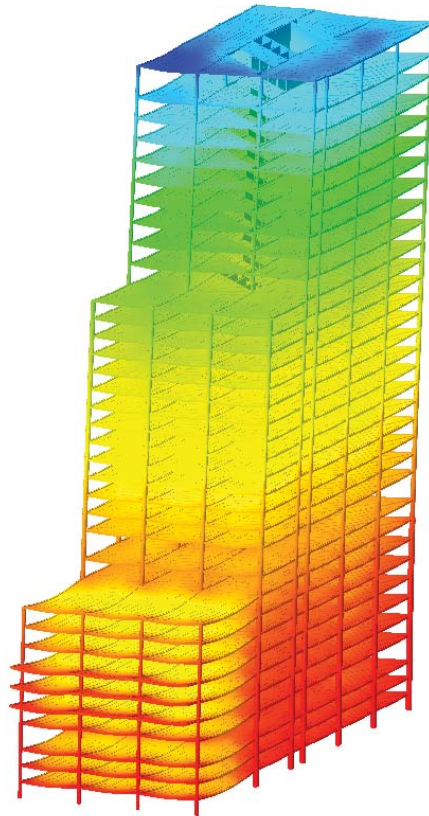




LUND
UNIVERSITY



STRUCTURAL DESIGN OF HIGH-RISE BUILDINGS

ERIK HALLEBRAND and WILHELM JAKOBSSON

Structural
Mechanics

Master's Dissertation

DEPARTMENT OF CONSTRUCTION SCIENCES
DIVISION OF STRUCTURAL MECHANICS

ISRN LUTVDG/TVSM--16/5213--SE (1-127) | ISSN 0281-6679

MASTER'S DISSERTATION

STRUCTURAL DESIGN OF HIGH-RISE BUILDINGS

ERIK HALLEBRAND and WILHELM JAKOBSSON

Supervisors: **PETER PERSSON**, PhD, Div. of Structural Mechanics, LTH
och **JESPER AHLQUIST**, MSc, Sweco.

Examiner: Professor **KENT PERSSON**, Div. of Structural Mechanics, LTH.

Copyright © 2016 Division of Structural Mechanics,
Faculty of Engineering LTH, Lund University, Sweden.

Printed by Media-Tryck LU, Lund, Sweden, June 2016 (*Pl*).

For information, address:

Division of Structural Mechanics,
Faculty of Engineering LTH, Lund University, Box 118, SE-221 00 Lund, Sweden.

Homepage: www.byggmek.lth.se

Abstract

High-rise buildings are exposed to both static and dynamic loads. Depending on the method used and how the structure is modelled in finite element software the results can vary.

Some of the issues and modelling techniques, introduced below, are investigated in this Master's thesis. Dynamic effects such as resonance frequencies and accelerations are considered. The variation in static results from reaction forces, overturning moments, deflections, critical buckling loads, forces between prefabricated elements and force distributions between concrete cores are investigated with different models. The models are evaluated by different elements and methods, such as construction stage analysis, to study the impact these have on the results.

Simplified calculations by hand according to different standards, regulations and codes such as SS-ISO, EKS and Eurocode have been compared with finite element analyses. The 3D-finite element software used for the analyses is Midas Gen.

From the results it can be observed, when modelling a high-rise building in a finite element software, that one model is often not sufficient to cover all different aspects. To see the global behaviour, one model can be used, and when studying the detailed results another model with a fine mesh, that have converged, is often needed. The same principle applies when evaluating horizontal and vertical loads, different models or methods are usually needed.

Keywords: High-rise buildings, resonance frequencies, accelerations, shear flow, displacements, critical buckling load, finite element.


Acknowledgements

This Master's thesis marks the end of 5 years of study at Lund University. It has been completed in association with Sweco AB and the Division of Structural Mechanics at the Department of Construction Sciences at Lund University.

We would like to thank Prof. Kent Persson, examiner, for the insight and assistance of problems encountered in this Master's thesis. Dr. Peter Persson, supervisor at Lund University, for the support, encouragement and assistance throughout the project. For providing help with the finite element software Midas Gen as well as useful knowledge about obstacles encountered, we thank Jesper Ahlquist at Sweco AB.



Erik Hallebrand



Wilhelm Jakobsson

Lund, June 2016

Contents

Abstract	i
Acknowledgements	iii
1 Introduction	1
1.1 Background	1
1.2 Objectives, aims and method	1
1.3 Limitations	2
1.4 Disposition	2
2 High-rise buildings	3
2.1 Stabilisation	4
2.2 Concrete buildings	6
2.2.1 Connections	6
2.3 Loads	7
2.4 Structural systems	7
2.4.1 Framed tube structures	8
2.4.2 Bundled tube	9
2.4.3 Tube in tube	9
2.4.4 Diagonalised- and rigid frame	9
2.4.5 Outrigger system	10
2.4.6 Hybrid structure	11
2.5 Wind-load effects	11
2.6 Comfort requirements	14
2.6.1 SS-ISO 10137	14
2.6.2 Human response	14
3 Finite element method	17
3.1 Linear elasticity	17
3.2 Structural dynamics	20
3.2.1 Resonance	21
3.3 Difficulties with the finite element method	22
3.3.1 Material	22
3.3.2 Load	23
3.3.3 Discretisation	23
3.4 Different types of elements	24
3.4.1 Beam elements	24

3.4.2	Plate elements	25
3.4.3	Plane shell element	25
3.5	Construction stage analysis	25
4	Method	31
4.1	Global critical load - Vianello method	31
4.2	Wind-load	33
4.2.1	Static wind-load	33
4.2.2	Dynamic wind-load	35
4.2.3	Along-wind response	38
4.2.4	Across-wind response	39
4.3	Empirical methods to determine the fundamental frequency	43
4.4	Forces between elements in a prefabricated concrete core	44
5	Case study in Midas Gen	47
5.1	Midas Gen elements	47
5.2	Description of Göteborg City Gate	47
5.2.1	Geometry	47
5.2.2	Modelling	49
5.3	Example case	51
6	Results	53
6.1	Analysis of Göteborg City Gate for vertical and horizontal loads	53
6.1.1	Vertical load	53
6.1.2	Horizontal load	57
6.1.3	Discussion of results	59
6.2	Analysis of reaction forces	60
6.2.1	Discussion of results	63
6.3	Analysis of overturning moment	64
6.3.1	Discussion of results	65
6.4	Analysis of horizontal deflection	65
6.4.1	Discussion of result	65
6.5	Analysis of critical load	66
6.5.1	Discussion of result	66
6.6	Analysis of resonance frequencies	67
6.6.1	Discussion of result	68
6.7	Analysis of acceleration	69
6.7.1	Along-wind acceleration	69
6.7.2	Across-wind acceleration	69
6.7.3	Discussion of results	72
6.8	Analysis of forces between elements in a prefabricated concrete core	72
6.8.1	Discussion of results	72
6.9	Vertical displacement	78
6.9.1	Vertical displacement in column	78
6.9.2	Discussion of results	79
7	Conclusions and further studies	85

Bibliography	87
Appendices	I
A Drawings of Göteborg City Gate	I
B Static wind-load - Strictly according to EC	XI
C Static wind-load with no c_s factor	XIII
D Static wind-load with τ factor	XV
E Wind-load according to EKS10	XVII
F Dynamic wind-load	XIX
G Deflection	XXI
H Vianello method	XXVII
I Buckling and P-delta analyses in Midas	XXIX
J Fundamental frequency according to Stafford Smith & Coull	XXXI
K Calculations of acceleration	XXXIII
L Calculation of shear-flow in a C-beam	XXXVII

1 Introduction

1.1 Background

The process of designing high-rise buildings have changed over the past years. In the most recent years it is not unusual to model full three-dimensional finite element models of the buildings. This due to the increased computational power and more advanced software. However, these models produce huge amount of data and results where possible errors are easily overlooked, especially if the model is big and complex. If the engineer is not careful and have a lack of knowledge of structural behaviour and finite element modelling, it is easy to just accept the results without critical thoughts. Furthermore, different ways of modelling have a big influence on the force and stress distribution. This can lead to time consuming discussion and disagreements between engineers as they often have different results from calculations on the same building.

Sweco AB were interested in initiating a Master's thesis that investigated different ways of modelling and how they affect the outcome. The Division of Structural Mechanics at Lund University were interested in a similar Master's thesis were the dynamics of high-rise buildings were to be analysed. Furthermore, investigations of how well analytical calculations by hand according to standards, codes and regulations of accelerations and resonance frequencies correspond to the results of large finite element models were to be conducted.

1.2 Objectives, aims and method

The objectives of this Master's thesis are to analyse different methods, codes and guidelines used when performing calculations on high-rise buildings in regards to deflections, resonance frequencies, accelerations and stability. The results from these methods are then compared with results from finite element models in order to evaluate differences and verify the methods and models.

The aims of the thesis are to provide insight on how different ways of modelling buildings in finite element programs affect the results. This is especially investigated when comparing vertical and horizontal loading with different modelling techniques and how the shear flow can be determined with a model using plate elements in a mesh compared to calculating it from the shear force in a model with wall elements. Furthermore, the accuracy of analytical calculations made by hand in comparison

to large finite element calculations are established. This to provide a helpful tool in discussions between engineers as well as provide basis for future research.

A comprehensive literature study has been made in the area of high-rise buildings regarding the history, design process, code regulations, finite element modelling as well as static and dynamic response. This translated into a case study of a high-rise building on which analytical calculations of deflection, critical buckling load, resonance frequencies and shear flow were made. The analytical calculations have then been compared to finite element calculations in Midas Gen. Furthermore, an analysis of accelerations and overturning moment from wind-load were made and compared to the comfort requirements.

1.3 Limitations

Analyses of high-rise buildings consists of many stages and factors and to evaluate all of these are beyond the scope of the Master's thesis. For concrete, no effects from creep, shrinkage or temperature effects have been analysed. The concrete have also been considered uncracked. Furthermore, no design of element cross-sections have been made and the accelerations of the building are calculated according to Eurocode, hence, no time-history analysis is performed.

1.4 Disposition

- | | |
|-----------|--|
| Chapter 1 | Gives an introduction to the subject and problem as well as the limitations that have been made. |
| Chapter 2 | Presents the fact gathered from the literature study and contains history as well as commonly used design methods for high-rise buildings. |
| Chapter 3 | Theory regarding the basis of the finite element method as well as different software applications are presented in this chapter. |
| Chapter 4 | Describes the chosen methods used for calculations on the building. |
| Chapter 5 | The case study and the different types of models used for analysis are presented in this chapter. |
| Chapter 6 | Shows the results from the analysis made and some discussion of the results. |
| Chapter 7 | Contains the conclusion drawn from the results as well as information about further studies on structural design of high-rise buildings. |

2 High-rise buildings

A building is defined as high-rise when it is considerably higher than the surrounding buildings or its proportion is slender enough to give the appearance of a tall building [14]. The construction of high-rise buildings started at the end of the 19th century in Chicago, with the evolution shown in Figure 2.1. This was made possible because of new inventions such as the safe elevator in 1853 [27] and the telephone in 1876 [5], that enabled transport of building materials and the ability to communicate to higher levels. In addition, the building materials changed as they went from wood and masonry to using steel frames with lighter masonry walls. Earlier buildings that were built with heavy masonry walls was limited to certain heights by its own self-weight. With steel frames the masonry could be thinner and act only as facade for weather protection and taller buildings could be constructed [19].

During the industrial revolution in Europe the need for warehouses, factories and multi-storey buildings were huge. Europe also played a major role in developing new materials such as glass, reinforced concrete and steel. Before 1945 the high-rise buildings in Europe were few and below the 100 meter limit and it was not until after the Second World War the construction of high-rise buildings excelled. This had to do with the reconstruction of all destroyed cities and the expanded demand for offices and residential [16].

In Sweden during the early 20th century there was a continued housing shortage and low housing conditions [26]. It was not until 1960 when the construction of new residencies skyrocketed. The politicians decided to build 100 000 new residencies a year for 10 years. This is known as the million-program. To be able to meet the requirements of the increased production the construction with prefabricated elements increased. In addition to faster production was that the decreased cost would give lower cost for living. During the time 1963–69 the production of prefabricated buildings was increased six fold. 20% of all residences built during the time was prefabricated and four major principles for building with prefabricated concrete elements were used [26] which are shown in Figure 2.2. In the 1970s the million-program was aborted due to the recession and oil-crisis which led to a drastic decrease in the production of new residencies [26]. The production dropped to only 30 000 residencies in 1986. In the end of the 1980s the production rose again to about 60 000 residences a year. The tallest building in Sweden today is Turning Torso in Malmö with its 190 meter and 54 stories above ground [20]. Turning Torso is an in-situ cast concrete building with the facade rotating 90 degrees from top to bottom. When constructing with precast concrete the height of the buildings is

2. High-rise buildings

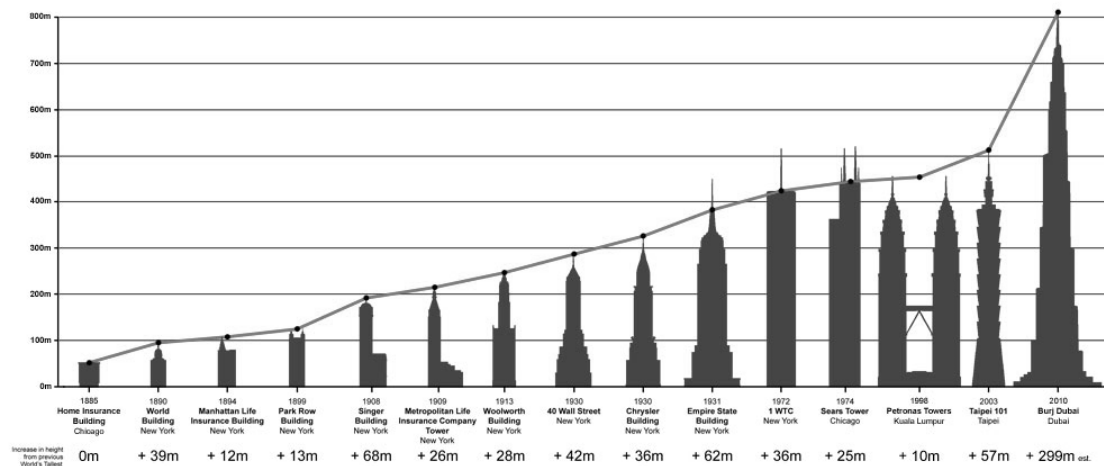


Figure 2.1: Diagram of buildings that have once claimed the title ‘World’s highest building’ [18].

usually much lower than buildings cast in-situ cast. The tallest building ever made with precast concrete is The Breaker Tower in Seef, Bahrain. The building reaches just above 150 meter and has 35 stories [11]. Comparing this with the tallest in-situ cast concrete building which is Burj Khalifa in Dubai, United Arab Emirates, see Figure 2.1, reaching 828 meters and has 163 stories [13]. High-rise buildings does not only give more residencies on smaller area but is also a landmark for the city or country and represents power.

2.1 Stabilisation

The buildings behaviour when excited to horizontal wind-load is described in this section, for more detailed information see [16].

Knowledge, technology and construction materials are constantly evolving and so is the strife for constructing higher buildings. However, it does not go without some challenges and issues. First off, the vertical loads increases with the height of the building. There is also the large effect from horizontal wind-load on the building. The buildings behaviour under the lateral loading can be seen as a cantilever fixed at the ground. If the wind is assumed to have a uniform distribution the base-moment increases quadratic with the height. However, the real shape of the wind pressure is increasing with the height, which gives even greater base-moment, see Figure 2.3. One of the main tasks when designing high-rise buildings is its ability to absorb the horizontal forces and to transmit the resulting moment into the foundation. One way to effectively achieve this are coupled load-bearing vertical walls. However, this will lead to tensile stresses in the concrete walls on the loaded side. In order to minimise these stresses, self-weight of slabs etc. are placed on the walls to get compressive stresses. Other ways of dealing with horizontal loading are presented more in detail in Section 2.4.

The higher a building is, the more important it is to consider the choice of cross-

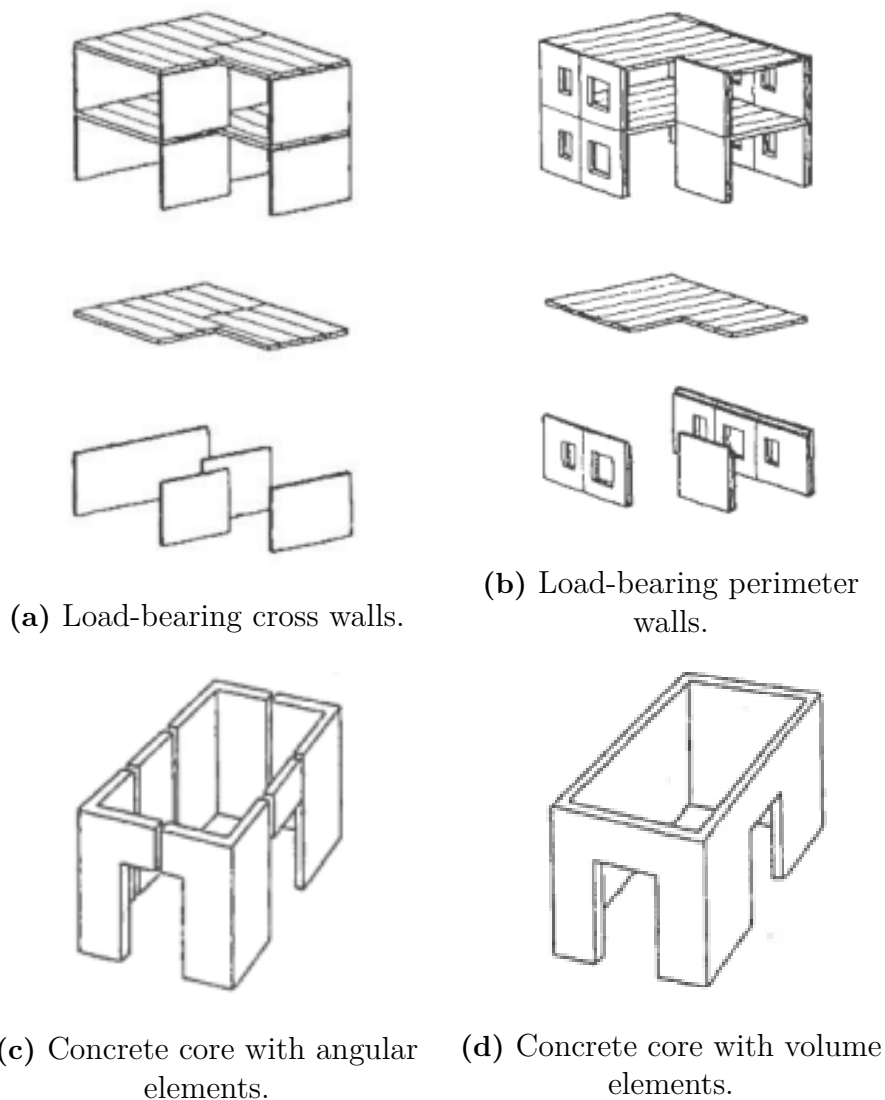


Figure 2.2: Four major principles of prefabricated construction [1].

sections, materials and structural systems as well as the demands on functionality. Factors that needs to be considered are deflections and accelerations from horizontal loading that mainly occurs from unexpected deflections, wind or earthquakes. Unexpected deflections may arise when imperfections in the elements occur during the manufacturing or if the foundation is uneven due to an inhomogeneous site. Any unexpected deflection causes additional lateral forces and must be considered. Horizontal loading from wind may also cause sway in the building. This since high-rise buildings are susceptible for oscillation. The wind should therefore not only be seen as a static load but also as a dynamic load. To determine how the building respond to wind-loads, wind tunnel experiments are often performed. The oscillation affects the building in several ways, how the people inside perceives the sway and the maximum horizontal deflection that arises.

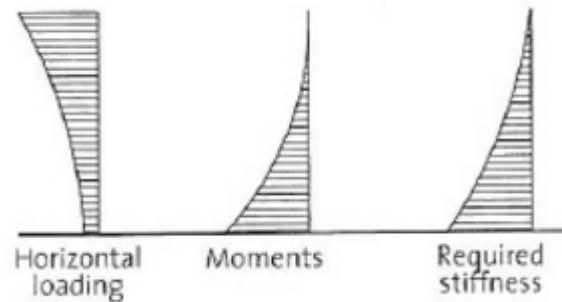


Figure 2.3: Wind-load, moment and stiffness diagram for a high-rise building [16].

2.2 Concrete buildings

In this section some differences between cast in-situ and precast concrete are explained as well as different types of connections, for more detailed information see [7].

Concrete buildings can either be cast in-situ, composed with precast elements or a combination of both. If the building is cast in-situ it is possible to start the activities on site in an early stage. Preparation for scaffolding and moulding can start as soon as the contract is assigned to the contractor and the design of the building starts. This is not possible when constructing with precast elements as all decisions regarding dimensions, shapes and so forth has to be taken long before the activities on site can start. When using precast elements it is of importance to industrialise the manufacturing. This implies manufacturing in covered factories, use of automatic tools and thoroughly plan the production process. There are some important differences regarding cast in-situ and precast buildings. When a building is cast in-situ the elements are created in moulds on site and are constantly checked to have the correct height. But when a building is constructed with precast elements the elements are created in a factory where the factory worker is fully dependent on the drawing. If for example a column have the wrong height on the drawing, no one will correct this in the factory and an incorrect column will be created causing problems on site.

2.2.1 Connections

When designing a precast building it is important to consider the connections between elements, which are part of the assembly procedure and should not interfere. Connections can be divided in wet and dry connections. The difference between these are the use of concrete or mortar. Wet connections are for example, mortar joints, cast in-situ blocks or cast in-situ slabs that are more fire resistant, less sensitive for tolerance criteria and more ductile than dry connections. Examples of dry connections are free supports, welded connections and cold joints which are quick to assemble.

2.3 Loads

Loads that has to be taken into consideration when designing a building are vertical loads from self-weight, imposed loads, snow loads and horizontal loads from both wind and unintended inclinations. For tall buildings, as earlier mentioned, the horizontal loading from wind is usually the design load. The vertical loads are the self-weights, finishing loads and live loads and they are transferred to the foundation through columns, load-bearing walls or towers. The live load depends on the type of usage in the building and on the standard used for designing [16]. In Eurocode [30], the live load varies from 0.5–5.0 kN/m². The higher value is often used for offices to take the variable partitioning and the greater live load in corridor areas into account [16]. Some reduction of the live load can be made depending on the number of stories, but may never exceed 40% for any construction element [16].

The horizontal load from wind working as a distributed load on the facade, which transfers the load to the slabs. The slabs are working as diaphragms and provides the lateral transfer of the shear load to the vertical elements and also as a stability unit for the compression flange of the steel beam beneath [36]. The shear forces in the diaphragms occur mainly in the concrete because of its in-plane stiffness. The horizontal loads are transferred from the slabs to the beams through welded studs. Depending on how the slabs are connected to the facade, the stress distributions in the slabs will vary. For example, the slabs can be connected directly to the facade, which gives a distributed load. The facade can also be connected to columns which will provide point loads instead. The load distribution depends on the stiffness of the elements as stiffer units attract more load than weaker.

When designing vertical walls in a building both shear and bending deformation may occur. For low robust walls the bending is negligible and for tall slender structures shear is negligible. Considering the entire building the shear wall becomes tall and slender, however, the walls in each plane are low and robust making it susceptible to both shear and bending. For a tall building the deformation shapes from bending and shear can be seen in Figure 2.4.

2.4 Structural systems

A building needs to be stabilised for horizontal load and to achieve this, several different structural systems can be chosen. Some of these are shown in Figure 2.5 and described in this section, for more detailed information see [34]. All of the different systems have evolved from the traditional rigidly jointed structural frame. The fundamental design for all these structural systems have been to place as much of the load-carrying material as possible around the buildings external fringe to maximise its flexural rigidity. For all structural systems, advantage can be taken by locating the main vertical members and, with the compressive stresses from self-weight, suppress the lateral load tensile stresses. This to avoid net tension in the vertical members and uplift in the foundations. For some structural systems it is necessary to have self-weight at the outer vertical members in order to achieve this.

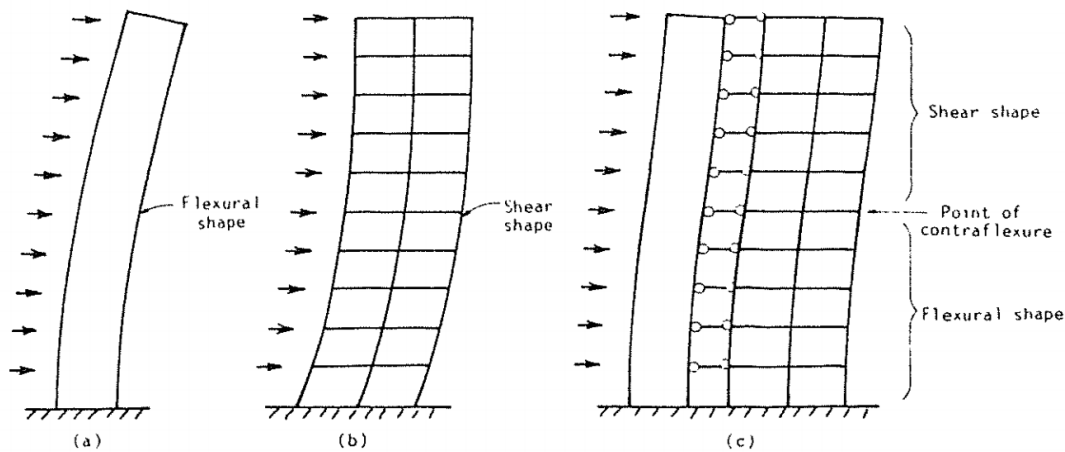


Figure 2.4: Deformation shapes of a tall building. a) Bending deflection, b) Shear deflection and c) Total deflection [34].

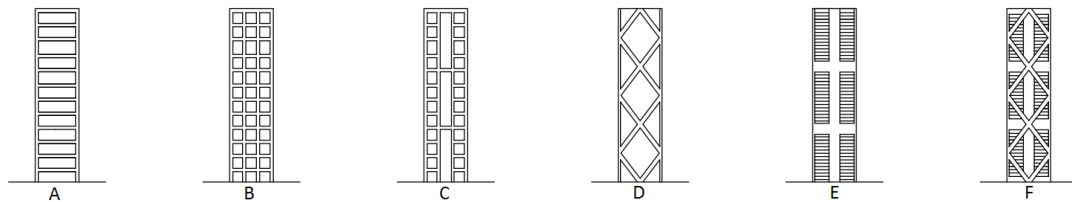


Figure 2.5: Different structural systems, where A) represents a framed tube system, B) a bundled tube system, C) a tube in tube system, D) a diagonalised system, E) a core and outrigger system and F) a hybrid system [15].

In the following sections, explanation are given of the structural systems shown in Figure 2.5.

2.4.1 Framed tube structures

For framed tube structures the lateral resistance is given by very stiff moment resisting frames that form a tube around the perimeter of the building. The frames consists of closely spaced columns, 2–4 meters between centres, connected by girders. The tube carries all the lateral load and the self-weight is distributed between the outer tube and the interior columns or walls. For the lateral loading the perimeter frames aligned in the load direction acts as webs of the tube cantilever and those perpendicular to the load direction acts as flanges. The tube structure is suitable for both steel and reinforced concrete buildings and have been used in the range of 40–100 stories. Framed tube systems have been the most significant modern development in high-rise structural forms and is easily constructed and usable for great heights. For the aesthetics of the tube structure the enthusiasm is mixed, some like the logic of the clearly expressed structure while others criticise the grid-like facade as small windowed and repetitious. A disadvantage with the tube structure is the efficiency for the flange frames, for lateral loading, which tend to suffer from shear lag with the result that the mid columns are less stressed than the corner columns and therefore not contributing as much as they could.

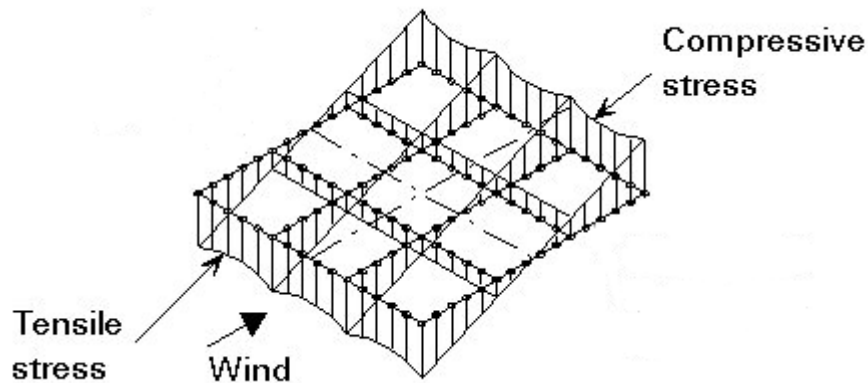


Figure 2.6: Bundled tube intersection [25].

2.4.2 Bundled tube

The bundled tube structure consists of four parallel rigid frames in each orthogonal direction, interconnected to form nine bundled tubes, see Figure 2.6. The principle is the same as for the single tube structure where the frames in the horizontal load direction acts as webs and the perpendicular frames acts as flanges. By introducing the internal webs the shear lag is drastically reduced and as a result the stresses in the columns are more evenly distributed and their contribution to the lateral stiffness is more significant. This allows for the columns to be spaced further apart and to be less striking.

2.4.3 Tube in tube

What differentiates the tube in tube concept from other structural systems is that an outer framed tube (hull), is working together with an internal tube (core), usually elevator shafts and stairs, to resist both the lateral and vertical loading, see Figure 2.7. This provides increased lateral stiffness and can be seen as the shear and flexural components of a wall-frame structure.

2.4.4 Diagonalised- and rigid frame

In braced frames the lateral resistance is given by diagonal members that, together with the girders, form a web of vertical trusses, where the columns acting as chords, see Figure 2.8. Bracing systems are highly efficient of resisting lateral loads. This due to the horizontal shear in the building is resisted by the horizontal components resulting in tensile and compressive actions in the web members. The bracing system is an almost steel exclusive system since the diagonals are inevitably subjected to tension for one or the other direction of the lateral loading. Braced systems are able to produce a very stiff lateral structure for a minimum of additional material which makes it economically efficient for any height. The major disadvantage with diagonal bracing is that it is limiting the internal planning and the location of windows. Furthermore, the connections to the diagonals are expensive to fabricate and erect.

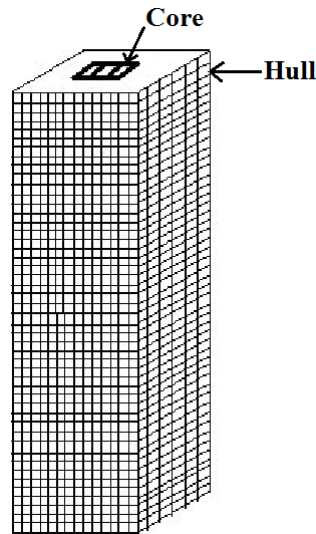


Figure 2.7: Tube in tube [2].

In rigid frame structures the columns and girders are joined together by moment resistant connections. The lateral stiffness of a rigid frame depends on the bending stiffness of the columns, girders and connections in-plane. This type of structure is ideally suited for reinforced concrete buildings because of the stiffness from reinforced concrete joints. For steel, these connections can be made although they are expensive. An advantage with rigid frame structures is the possibility of planning and fitting of windows because of the open rectangular arrangement. A disadvantage is that the self-weight is resisted by the action from rigid frames. Negative moments are induced in girders adjacent to columns causing the mid-span positive moments to be significantly less than in a simply supported span. For buildings where self-weights dictate the design, usually below 10 stories, economics in member sizes that arise from this effect tend to be offset by the increased cost of the rigid joints.

2.4.5 Outrigger system

The outrigger system is an efficient structural form that consists of a central core with outriggers, connecting the core to the outer columns. The central core contains of either braced frames or shear walls. When the building is loaded laterally the vertical plane rotations are resisted by the outriggers through tension in the windward columns and compression in the leeward columns, see Figure 2.9. This is augmenting the lateral stiffness of the building and reducing the lateral deflections as well as the moments in the core. In addition, the outriggers join the columns and makes the building behave almost as a composite cantilever. Even the perimeter columns, those not directly connected to the outriggers, can be used to increase the lateral resistance of the building by connecting all the perimeter columns with a horizontal girder around the building's facade. Multilevel outrigger systems can provide up to five times the moment resistance of a single outrigger system. Outrigger systems have been used for buildings up to 70 stories but the concept should hold for even higher buildings.

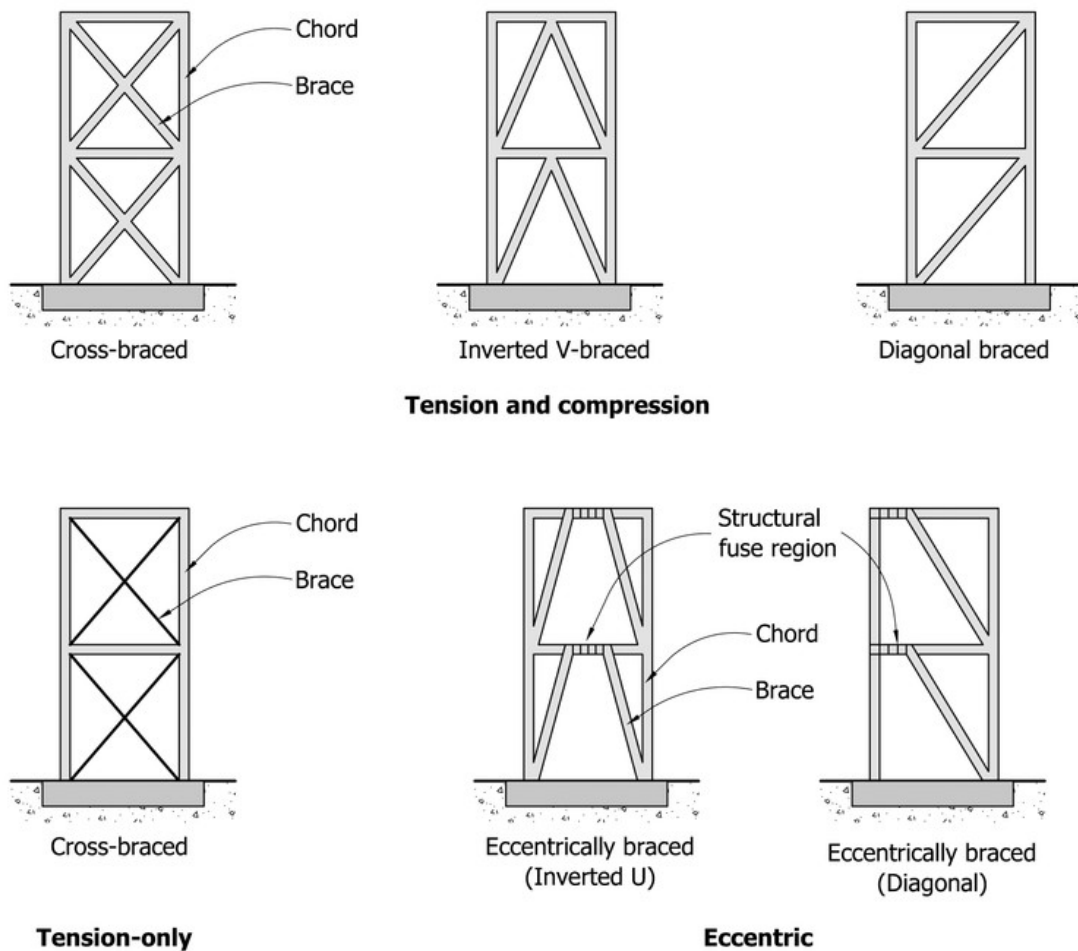


Figure 2.8: Different types of diagonal bracing [9].

2.4.6 Hybrid structure

Hybrid structures are often used for non-prismatic structure where two or more of the basic structures described earlier are used in the same building. This concept can be used for either direct combination of, for example, a tube and an outrigger system or by adopting different systems for different parts of the building, for example a tube system on three walls and a frame on the fourth wall.

2.5 Wind-load effects

The effects from wind-load will be described in this section, for more detailed information see [34].

As mentioned earlier wind-load has to be considered when designing high-rise buildings. Up to 10 stories the wind-load rarely affects the design. However, for taller buildings the effect is more crucial. Over the past years new materials with higher strength have been developed. This in combination with more innovations in architectural treatment and advances in methods of analysis have made high-rise build-

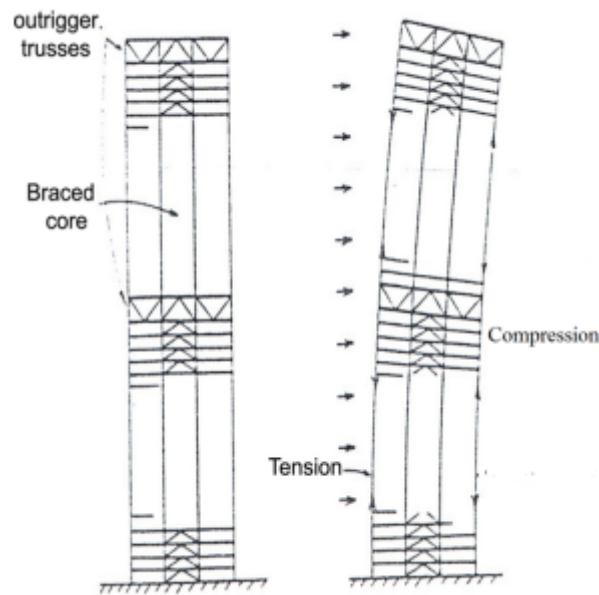


Figure 2.9: Outrigger-braced system [35].

ings more efficient and lighter, which also means more prone to deflections and sway. Wind-load can be divided into both static and dynamic loading depending on the time period. For long periods of time the load can be seen as static and for shorter time periods as dynamic. In this section the dynamic response from wind is investigated. The dynamic wind pressure produces sinusoidal or narrow-band random vibration motions on the building in both along- and across-wind direction as well as rotation about the vertical axis, see Figure 2.10. The magnitudes of the displacements depends on the wind velocity distribution and direction but also on the mass, stiffness and shape of the building. For some cases the effects from the across-wind actions are greater than the along-wind actions on the building. Even though the wind-load is dynamic in short periods of time it is often replaced by an equivalent static load representing the maximum magnitude in the design stage. The dynamic response is considered when a building is relatively flexible to investigate the stress levels and the accelerations that may affect the comfort of the occupants.

Natural frequencies and resonance

The first modes of a building are of interest when investigating the dynamic response from wind-load. These are the lateral deflection in both directions as well as the rotational mode around the vertical axis. The modes being excited when a building is relatively tall or large, making the wind gusts not acting simultaneously on all parts and thus will tend to offset each other's effect. The stiffness of the building affects the resonance frequencies. If the building is stiff, the resonance frequencies will be relatively high and the dynamic deflections will not be significant. In addition, the main design parameter to be considered is the maximum loading during the building's lifetime. The building can then be seen as static and analysed for an

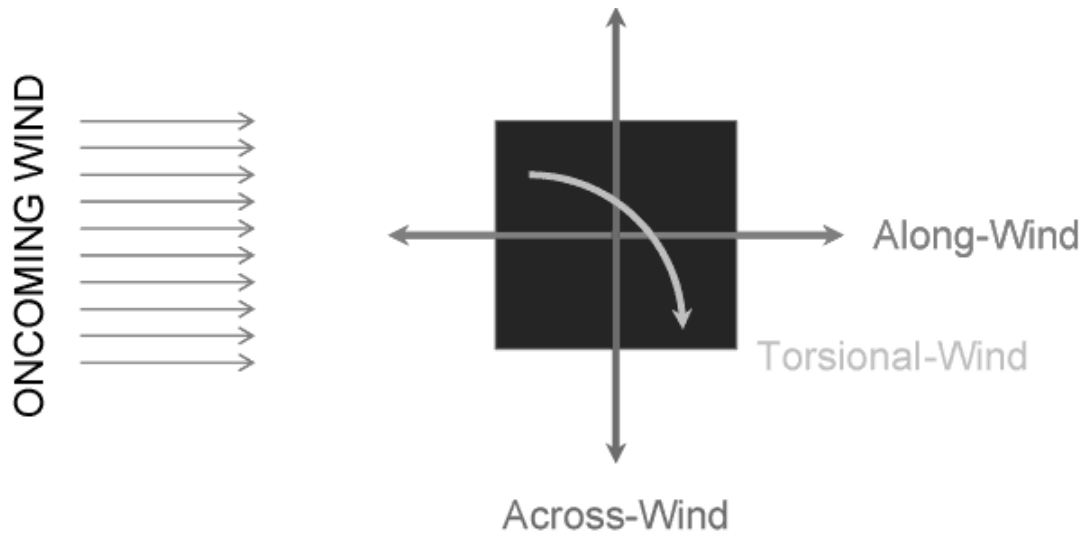


Figure 2.10: The response of a building when excited to wind-load [17].

equivalent wind-load. On the other hand if the stiffness is low the building is flexible and the resonance frequencies will become lower. This leads to that the response will depend on the frequency of the fluctuating wind forces. The building will tend to follow the fluctuating wind actions below the fundamental frequency and will be attenuated at frequencies above. However, at frequencies at or close to the natural frequencies the response will be amplified which may cause the dynamic deflections to be greater than the static deflections. In this case the lateral deflection becomes an important design parameter and the building is classified as dynamic. For flexible buildings the oscillations may interact with the aerodynamic forces which may lead to instability in form of galloping oscillations, vortex-capture resonance, divergence and flutter. To predict the structural response from wind-load there are two important evaluations to do:

- The prediction of the occurrence of various mean wind velocities and their associated directions.
- The prediction of the maximum dynamic response of the building with the given occurrence of the wind.

When a building is excited by wind-load the wind-force tend to be random in amplitude and spread over a wide range of frequencies. The building's response is then decided by the wind energy available in the narrow bands close to the natural frequencies of the building. The major part of the exciting wind energy often occurs at frequencies lower than the fundamental frequency of the building and the energy decreases with increasing frequency. This makes it necessary to only consider the building's response at the three first modes, two lateral and one rotational, higher modes being rarely significant. The response to the along- and across-wind arises from different forcing mechanics where the along-wind is primarily to buffeting effects caused by turbulence and the across-wind primarily to vortex shedding. The across-wind response is of special interest with regard to the comfort of the occupants.

2.6 Comfort requirements

The dynamic effects should be considered both for serviceability and safety [33]. When considering safety, the risk of resonance are of interest and when considering serviceability, the human response to motion are of interest [33]. Movement in a tall building can have a wide range of human response, from anxiety to acute nausea [34]. This can make a building undesirable and may produce difficulties renting floor area. Why it is of importance to not just consider stability issues but also consider motions [34]. Movements in buildings are commonly generated from wind, earthquakes, machinery, nearby industrial plants and various types of transportation [34]. It would be expensive to construct a high-rise building that could withstand all movements [34]. That is why there are various recommendations regarding accelerations in buildings depending on the occupancy.

2.6.1 SS-ISO 10137

SS-ISO 10137 is a Swedish standard that gives recommendations regarding the serviceability limit state [33]. Different aspects has to be taken into account when evaluating the serviceability limit state criteria regarding vibrations. For instance, the variation of human tolerance due to cultural, regional or economic factors. Other aspects to consider when evaluating serviceability are sensitive contents in the building and the possibility in change of use and occupancy. Materials whose dynamic characteristics may change with time and social or economic consequences of unsatisfactory performance may also be of interest [33]. The variation of human tolerance regarding vibrations in a building depends on both direct and indirect effects. The direct effects are the frequencies, magnitude, duration, variability, form, directions of the vibration and intervals between vibration events or exposure of the human subjects to the vibration. Indirect effects are audible noise and infra sound, visual cues, population type, familiarity with vibration, structural appearance, confidence in a buildings structure and knowledge of the vibration source [33]. SS-ISO 10137 have different levels of acceptable vibrations in buildings depending on the occupancy. For instance, the acceptable accelerations are higher for offices than residencies [33], shown in Figure 2.11.

2.6.2 Human response

Besides the SS-ISO standard a lot of investigations have been made regarding human response to motions in buildings. Subjects have been called to undertake different tasks when subjected to motion. The result of these studies are presented in Table 2.1. These studies are based on the motion caused by the peak during 10 minutes of the worst windstorm with a return period of 5 years and that not more than 2% of those occupying the building complain about the motions. Guidelines regarding acceptable motions depending on the occupancy of the building have been developed from these [34].

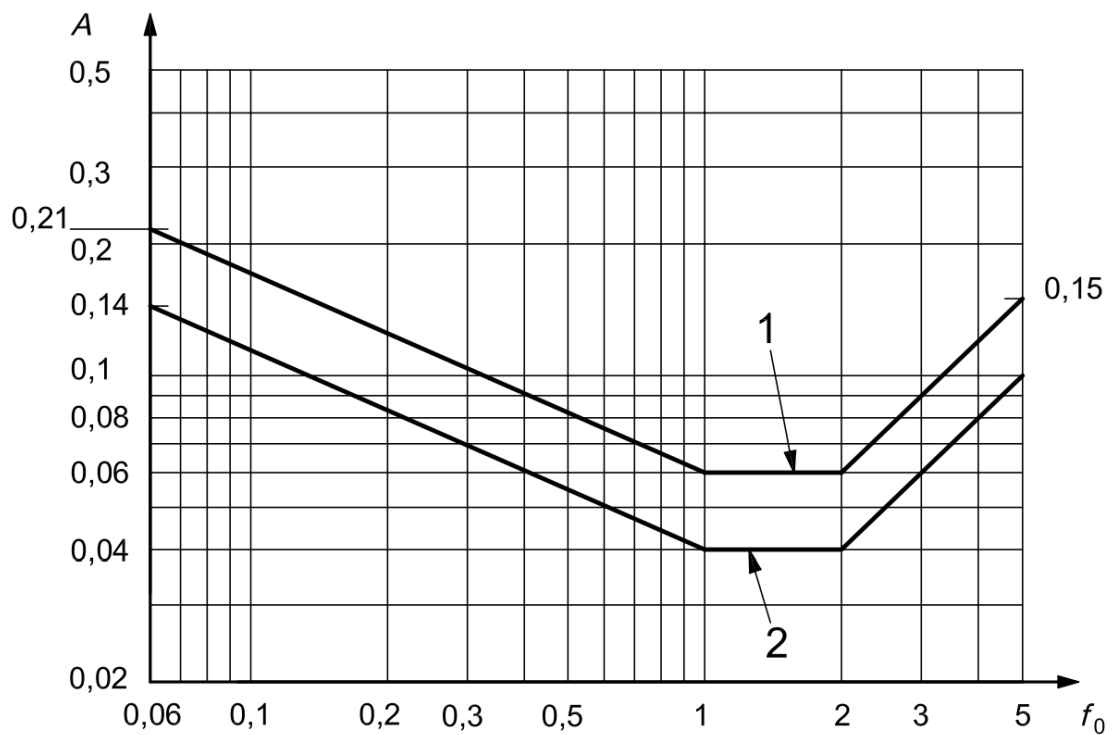


Figure 2.11: Evaluation curves for horizontal wind induced vibrations in a building caused by a one-year return wind. Line 1 represents office and line 2 represents residence. The axis represents the acceleration [m/s^2] and the fundamental frequency of the building [Hz] [33].

Table 2.1: Human perception levels [34]

Range	Acceleration [m/s ²]	Effect
1	<0.05	Humans cannot perceive motion
2	0.05–0.10	Sensitive people can perceive motion; hanging objects may move slightly
3	0.1–0.25	Majority of people will perceive motion level of motion may affect desk work long-term exposure may produce motion sickness
4	0.25–0.4	Desk work becomes difficult or almost impossible ambulation still possible
5	0.4–0.5	People strongly perceive motion difficult to walk naturally standing people may lose balance
6	0.5–0.6	Most people cannot tolerate motion and are unable to walk naturally
7	0.6–0.7	People cannot walk or tolerate motion
8	>0.85	Objects begin to fall and people may be injured

3 Finite element method

In this chapter the finite element (FE) method will be introduced briefly, for more detailed information see [4, 10, 12, 37]. Various types of elements and some difficulties working with the method will also be mentioned.

To describe various physical problems, the use of partial differential equations (PDEs) is a good option. These PDEs can be solved with numerical methods when the system is too complicated for an analytical solution. To solve this numerically, the (FE) method can be used. Using FE modelling, the structure is subdivided, discretised, into a finite number of individual elements. The behaviour of these elements, the relation between their nodal displacements and reactions, can be specified by shape functions. By means of the shape functions and their corresponding derivatives, all displacements, strains and stresses within an element can be calculated. The individual elements are only interconnected by their nodes and to get the complete solution for the entire structure all elements are assembled [29]. The amount of elements affects the result as more elements give a more accurate result. However, the more complex and larger the structure is, the more the computation time increases.

A few years ago, modelling entire 3D models of a complex building was not possible due to insufficient processing power and software. The building had to be disassembled into its different structural parts, beams, columns, plates, walls etc. and designed separately [29]. This made complex architectural forms difficult to design. Nowadays, with improved computational power and software, it is possible to calculate more complex and bigger structures. However, trusting the FE analysis blindly can have large complications and it is up to the user to verify the result to prevent a collapse of the structure. The more complicated the numerical model is, the more difficult it is to interpret the accuracy of the result and maintain a global overview of the structure [29].

3.1 Linear elasticity

The dynamic equilibrium for a linear elastic continuum body can be described with the following differential equation

$$\tilde{\nabla}^T \boldsymbol{\sigma} + \mathbf{b} = \rho \frac{\partial^2 \mathbf{u}}{\partial t^2} \quad (3.1)$$

where:

- $\tilde{\nabla}$ is a matrix differential operator
- $\boldsymbol{\sigma}$ is a vector composed of all the stress components involved
- \mathbf{b} is a body force vector containing the body forces present per unit volume

The matrix and vectors contains the following components

$$\tilde{\nabla}^T = \begin{bmatrix} \frac{\partial}{\partial x} & 0 & 0 & \frac{\partial}{\partial y} & \frac{\partial}{\partial z} & 0 \\ 0 & \frac{\partial}{\partial y} & 0 & \frac{\partial}{\partial x} & 0 & \frac{\partial}{\partial z} \\ 0 & 0 & \frac{\partial}{\partial z} & 0 & \frac{\partial}{\partial x} & \frac{\partial}{\partial z} \end{bmatrix}; \quad \boldsymbol{\sigma} = \begin{bmatrix} \sigma_{xx} \\ \sigma_{yy} \\ \sigma_{zz} \\ \sigma_{xy} \\ \sigma_{xz} \\ \sigma_{yz} \end{bmatrix}; \quad \mathbf{b} = \begin{bmatrix} b_x \\ b_y \\ b_z \end{bmatrix}; \quad \mathbf{u} = \begin{bmatrix} u_x \\ u_y \\ u_z \end{bmatrix}. \quad (3.2)$$

The body force vector, \mathbf{b} , acts on the body-per-unit volume, while the traction vector, \mathbf{t} , acts on the surface of the body, as a force-per-unit area. As long as the traction vector is present on the surface, it must fulfil the following boundary condition

$$\mathbf{t} = \mathbf{S}\mathbf{n} \quad (3.3)$$

where:

- \mathbf{S} is the stress tensor
- \mathbf{n} is the unit normal vector

For deriving the weak formulation, the arbitrary vector \mathbf{v} is established as

$$\mathbf{v} = \begin{bmatrix} v_x \\ v_y \\ v_z \end{bmatrix}. \quad (3.4)$$

By multiplying Equation 3.1 with Equation 3.4 and integrating the expressions over the volume, V , gives

$$\int_V \mathbf{v}^T (\tilde{\nabla}^T \boldsymbol{\sigma} + \mathbf{b} - \rho \frac{\partial^2 \mathbf{u}}{\partial t^2}) dV = 0. \quad (3.5)$$

An integration by parts is then performed using the Green-Gauss theorem on the first term in Equation 3.5 and the components of the traction vector appear as

$$\int_V \mathbf{v}^T \tilde{\nabla}^T \boldsymbol{\sigma} dV = \int_S \mathbf{v}^T \mathbf{t} dS - \int_V (\tilde{\nabla} \mathbf{v})^T \boldsymbol{\sigma} dV. \quad (3.6)$$

The weak form is found by adding the terms together, resulting in

$$\int_V \mathbf{v}^T \rho \frac{\partial^2 \mathbf{u}}{\partial t^2} dV + \int_V (\tilde{\nabla} \mathbf{v})^T \boldsymbol{\sigma} dV = \int_S \mathbf{v}^T \mathbf{t} dS + \int_V \mathbf{v}^T \mathbf{b} dV. \quad (3.7)$$

To be able to apply this in the FE formulation, the displacement vector, \mathbf{u} , is approximated by

$$\mathbf{u} = \mathbf{N}\mathbf{a} \quad (3.8)$$

where:

- \mathbf{N} are the global shape functions
- \mathbf{a} are the displacements

The use of the Galerkin method implies that

$$\mathbf{v} = \mathbf{Nc} \quad (3.9)$$

where:

- \mathbf{c} is a vector with arbitrary constants

Introducing $\tilde{\mathbf{B}} = \tilde{\nabla}\mathbf{N}$, gives

$$\tilde{\nabla}\mathbf{u} = \boldsymbol{\varepsilon} = \mathbf{Ba} \quad (3.10)$$

and

$$\tilde{\nabla}\mathbf{v} = \mathbf{Bc} \quad (3.11)$$

By inserting Equation 3.9 and Equation 3.11 into the weak formulation shown in Equation 3.7 the elimination of \mathbf{c} is possible. The introduction of the constitutive matrix \mathbf{D} , which contains the behaviour of linear elastic material, is given as

$$\boldsymbol{\sigma} = \mathbf{D}\boldsymbol{\varepsilon}. \quad (3.12)$$

By using the kinematic relationship for elastic strains derived with Equation 3.10, Equation 3.12 can be written as

$$\boldsymbol{\sigma} = \mathbf{DBa}. \quad (3.13)$$

It is now possible to rewrite the FE formulation for a linear elastic case as

$$\int_V \mathbf{N}^T \rho \mathbf{N} dV \ddot{\mathbf{a}} + \int_V \mathbf{B}^T \mathbf{D} \mathbf{B} dV \mathbf{a} = \int_S \mathbf{N}^T \mathbf{t} dS + \int_V \mathbf{N}^T \mathbf{b} dV. \quad (3.14)$$

There are two ways to state the boundary conditions involved. Either as the essential boundary condition, i.e. prescribed displacements \mathbf{u} , or as the natural boundary condition, i.e. prescribed traction vector \mathbf{t} .

A more compact formulation is obtained by defining the matrices and vectors as

$$\mathbf{M} = \int_V \mathbf{N}^T \rho \mathbf{N} dV; \quad \mathbf{K} = \int_V \mathbf{B}^T \mathbf{D} \mathbf{B} dV; \quad \mathbf{f} = \int_S \mathbf{N}^T \mathbf{t} dS + \int_V \mathbf{N}^T \mathbf{b} dV \quad (3.15)$$

which can be written as

$$\mathbf{M}\ddot{\mathbf{a}} + \mathbf{K}\mathbf{a} = \mathbf{f}. \quad (3.16)$$

where:

- \mathbf{M} is the mass matrix
- \mathbf{K} is the stiffness matrix
- \mathbf{f} is the force vector
- $\ddot{\mathbf{a}}$ is the acceleration vector
- \mathbf{a} is the displacement vector

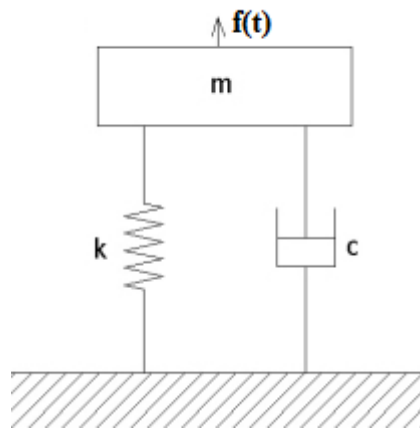


Figure 3.1: Mass-spring-damper system for a single degree of freedom system.

3.2 Structural dynamics

Structural dynamics treats forces and displacements caused by motion. This can be described with Newton's second law as shown in Equation 3.17.

$$f - c\dot{u} - ku = m\ddot{u} \quad (3.17)$$

where:

- f is the time dependent load
- c is the damping
- \dot{u} is the velocity
- k is the stiffness
- u is the displacement
- m is the mass
- \ddot{u} is the acceleration

To describe a structural dynamic system the easiest way is to start with a single degree of freedom system (s dof). An easy sdof system is shown in Figure 3.1 and Equation 3.17 and can be rewritten for a sdof system as shown in Equation 3.18.

$$m\ddot{u} + c\dot{u} + ku = f. \quad (3.18)$$

All systems cannot be described as a sdof system. When a more complex structure has to be described a multi degree of freedom system (mdof) can be used. The accuracy of the result of a mdof system will, for most cases, be better with a larger number of degrees of freedom. The equation of motion for a mdof system is described by a differential equation shown in Equation 3.19, assuming small deformations.

$$\tilde{\nabla}^T \boldsymbol{\sigma} + \mathbf{b} = \rho \frac{\partial^2 \mathbf{u}}{\partial t^2} \quad (3.19)$$

where:

- $\tilde{\nabla}$ is the differential operator matrix

$\boldsymbol{\sigma}$	is the stress vector
\mathbf{b}	is the body force vector
ρ	is the mass density
\mathbf{u}	is the displacement vector
t	is the time

From Equation 3.19 the equation of motion for a dynamic system can be derived as shown in Equation 3.20

$$\mathbf{M}\ddot{\mathbf{u}} + \mathbf{C}\dot{\mathbf{u}} + \mathbf{K}\mathbf{u} = \mathbf{f} \quad (3.20)$$

where:

\mathbf{M}	is the mass matrix
\mathbf{C}	is the damping matrix
\mathbf{K}	is the stiffness matrix
\mathbf{f}	is the load vector
\mathbf{u}	is the nodal displacement vector
$\dot{\mathbf{u}}$	is the nodal velocity vector
$\ddot{\mathbf{u}}$	is the nodal acceleration vector

3.2.1 Resonance

Resonance occurs when a structure is exposed to dynamic loading with a frequency near a natural frequency. This phenomenon means that the amplitude of vibrations in the structure starts to increase drastically. Resonance can occur at all natural frequencies which are unlimited in reality and are equal to the number of degrees of freedom in a numerical model. The steady-state response of the displacement amplitude of an undamped sdof system is shown in Equation 3.21.

$$u(\omega) = \frac{f}{k} \frac{1}{1 - (\omega/\omega_n)^2} \quad (3.21)$$

where:

ω_n	is the angular eigenfrequency of the structure
f	is the frequency of the load
k	is the stiffness of the structure
ω	is the exciting frequency

From Equation 3.21 it can be observed that if the eigenfrequency and the exciting frequency coincide the displacement will go to infinity. However this is not the case in reality since damping always exists in some way. To all natural frequencies there is a corresponding eigenmode which represents a certain deformed shape. To determine this shape and corresponding eigenfrequency for a mdof system the equation of motion for an undamped system ($\mathbf{C} = 0$) can be evaluated, where the load vector is equal to zero ($\mathbf{f} = 0$), see Equation 3.22.

$$\mathbf{M}\ddot{\mathbf{u}} + \mathbf{K}\mathbf{u} = \mathbf{0}. \quad (3.22)$$

Equation 3.22 could then be solved with the initial conditions at $t = 0$, see Equation 3.23.

$$\mathbf{u} = \mathbf{u}(0); \quad \dot{\mathbf{u}} = \dot{\mathbf{u}}(0). \quad (3.23)$$

The free vibration of an undamped mdof system in a given eigenmode can then be written as Equation 3.24

$$\mathbf{u}(t) = q_n(t)\phi_n \quad (3.24)$$

where:

$q_n(t)$ is the time-dependent and can be described by the harmonic function in Equation 3.25
 ϕ_n is the eigenmode

$$q_n(t) = A_n \cos \omega_n t + B_n \sin \omega_n t \quad (3.25)$$

If no load is applied to the structure and thereby no motion is implied which leads to the deformed shape becomes equal to zero. In this case the natural frequency and corresponding eigenmode can be determined by solving the eigenvalue problem in Equation 3.26.

$$(-\omega_n^2 \mathbf{M} + \mathbf{K})\phi_n = \mathbf{0}. \quad (3.26)$$

The solution to the eigenvalue problem gives the eigenfrequencies $\omega_1, \dots, \omega_n$ where n is the number of degrees of freedom. From the eigenfrequencies the eigenmodes can then be determined by solving Equation 3.26 with the known eigenfrequencies.

3.3 Difficulties with the finite element method

Using the finite element method when evaluating a structure is a powerful tool. However, it does not come without difficulties where some are described in this section, for more details see [29]. The more complex a structure is the more controlling of the model is required. This in combination with more complex and advanced software results in difficulties for the engineer to examine all possible eventualities in advance. In addition, computers have a limitation regarding accuracy exists shown in an example below.

$$2^{45} - 0.8 - 2^{45} = -0.8008 \neq -0.8000$$

$$2^{50} - 0.8 - 2^{50} = 0.0 \neq -0.8000$$

3.3.1 Material

Difficulties commonly occurs regarding the modelling of the materials. Concrete for instance is a highly nonlinear material. Although it is often considered as a linear elastic material when calculating internal forces and moments, because of the large amount of work needed and getting the correct material description. However, this

is sufficient for most cases, except when designing slender columns and thin shell structures where the internal forces are significantly influenced by the deflection of the member. Other cases where nonlinear material behaviour should be taken into account are when:

- optimising the load redistribution of a structure.
- reduction of member forces in case of restraints is needed.
- the member forces of a structure are significantly influenced by the deformation in the ultimate limit state.
- an exact determination of the deformation of a structure is needed.
- analysing structural failures and damages.
- performing post-calculation of tests.

3.3.2 Load

When a load is applied in a finite element model it is distributed to the nodes, which can result in incorrect shear forces. For example, a beam that is divided into three elements and loaded in one case with a uniform distributed load of 10 kN/m and in another case with a concentrated load of 100 kN in the middle of the span gives the same resulting deflection, see Figure 3.2. This is due to the fact that the uniform distributed load is divided into point loads of 50 kN in each of the inner nodes. The concentrated load of 100 kN is also divided into two point loads of 50 kN each in the inner nodes. It should also be noted that the shear force calculated by the FE method is misleading in comparison to the analytical result.

Common for FE programs is that loads on fixed nodes are often neglected which can give an incorrect result. The support force is calculated only by the loads on the unrestrained nodes. This is essential when support forces from one FE analysis is used for loading another member. Fully restrained columns and walls that are loaded are neglected by some software. Furthermore, the choice of element type can have an important role in the load distribution. For example, if a four-noded plate element and an eight-noded plate element is loaded by a uniform distributed load the resulting nodal forces will differ. In the four-noded element all nodal forces will be in the same direction but in the eight-noded element the nodal forces will change direction from node to node, see Figure 3.3.

3.3.3 Discretisation

When creating a numerical model the structure is subdivided into a finite number of different elements. This is called discretisation and most errors occur in this step. These errors are related to the size of the elements, shape functions, supports, occurrence of singularity and kinematic effects which will be described briefly hereafter.

Element size

The size of the elements can have a major effect of the result of an analyses and can give considerably large errors. In regions with high deformations and stress

gradients a sufficiently fine mesh is required to give a satisfying result and accurate design. To perform this an engineering knowledge is required even though many software have automatic meshing tools.

Form functions

The user of a finite element program should have the knowledge that all types of elements cannot be joined together, even if the software allows it. This is because different elements have different shape functions. It is not necessary for the user of a FE program to know about the numerical algorithms and shape functions for which the software is based on. But it is essential that the user know the difference between a beam, a plate and a shell element to be able to make a safe and accurate design of a structure.

Singularity

Singularity is a phenomenon that occurs in numerical models in slabs and shear walls under highly concentrated point loads. It is recognised by infinite stresses and internal forces and is caused by simplifications and assumptions of the element's behaviour. In the real structure singularity will not occur because the concrete will yield or crack by the compression or tensile forces. All though singularities do not need to be considered in the design, the user should be aware of it to be able to make a good interpretation of the result.

Kinematic effects

A structure becomes kinematic when the system of equations has no unique solution. Most FE software will give warnings if this occurs. But it is easily overlooked because of the huge amount of data produced, especially if the force distribution is reasonable. This may result in an improper design of the structure caused by incorrect actions of a kinematic structure.

3.4 Different types of elements

In modelling of a structure, there are different types of elements to represent different structure types. The elements have various properties and behave differently when loaded. Some of the elements used are described in this section, for details see [29].

3.4.1 Beam elements

A beam element is a line element with six degrees of freedom in each node representing rotation and translation in each axis [3], see Figure 3.4. They are suitable to use when modelling a beam in bending, a truss element and a torsion bar. Should not be used for structures with complex geometry, holes and points of stress concentrations. The cross section of a beam element is uniformed and it represents a slender structure [3].

3.4.2 Plate elements

A plate element has no internal normal forces or in-plane deformations. It can be based on Kirchhoff's plate theory and consist of bending moment M_x and M_y , twisting moment M_{xy} and shear forces V_x and V_y , see Figure 3.5. The plate element has three degrees of freedom in each node, see Figure 3.6. A common use are for slabs, since the general assumptions for a slab is that:

- it is thin (depth \ll length)
- the stresses: $\sigma_z = \tau_{xy} = \tau_{yz} = 0$
- the depth is constant
- there are small vertical displacements in first order theory
- there are no strains at the middle plane (no normal or membrane forces)
- stresses in normal direction are negligible
- Bernoulli-Euler's theory about that plane sections remain plane before and after loading is valid.

If normal forces are of interest in a slab a shell element is a better choice.

3.4.3 Plane shell element

A plane shell element has two degrees of freedom in each node for deflection but no degree of freedom for rotation, see Figure 3.7. This element can be used to model columns, but should be done with care since no moment will occur in the column. This may lead to major errors especially if a plane shell element is connected to a beam element which has an extra degree of freedom for rotation, see Figure 3.7.

3.5 Construction stage analysis

A construction stage analysis is performed to look at the force- and stress distributions as well as deformations at different steps in the construction sequence defined by the engineer, usually one step per storey. For high-rise buildings this is a good option because the deflections in the top slabs and columns will otherwise be very large [29].

For a usual FE analysis all self-weight is applied in one step. This causes the elements with lower stiffness, such as columns, to have large deflections compared to the very stiff walls. When constructing a building on site, the deflection on each floor is compensated for, which leads to very small deflections in the top floor. The construction stage analysis performs these step where one storey is constructed at a time and the load on that storey is applied before the next storey is constructed. The engineer have the ability to choose the individual member age of each element and also how long each storey takes to construct. This will affect the deflections and the stress distributions of the building. However, performing a construction stage analysis is a difficult and time consuming task but gives good indications of whether or not creep and shrinkage effect have to be considered in the design of the building [29].

3. Finite element method

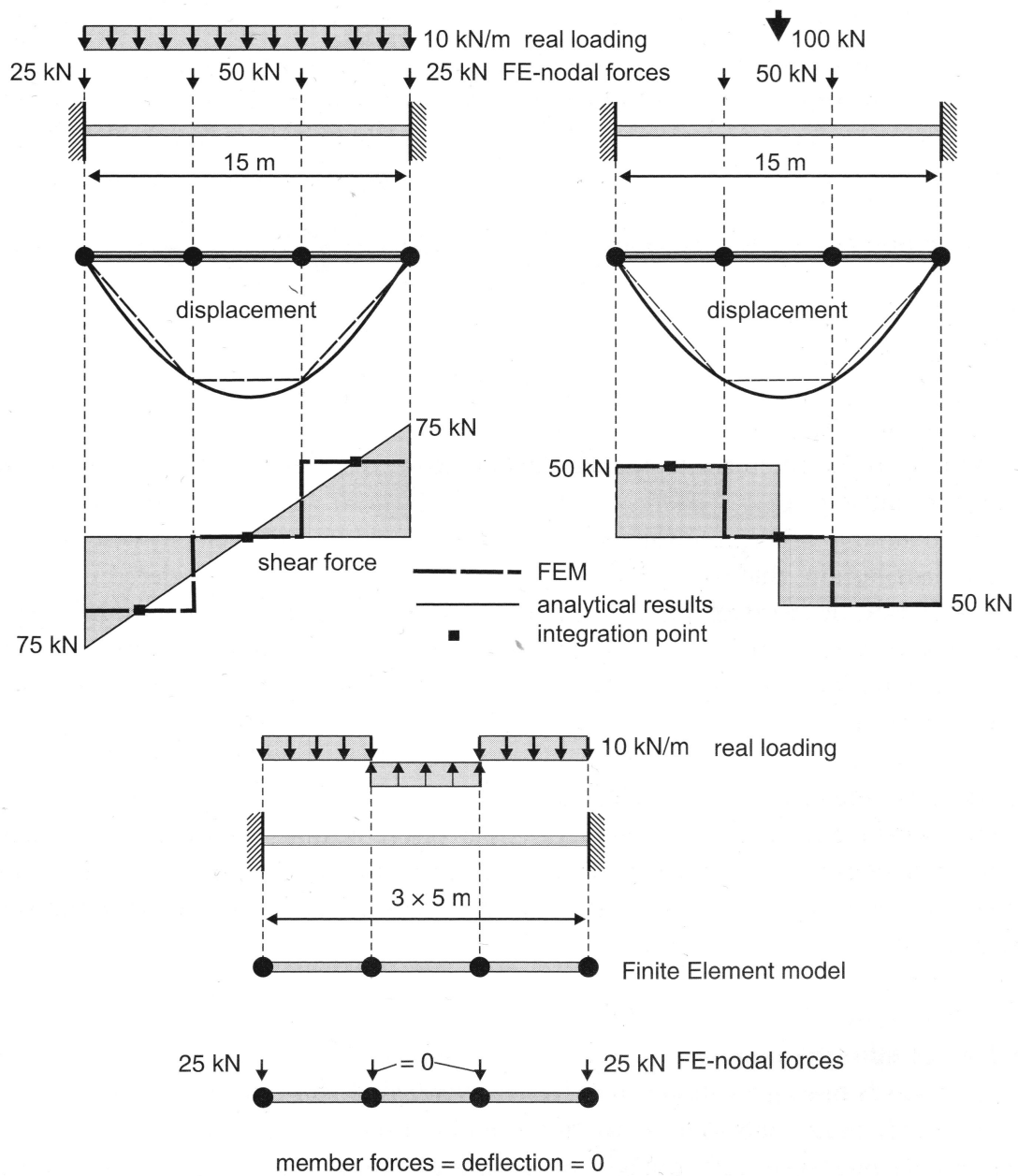


Figure 3.2: A beam divided into three elements and loaded in one case with a uniform distributed load and in another case with a concentrated load in the middle of the span [29].

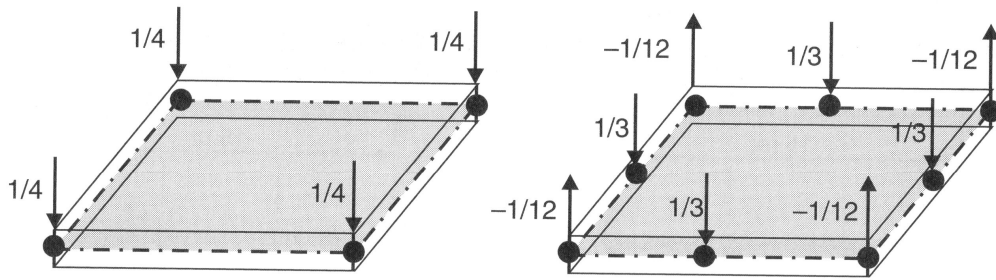


Figure 3.3: Nodal forces in a four-noded plate element and an eight-noded plate element under uniform vertical loading [29].

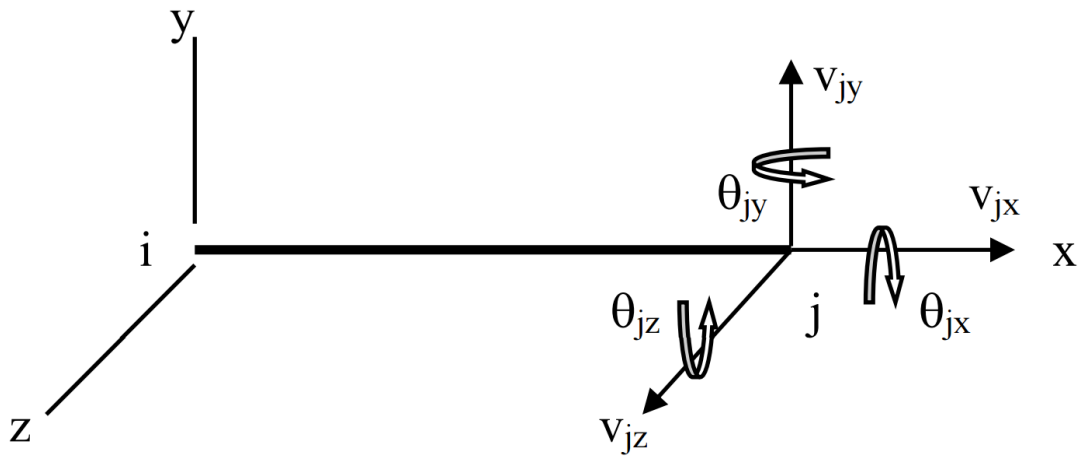


Figure 3.4: Beam element with six degrees of freedom in each node [3].

3. Finite element method

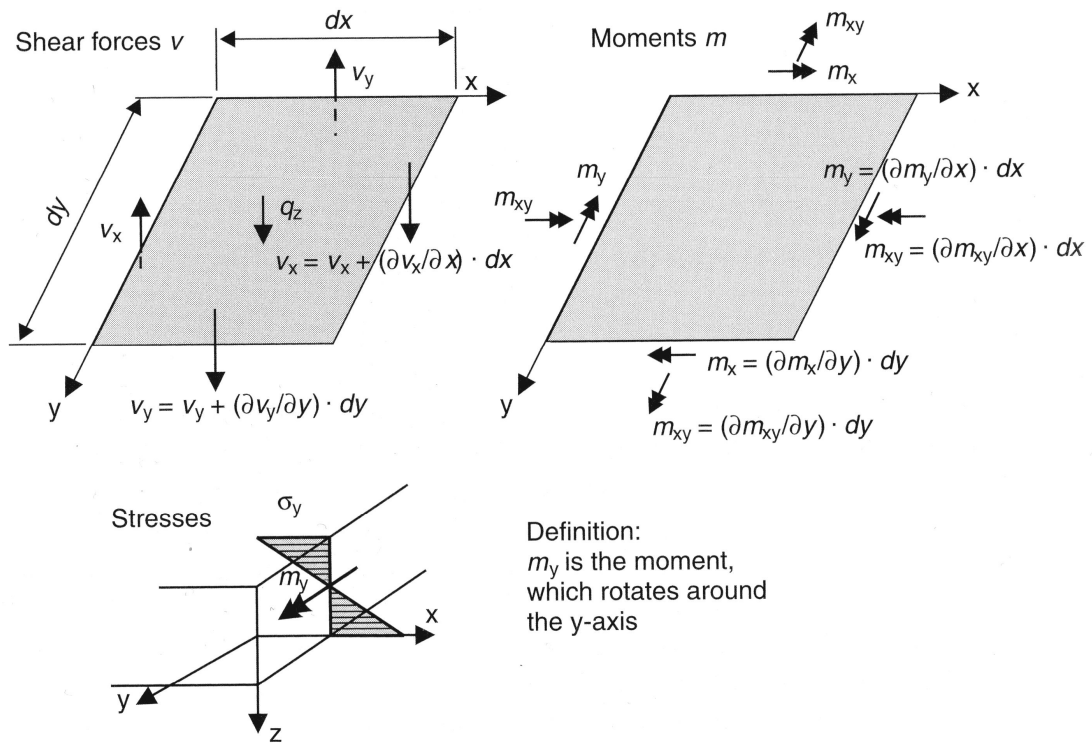


Figure 3.5: Internal actions in a plate element [29].

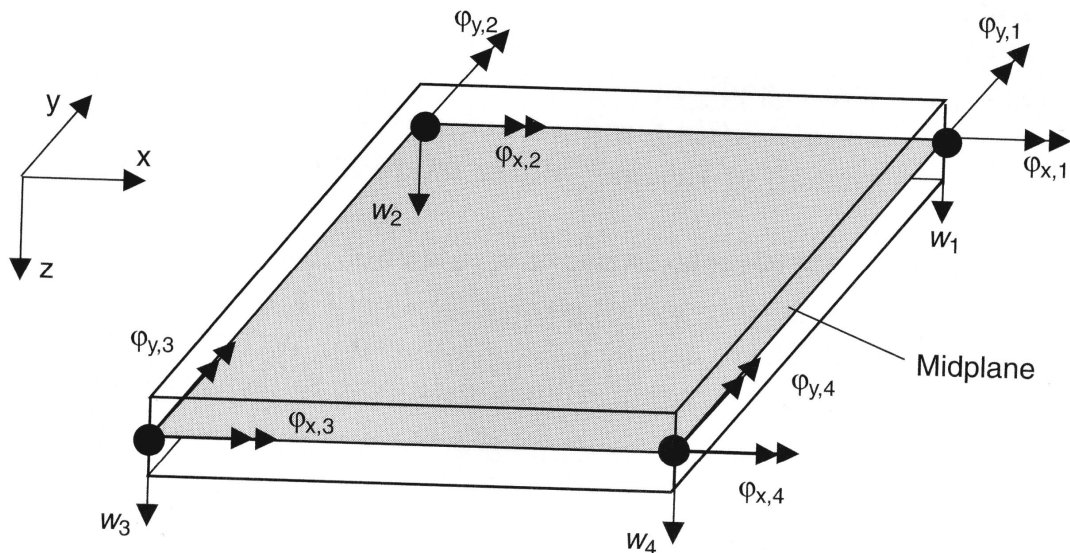


Figure 3.6: Plate element with three degrees of freedom in each node [29].

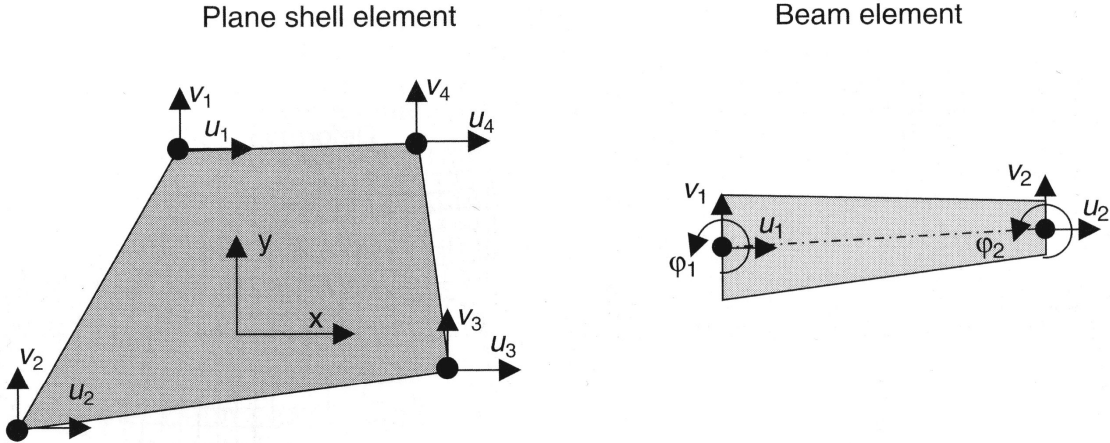


Figure 3.7: Plane shell element with two degrees of freedom in each node and a plane beam element with three degrees of freedom in each node [29].

4 Method

This chapter describes all the different methods used for calculations by hand to verify the FE model.

4.1 Global critical load - Vianello method

To determine the global critical load for a structure different methods exist. The Vianello method will be described in this section since it was used in the thesis. The Vianello method is used to calculate the global critical load for a structure with varying stiffness [28]. It only considers in-plane buckling. In comparison with the Euler method, where a cantilever is fixed in one end and a single concentrated load is applied in the other, the Vianello method is available when there are several stories with different forces acting on each one of them. To calculate the critical load, N_{cr} , the following equation is used

$$N_{cr} = k_v \frac{EI}{L_h^2} \quad (4.1)$$

where:

- E is the Young's modulus
- I is the moment of inertia
- L_h is the total height of the building
- k_v is a factor for the amount of stories

For a case with constant stiffness, EI , along the height of the building and with the same value on the force acting on each storey the value of k_v can be taken directly from Figure 4.1. In cases where the stiffness varies, the factor k_v has to be calculated. This is made by using an iteration process which converges towards a true value. The method is based on the equation for an elastic line

$$EI_x v'' + M_x = 0 \quad (4.2)$$

where:

- E is the Young's modulus
- I_x is the moment of inertia
- v'' is the curvature
- M_x is the moment

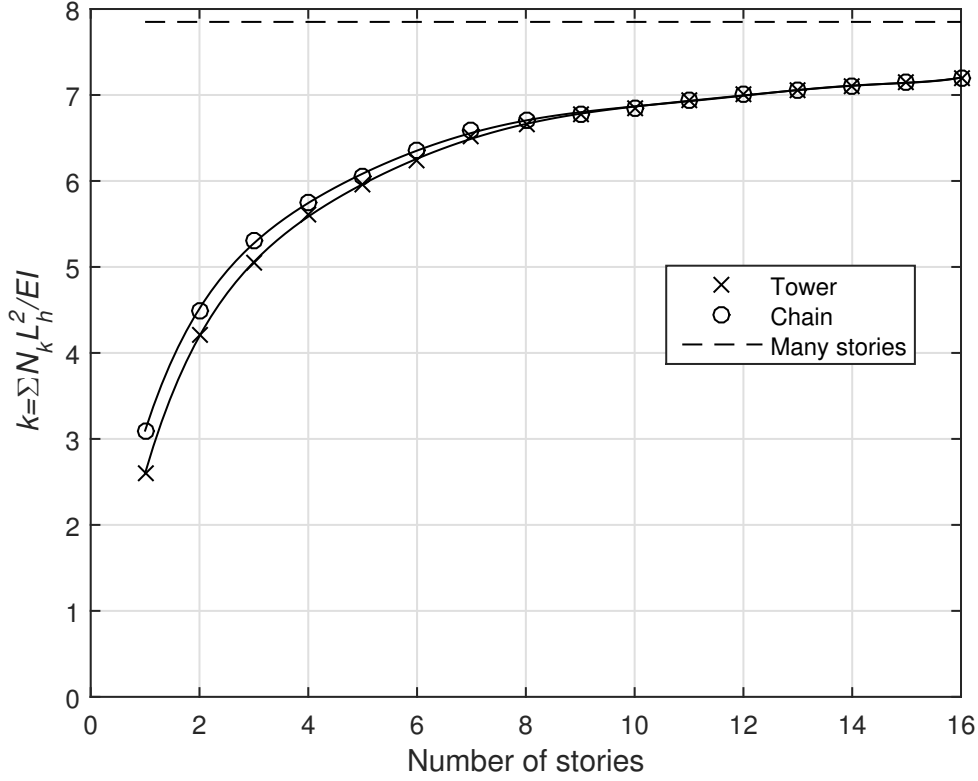


Figure 4.1: Factor k_v for buildings with constant stiffness and with the same force on each storey [22].

The steps to calculate the global critical load are as follows

1. Assume a function for the initial deflection, $v_a(x)$, for the building.
2. Divide the structure into elements and assign their respective stiffness, EI_x and force, P . Smaller elements give a more accurate result.
3. Calculate the moment acting on each element, $M_x = \sum P v_a$. Note that the method only considers vertical forces and neglects all horizontal forces acting on the building.
4. Calculate the curvature, v'' , using Equation 4.2

$$v'' = -\frac{M_x}{EI_x} \quad (4.3)$$

5. Integrate the curvature two times to get a new deflection for the building. First integration of the curvature gives the angle

$$v' = -\sum_0^x \left(\frac{M_x}{EI_x} \right) \Delta x + C1 \quad (4.4)$$

Integration of the angle provides the new deflection

$$v_{calc} = \sum_0^x v' \Delta x + C2 \quad (4.5)$$

where $C1$ and $C2$ are integration constants which have to be decided depending on the boundary conditions. For the case with a fixed cantilever the deflection and the angle is zero at the ground, $v(0) = 0$ and $v'(0) = 0$.

6. Compare the initial deflection with the new deflection

$$s = \frac{\sum v_a}{\sum v_{calc}} \quad (4.6)$$

v_{calc} is then normalised and set to v_a and the process is repeated until s converges. This usually takes around three iterations. Then, the critical load factor can be calculated as

$$k_v = ns = n \frac{\sum v_a}{\sum v_{calc}} \quad (4.7)$$

where:

n is the number of stories

4.2 Wind-load

As earlier mentioned, a buildings response from wind-load is in the along- and across wind direction as well as rotation around the vertical axis, see Figure 2.10. In this section the along- and across wind response is evaluated.

In this section the Eurocode standard [31] has been followed since the purpose of these calculations are to compare the results with an FE analysis based on the Eurocode standard.

4.2.1 Static wind-load

When analysing the wind-load actions on a building the first step is to determine the static wind-load effects. To do this the peak velocity pressure, $q_p(z)$, on each floor of the building is calculated. This is done with Equation 4.8.

$$q_p(z) = [1 + 7l_v(z)] \frac{1}{2} \rho v_m^2(z) \quad (4.8)$$

where:

$l_v(z)$ is the wind turbulence according to Equation 4.9

ρ is the air density

$v_m(z)$ is the mean wind velocity at height z according to Equation 4.12

z is the height of the structure

$$l_v(z) = \begin{cases} \frac{\sigma_v}{v_m(z)} = \frac{k_t}{c_0(z) \ln\left(\frac{z}{z_0}\right)} & \text{if } z_{min} \leq z \leq z_{max} \\ l_v(z_{min}) & \text{if } z \leq z_{min} \end{cases} \quad (4.9)$$

4. Method

where:

σ_v	is the standard deviation of turbulence according to Equation 4.10
k_l	is the turbulence factor
$c_0(z)$	is the orography factor = 1.0, if nothing else is given in clause 4.3.3 in Eurocode [31]
z_0	is the roughness length
z_{min}	is the minimum height
z_{max}	is 200 meters

$$\sigma_v = k_r v_b k_l \quad (4.10)$$

where:

k_r	is the terrain factor according to Equation 4.11
v_b	is the basic wind velocity

$$k_r = 0.19 \left(\frac{z_0}{z_{0,II}} \right)^{0.07}, \quad z_{0,II} = 0.05 \quad (4.11)$$

$$v_m(z) = c_r(z) c_0(z) v_b \quad (4.12)$$

where:

$c_r(z)$	is the terrain roughness factor according to Equation 4.13
----------	--

$$c_r(z) = k_r \ln \left(\frac{z}{z_0} \right) \quad (4.13)$$

When the peak velocity pressure is determined the wind force, F_w , on each floor can be calculated according to Equation 4.14.

$$F_w = c_s c_f q_p(z_e) A_{ref} \quad (4.14)$$

where:

c_s	is the size factor according to Equation 4.15
c_f	is the force coefficient according to Equation 4.16
A_{ref}	is the reference area for each floor

$$c_s = \frac{1 + 7l_v(z_s)\sqrt{B^2}}{1 + 7l_v(z_s)} \quad (4.15)$$

where:

z_s	is the reference height, $z_s = 0.6h$ for vertical extracted structures e.q. buildings
B^2	is the background factor according to Equation 4.18

$$c_f = c_{f,0} \Psi_r \Psi_\lambda \quad (4.16)$$

where:

- $c_{f,0}$ is the force coefficient according to Equation 4.17
- Ψ_r is the reduction factor for square sections with rounded corners
- Ψ_λ is the end effect factor

$$c_{f,0} = \begin{cases} 2.0 & \text{if } d/b \leq 0.2 \\ 0.3193 \ln(d/b) + 2.5139 & \text{if } 0.1 \leq d/b \leq 0.7 \\ -0.7121 \ln(d/b) + 2.1460 & \text{if } 0.7 \leq d/b \leq 5.0 \\ -0.1443 \ln(d/b) + 1.2322 & \text{if } 5.0 \leq d/b \leq 10.0 \\ 0.9 & \text{if } 10.0 \leq d/b \end{cases} \quad (4.17)$$

where:

- d is the depth of the structure
- b is the width of the structure

$$B^2 = \frac{1}{1 + 0.9 \left(\frac{b+h}{L(z_s)} \right)^{0.63}} \quad (4.18)$$

where:

- h is the height of the structure
- $L(z_s)$ is the turbulent scale length according to Equation 4.19

$$L(z_s) = \begin{cases} L_t \left(\frac{z}{z_t} \right)^\alpha & \text{if } z \geq z_{min} \\ L(z_{min}) & \text{if } z < z_{min} \end{cases} \quad (4.19)$$

where:

- L_t is the reference length $L_t = 300$ meters
- z_t is the reference length $z_t = 200$ meters
- $\alpha = 0.67 + 0.05 \ln(z_0)$

With the force, F_w , known the static overturning moment can be determined.

4.2.2 Dynamic wind-load

When calculating the overturning moment from dynamic wind-load an extra coefficient, c_d , is applied to Equation 4.14 when calculating the wind force on each floor, see Equation 4.20.

$$F_w = c_s c_d c_f q_p(z_s) A_{ref} \quad (4.20)$$

where:

- c_s is the size factor according to Equation 4.15
- c_d is the dynamic factor according to Equation 4.21
- c_f is the force coefficient according to Equation 4.16
- $q_p(z_s)$ is the peak velocity pressure according to Equation 4.8

4. Method

z_s is the reference height, $z_s = 0.6h$ for vertical extracted structures
 e.g. buildings
 A_{ref} is the reference area for each floor

$$c_d = \frac{1 + 2k_p l_v(z_s) \sqrt{B^2 + R^2}}{1 + 7l_v(z_s) \sqrt{B^2}} \quad (4.21)$$

where:

k_p is the peak factor according to Equation 4.22
 $l_v(z)$ is the wind turbulence according to Equation 4.9
 B^2 is the background factor according to Equation 4.18
 R^2 is the resonance response factor according to Equation 4.24

$$k_p = \max \left(\sqrt{2 \ln(vT)} + \frac{0.6}{\sqrt{2 \ln(vT)}}; 3 \right) \quad (4.22)$$

where:

v is the up-crossing frequency according to Equation 4.23
 T is the averaging time for the mean wind velocity, $T = 600$ seconds

$$v = n_{1,x} \sqrt{\frac{R^2}{B^2 + R^2}} \quad ; \quad v \geq 0.08 \text{ Hz} \quad (4.23)$$

where:

$n_{1,x}$ is the fundamental frequency of the structure

$$R^2 = \frac{\pi^2}{2\delta} S_L(z_s, n_{1,x}) R_h(\eta_h) R_b(\eta_b) \quad (4.24)$$

where:

$S_L(z_s, n_{1,x})$ is the non-dimensional power spectral density
 function according to Equation 4.25
 $R_h(\eta_h), R_b(\eta_b)$ is the aerodynamic admittance functions according
 to Equations 4.28 and 4.29
 δ is the total logarithmic decrement of damping
 according to Equation 4.30

$$S_L(z, n) = \frac{n S_v(z, n)}{\sigma_v^2} = \frac{6.8 f_L(z, n)}{(1 + 10.2 f_L(z, n))^{5/3}} \quad (4.25)$$

where:

n is the frequency with $n = n_{1,x}$ as the fundamental frequency of the structure
 $S_v(z, n)$ is the one-sided variance spectrum
 z is the height of the structure
 σ_v is the standard deviation of turbulence according to

Equation 4.10

$f_L(z, n)$ is a non-dimensional frequency according to Equation 4.26

$$f_L(z, n) = \frac{nL(z)}{v_m(z)} \quad (4.26)$$

where:

$L(z)$ is the turbulence length scale

$v_m(z)$ is the mean wind velocity at height z according to Equation 4.12

For buildings higher than 50 stories the fundamental frequency can be estimated with Equation 4.27

$$n_1 = \frac{46}{h} \quad (4.27)$$

The aerodynamic admittance functions are calculated as

$$R_h = \frac{1}{\eta_h} - \frac{1}{2\eta_h^2}(1 - e^{-2\eta_h}) \quad (4.28)$$

$$R_b = \frac{1}{\eta_b} - \frac{1}{2\eta_b^2}(1 - e^{-2\eta_b}) \quad (4.29)$$

where:

$$\eta_h = \frac{4.6h}{L(z_s)} f_L(z_s, n_{1,x})$$

$$\eta_b = \frac{4.6b}{L(z_s)} f_L(z_s, n_{1,x})$$

The total logarithmic decrement of damping is then calculated as

$$\delta = \delta_s + \delta_a + \delta_d \quad (4.30)$$

where:

δ_s is the logarithmic decrement of structural damping

δ_a is the logarithmic decrement of aerodynamic damping for the fundamental mode according to Equation 4.31, given that the modal deflection $\phi(y, z)$ is constant

δ_d is the logarithmic decrement of damping due to special devices

$$\delta_a = \frac{c_f \rho b v_m(z_s)}{2n_1 m_e} \quad (4.31)$$

With the new dynamic force, F_w , known the overturning moment from dynamic wind-load can be determined.

4.2.3 Along-wind response

The along-wind acceleration of a building can be calculated with Equation 4.32.

$$\ddot{X}_{max}(z) = k_p \sigma_{a,x}(z) \quad (4.32)$$

where:

- k_p is the peak factor according to Equation 4.22
- $\sigma_{a,x}(z)$ is the standard deviation of the characteristic along-wind acceleration according to Equation 4.33
- z is the height of the structure

$$\sigma_{a,x}(z) = \frac{c_f \rho b l_v(z_s) v_{m,s}^2(z_s)}{m_{1,x}} R K_x \phi_{1,x}(z) \quad (4.33)$$

where:

- c_f is the force coefficient according to Equation 4.16
- ρ is the air density
- b is the with of the structure
- $l_v(z_s)$ is the wind turbulence according to Equation 4.9
- z_s is the reference height, $z_s = 0.6h$ for vertical extracted structures
- $v_{m,s}(z_s)$ is the characteristic mean wind velocity at height z_s for a 5 year return period according to Equation 4.36
- R is the square root of the resonance response, Equation 4.24
- K_x is the aerodynamic damping parameter according to Equation 4.34
- $\phi_{1,x}(z)$ is the fundamental along wind modal shape according to Equation 4.35
- $m_{1,x}$ is the along wind fundamental equivalent mass

$$K_x = \frac{(2\zeta + 1) \left\{ (\zeta + 1) \left[\ln \left(\frac{z_s}{z_0} \right) + 0.5 \right] - 1 \right\}}{(\zeta + 1)^2 \ln \left(\frac{z_s}{z_0} \right)} \quad (4.34)$$

where:

- ζ is the exponent of the mode shape
- z_0 is the roughness length

The fundamental along-wind modal shape is calculated as

$$\phi_{1,x}(z) = \left(\frac{z}{h} \right)^\zeta \quad (4.35)$$

where:

- h is the height of the structure
- ζ is set to 1 for buildings with a central core with peripheral columns or larger columns with shear bracing

The characteristic mean wind velocity for a reduction of the return period according to the Swedish national annex [6] is calculated as

$$v_{m,s} = 0.75v_{50}\sqrt{1 - 0.2 \ln\left(-\ln\left(1 - \frac{1}{T_a}\right)\right)} \quad (4.36)$$

where:

- v_{50} is the basic wind velocity
- T_a is the number of years

The calculated accelerations should then be compared to national annex guidelines [33].

4.2.4 Across-wind response

Generally the maximum wind-load and deflection of a building occurs in the along-wind direction. However, the maximum acceleration often occurs in the across-wind direction [34]. This occurs especially when the building is slender about both axis with a ratio of $\sqrt{WD}/H < 1/3$, where W is the width, D is the depth and H is the height of the structure [34]. The Eurocode standard does not give any regulations on how to calculate the across-wind response. However, Stafford Smith & Coull [34] in the National Building Code of Canada (NBCC) gives a suggestion on how to consider this, although it is very difficult to predict the outcome. This due to the fact that many parameters affects the across-wind response. Parameters like the buildings geometry, density, structural damping, turbulence, operating reduced frequency range and interference from upstream buildings [34]. The best way to determine the across-wind response is from wind tunnel tests [34].

However, the peak acceleration at the top of a building can be predicted with Equation 4.37 [34].

$$a_w = n_0^2 g_p [WD]^{1/2} \left(\frac{a_r}{\rho g \sqrt{\beta}} \right) \quad (4.37)$$

$$a_r = 78.5 \cdot 10^{-3} [V_H / (n_0 \sqrt{WD})]^{3.3}$$

where:

- a_w is the peak acceleration at the top of the building
- n_0 is the estimated fundamental frequency
- g_p is the peak factor according to Figure 4.2
- W is the width of the building
- D is the depth of the building
- ρ is the average building density
- g is the acceleration due to gravity
- β is the estimated critical damping ratio
- V_H is the mean wind speed at top of building

$$v = \frac{n_0}{\sqrt{(1 + B/R)}} \quad (4.38)$$

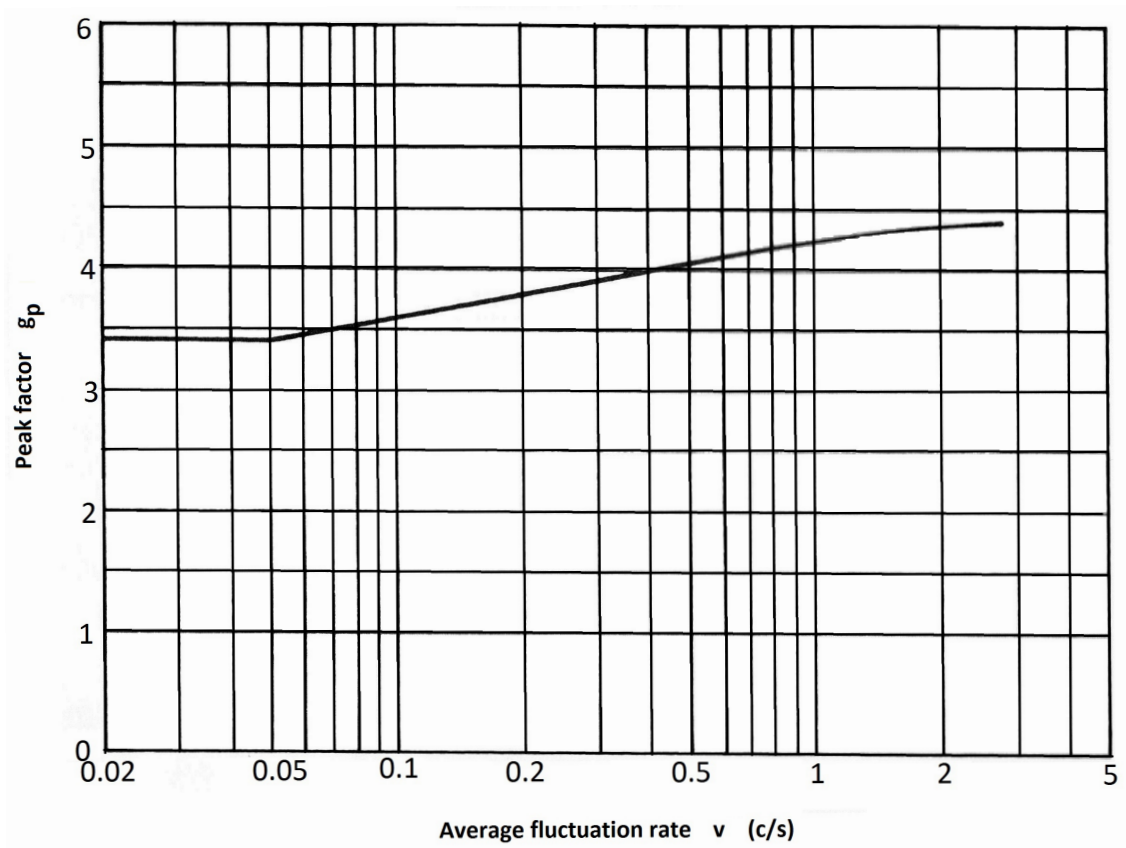


Figure 4.2: Variation of peak factor with average fluctuation rate v [34], which can be calculated with Equation 4.38.

where:

- B is the background factor according to Equation 4.18 or Figure 4.3
- R is the resonance response factor according to Equation 4.24 or 4.39

$$R = \frac{SF}{\beta} \quad (4.39)$$

where:

- S is the size reduction factor according to Figure 4.4
- F is the gust energy ratio according to Figure 4.5

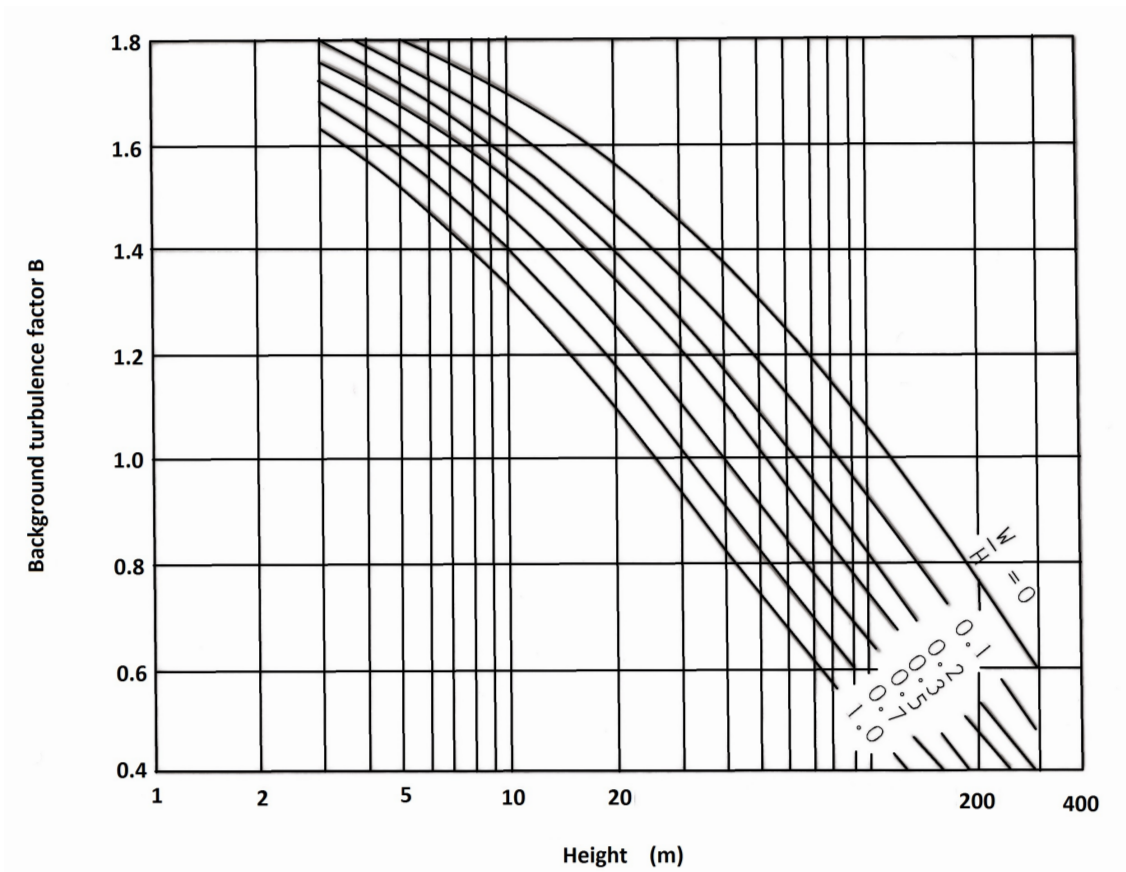


Figure 4.3: Variation of background turbulence factor [34].

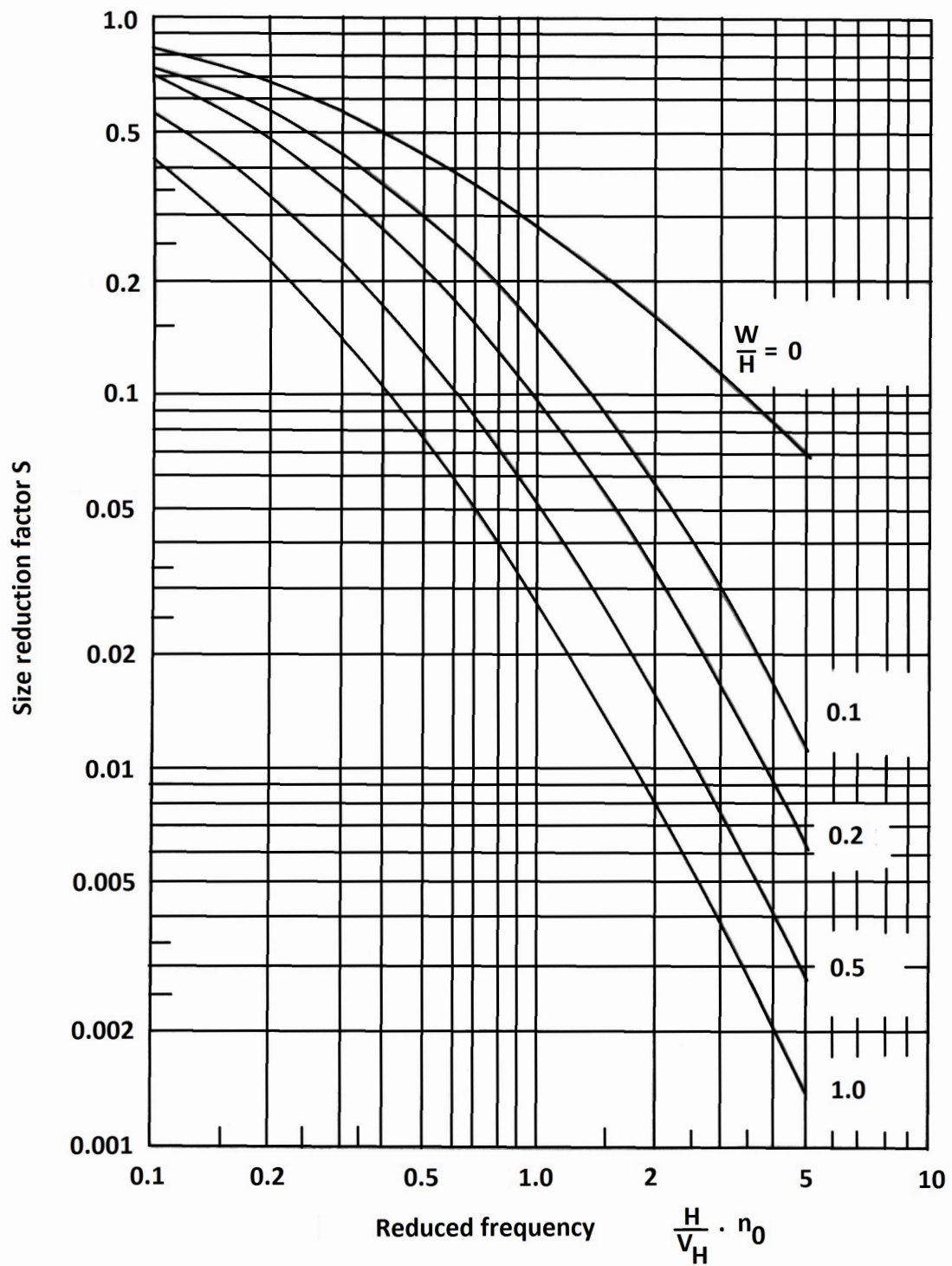


Figure 4.4: Variation of size reduction factor [34].

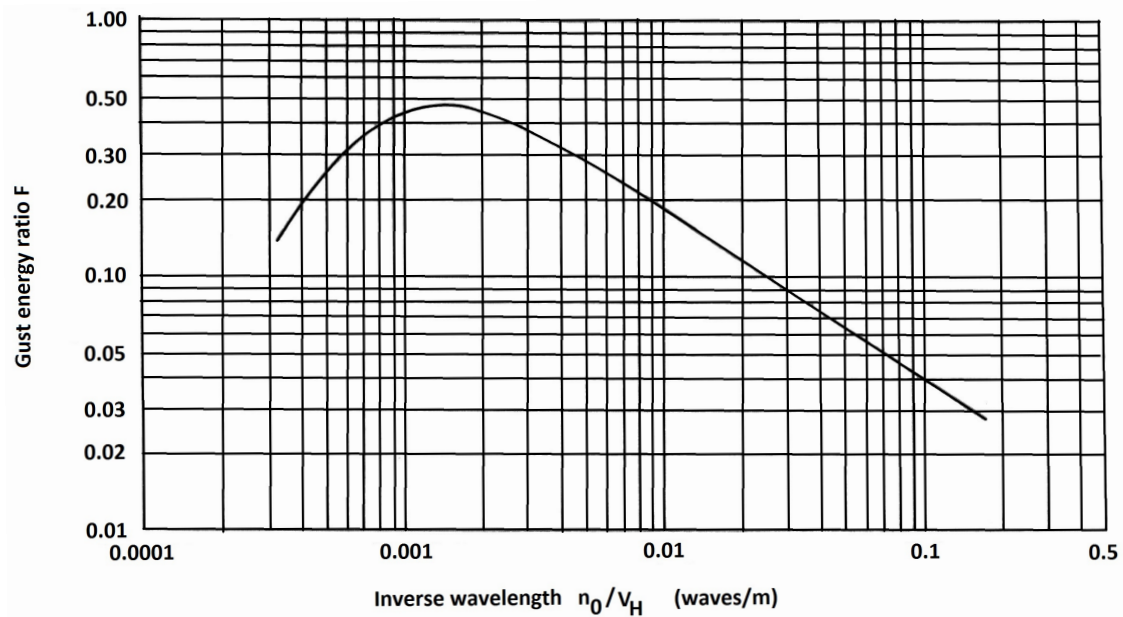


Figure 4.5: Variation of gust energy ratio [34].

4.3 Empirical methods to determine the fundamental frequency

When designing a high-rise building the actions from motions and vibrations has to be considered. To do this the fundamental frequency of the building has to be estimated in an early design stage. This can be difficult if the structural form has not been decided in detail. As mentioned earlier, a method to estimate the fundamental frequency is presented in Eurocode [31], as shown in Equation 4.27. Stafford Smith & Coull [34] present some different equations to estimate the fundamental frequency. These are presented in Equations 4.40–4.43 and are applicable to different kinds of structural systems.

$$n_0 = \frac{\sqrt{D}}{0.091H} \quad (4.40)$$

Equation 4.40 is suggested to be used for reinforced concrete shear wall buildings and braced steel frames where D is the depth and H is the height of the structure in meters [34].

$$n_0 = \frac{10}{N} \quad (4.41)$$

For structural systems where the lateral forces are resisted entirely by space frames Equation 4.41 can be used where N is the number of stories in the building [34]. A requirement to use this formula is that the space frames are not enclosed or adjoined by more rigid elements that would prevent the frames from resisting lateral forces.

Studies have been made regarding Equations 4.40 and 4.41 with the result that these could give an error of $\pm 50\%$ [34]. Another method for estimating the fundamental frequency is presented in Equation 4.42.

$$n_0 = \frac{1}{C_T H^{3/4}} \quad (4.42)$$

Equation 4.42 can be used when moment resisting frames are the only lateral load resisting element in the structure [34]. Where C_T is equal to 0.035 or 0.025 for steel and concrete structures respectively and H is the height of the building in feet. Evaluations of the first equations for fundamental frequencies have been made. This together with measurements of the fundamental frequencies of 163 buildings with rectangular shape have resulted in Equation 4.43, where H is the height of the building in meters [34].

$$n_0 = \frac{46}{H} \quad (4.43)$$

Equation 4.43 is the same equation as the equation presented in Eurocode for estimating the fundamental frequency. Similar studies have been made for estimating the first orthogonal translational mode and the first torsional mode which has resulted in similar equations. The frequency for the first orthogonal translational mode can be estimated with Equation 4.44 and the frequency for the first torsional mode can be estimated with Equation 4.45 where H is the height of the building in meters [34].

$$n_1 = \frac{58}{H} \quad (4.44)$$

$$n_2 = \frac{72}{H} \quad (4.45)$$

A more accurate equation for estimating the fundamental frequency is presented in Equation 4.46. This equation cannot, however, be used until the preliminary design is made and the stiffness of the structure is known [34].

$$n_0 = \frac{1}{2\pi} \left(\frac{g \sum F_i u_i}{\sum W_i u_i^2} \right)^{1/2} \quad (4.46)$$

where:

- g is the acceleration due to gravity
- F_i is the equivalent lateral load at the floor levels
- u_i is the calculated static horizontal deflection at level i
- W_i is the weight of floor i

4.4 Forces between elements in a prefabricated concrete core

When constructing with prefabricated concrete elements the forces between the elements have to be considered to design the connections. Evaluating these forces

can be a difficult task, but they can be estimated by calculating the shear flow in the structure. It is possible in FE software as Midas Gen to calculate the linear-elastic shear flow in a structure. An experiment to validate this method was carried out with a simple C-beam with the outcome presented in Appendix L.

Concrete, however, is not a linear-elastic material and to calculate the shear flow in concrete Eurocode [32] presents the following equation

$$v_{Ed} = \frac{\beta V_{Ed}}{zb} \quad (4.47)$$

where:

- v_{Ed} is the shear stress
- β is the factor between the along force in the new concrete and the total along force, in compressive or tensile zone, calculated for actual cut
- V is the shear force
- z is the composite cross section internal lever
- b is the width

5 Case study in Midas Gen

In this chapter the building used in the case study is described with geometry and how the 3D FE model was composed.

5.1 Midas Gen elements

Different models have been assembled in Midas Gen. One model have been using the unique Midas Gen wall element, which consists of two subtypes: membrane and plate. The other model have been meshed with plate elements. Both the wall elements have in-plane stiffness and a rotational stiffness about the vertical axis. The wall-plate element has an out-of-plane bending stiffness which makes the difference between the two types [24]. When performing an FE analysis with wall elements in Midas Gen, the software creates stories at each level of nodes in the model in the story data. If an element for some reason needs to be divided, it is of importance for the user to manually update the stories or the result will have huge errors. The plate element used in the meshed model have five degrees of freedom in each node, two for rotation and three for deflection. The rotation about the z-axis is the difference between a plate element and a shell element with six degrees of freedom in each node.

5.2 Description of Göteborg City Gate

A case study has been performed on Göteborg City Gate (GCG), see Figure 5.1. In this Masters thesis only the high-rise part of the building is considered. This building was yet to be built when the Masters thesis was conducted. The high-rise building contains 31 stories with two concrete cores built with shear walls functioning as staircases and elevator shafts. The dimensions and stiffness changes at two levels in the building, at 27.3 meters and at 83.7 meters up in the building. At the second change the smaller core ends and two columns are placed on top of the core, see Figure 5.2. The total height above the ground of the building is 120.8 meters. The concrete cores and columns are modelled with concrete of quality C40/50 and the deck as hollow-core slabs. The geometry of the building can be found in Appendix A.

5.2.1 Geometry

As mentioned, the building contains of three different levels. At each level the dimensions of the vertical load-bearing elements are changed. The first level reaches



Figure 5.1: Rendered image of Göteborg City Gate [8].

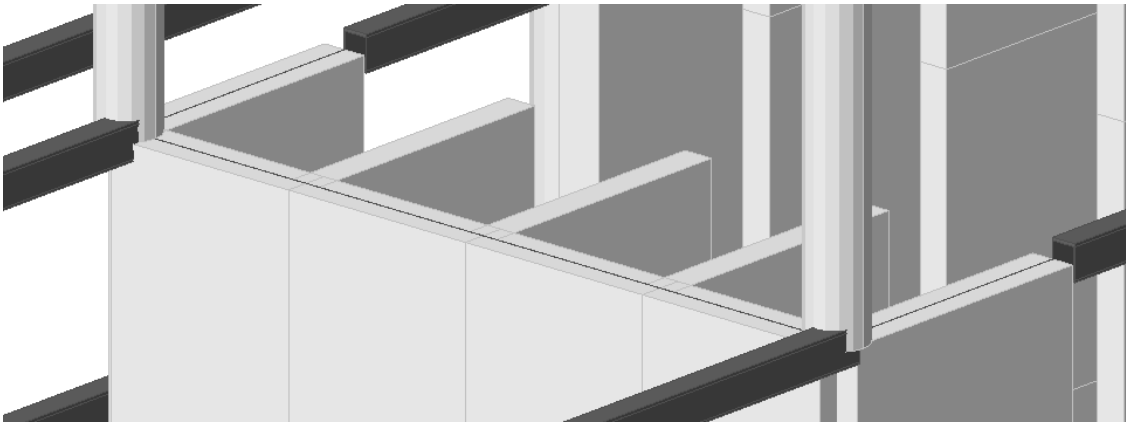


Figure 5.2: End of the smaller concrete core at height 83.7 meters, where two columns are placed on top.

from the bottom, -9 meters, up to 27.3 meters. The second level starts at 27.3 meters and continues up to 83.7 meters where the smaller core ends. The third and last level reaches from 83.7 meters up to the top of the building at 120.8 meters. The walls in the first level has a thickness of 0.55 meters and the columns are circular with a diameter of 1 meter. In the second level the thickness of the walls are 0.45 meters and the diameter of the columns are 0.8 meters. For the third level the thickness of the walls are 0.35 meters and the diameter of the columns are 0.6 meters. Common for the entire building are the walls in the elevator shafts which have a thickness of 0.3 meters for the whole length, for detailed floor plans see Appendix A. The slab, in the meshed models, are modelled with plate elements with a thickness of 0.148 meters to correspond to the floor load applied in the models with wall elements of 3.7 kN/m^2 . The floor load is applied in the model with wall elements since no slab is modelled but floor diaphragms are used for in-plane stiffness.

Different variations of the model have been used in the Masters thesis. The difference between the models have been the connections between the cores, the consideration

Table 5.1: Material properties.

Material	Density [kN/m ³]	Young's modulus [GPa]	Poisson's ratio
Steel, S450	77	210	0.3
Concrete, C40/50	25	35	0.2

Table 5.2: Initial conditions for Göteborg City Gate.

Type	Condition
Location	Göteborg
Terrain class	III
Reference wind-speed	25 m/s
Self-weight, hollow-core slab	3.7 kN/m ²

of floor diaphragms or not, whether construction stage analysis is considered or not and the use of different element types described in Section 5.1. The initial conditions for GCG are shown in Table 5.2, the material properties are described in Table 5.1 and for more details about the element cross sections and floor plans, see Appendix A.

5.2.2 Modelling

In the models with the element type walls, the feature floor diaphragm is used to simulate a slab. The floor diaphragm works as a rigid link where each node in each storey are linked to a master node located in or close to the stories' centre of mass. The nodes linked to the master node are called slave nodes. The stiffness of the diaphragms are close to infinitely stiff, to simulate a slab transferring the lateral loads to the vertical elements. The diaphragms only transfers axial force and no out-of-plane shear or bending. For the meshed models there is no need for floor diaphragms since the slab is meshed with plate elements and have stiffness, both in-plane and out-of-plane bending, and connects all nodes in the plane. This provides stiffness in-plane and the load can be transferred to the vertical elements. A general modelling feature that is unchanged for all models are the connections between the columns and all beams except those running between the two cores. These connections are modelled as hinged in order to avoid statically indeterminate load distributions.

Cumulative load distribution

For analysing the cumulative load distribution and comparing to the calculations made by hand a model with wall elements for the concrete core was used. In addition, the hollow core slabs were modelled as one-way floor loads to give a correct representation. The models was analysed with and without floor diaphragms to show the discrepancies.

Eigenfrequency analysis

For the eigenfrequency analysis of the structure, all models were analysed in order to determine the discrepancies between them. For all models where a floor load was used to simulate the slab, the self-weight had to be changed to get the correct mass of the building when performing the eigenfrequency analysis. This due to the fact that the floor load acting on the building is not a mass but a load and will therefore not be including in the eigenvalue analysis resulting in higher eigenfrequencies. A modification on the weight property was made where the density of the materials was increased to get the total weight included.

Forces between elements in a prefabricated concrete core

When analysing the forces between elements in the the concrete cores two models were used. One meshed model where linear-elastic shear flow was calculated and one model with wall elements where the shear flow was calculated from the shear forces according to Eurocode, Equation 4.47. These models were then compared to evaluate if the equation in Eurocode is reliable. In the models, three cuts in the cores at different heights were checked, placed at heights 21.3, 60 and 90 meters, one cut for each change in the buildings cross-section. The first model that was analysed was a meshed model where the elements were of plate type with sizes of one meter each. The shear flow was here given as linear-elastic in the same way as for the C-beam in Appendix L, as F_{xy} [kN/m]. The second model used for analysis was composed with wall elements of subtype membrane. The shear forces was given for each wall respectively and with a modification of Equation 4.47 the shear flow was calculated as

$$F_{xy} = \frac{\beta V}{z} \quad (5.1)$$

The shear flow is calculated with both a maximum and minimum value of the internal lever arm, z , which for a concrete cross section is somewhere between $0.67h$ and h depending on acting forces and moments, where h is the height of the cross section. The minimum and maximum value of the lever arm is taken from the stress distribution of a beam exposed for bending. If all the compression is taken just at the upper part and all tension at the lower part the distance is almost equally to the height of the cross section, see Figure 5.3. If however, the stress distribution is evenly spread over the cross section the distance of z will be two-thirds of the total height, see Figure 5.4.

Global buckling

The global buckling analysis in Midas Gen is only applicable on meshed models and was performed on two models with quadratic and triangular plate elements with size three and one meter, respectively. Both the concrete walls and slabs were meshed using these models. Furthermore, the analysis was performed without floor diaphragms. The loads applied to the structure was only self-weight to get a critical load factor to be compared with the other critical load analyses.

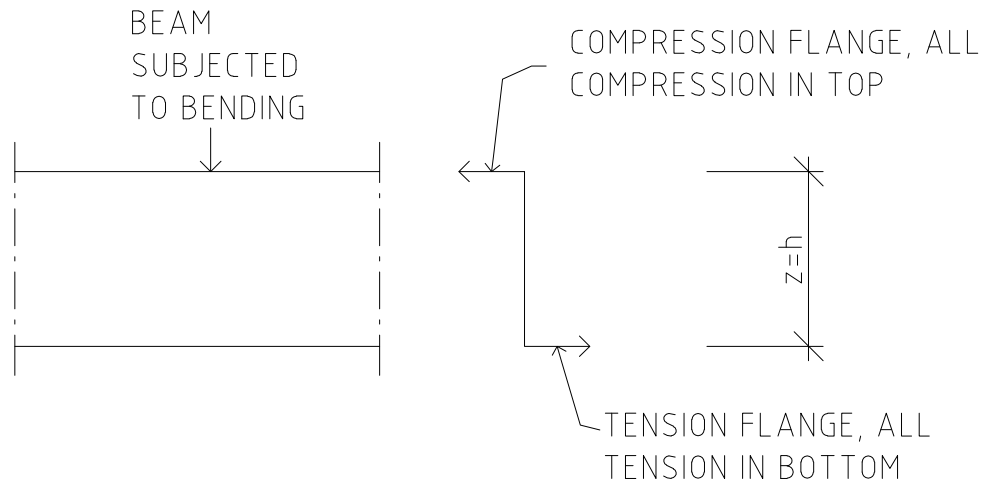


Figure 5.3: Calculation model for maximum value on the internal lever arm, z .

P-delta

Two different P-delta analyses were performed. One with wall elements, subtype plate, and the other with wall elements, subtype membrane. No wind-load was applied in order to get a comparable result with the other critical load analyses. To find the critical load factor, the load factor was increased until the model where unstable and did not converge, which meant that the critical load factor was found.

Construction stage analysis

The constructions stage analysis was constructed by adding the elements storey by storey. This was done on two different models, one where the floor diaphragms were added directly for each storey and the other where the floor diaphragms were added at the end. Both models had no connection between the concrete cores and only vertical actions were considered.

5.3 Example case

In order to investigate how the different connections between the concrete cores affects the force distribution, an example case was used. The example case was modelled with wall elements with a dimension of three times four meters and a thickness of 0.55 meters, see Figure 5.5. The total height of the walls are 12 meters and the distance between them are four meters.

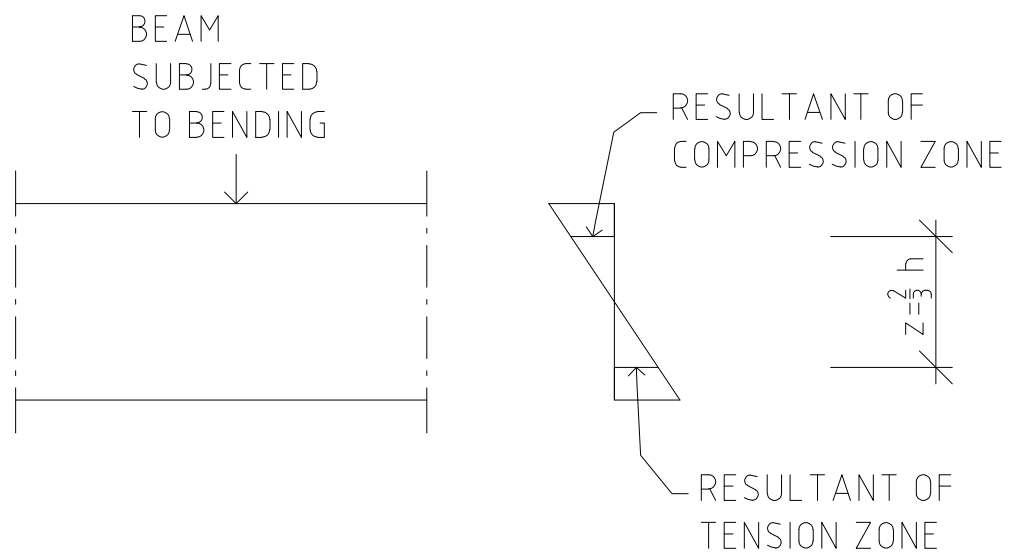


Figure 5.4: Calculation model for minimum value on the internal lever arm, z .

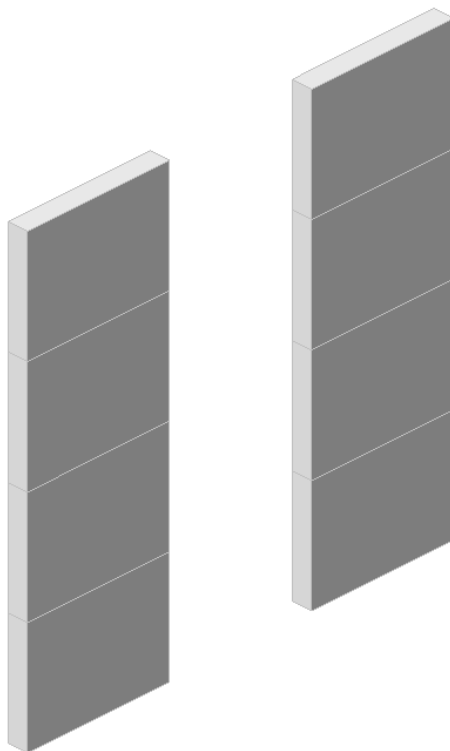


Figure 5.5: Example model to illustrate the effect of floor diaphragms between cores.

6 Results

In this chapter the results from the different FE analyses and calculations made by hand will be presented.

6.1 Analysis of Göteborg City Gate for vertical and horizontal loads

In this section the result for the force distributions are presented for the building with the comparison of considering floor diaphragms and by not considering it. For the models of Göteborg City Gate (GCG) there are no beams connecting the concrete cores in the structure when studying the effect from vertical and horizontal loading. This makes the force and moment distributions between the concrete cores very clear.

6.1.1 Vertical load

For the vertical load case, the structure is exposed to self-weight and load from the hollow-core slabs. The results are shown in Figure 6.1 and Figure 6.2. The shear force between the cores at the end of the smaller core are shown and the cores are dependent on each other when floor diaphragms are considered. When floor diaphragms are not considered, very small, or no, shear forces occur between the cores, as shown in Figure 6.1b. The moment distribution is shown in Figure 6.2, with and without the consideration of floor diaphragms. It is clear, when floor diaphragms are considered, that the shear forces create a moment couple at the top storey, where the small core ends, and since the bigger, right, core have a much greater stiffness than the left, the moment is distributed to it. For the case when floor diaphragms are not considered, the moment is absorbed in each core separately and no distribution between them can be observed.

6. Results

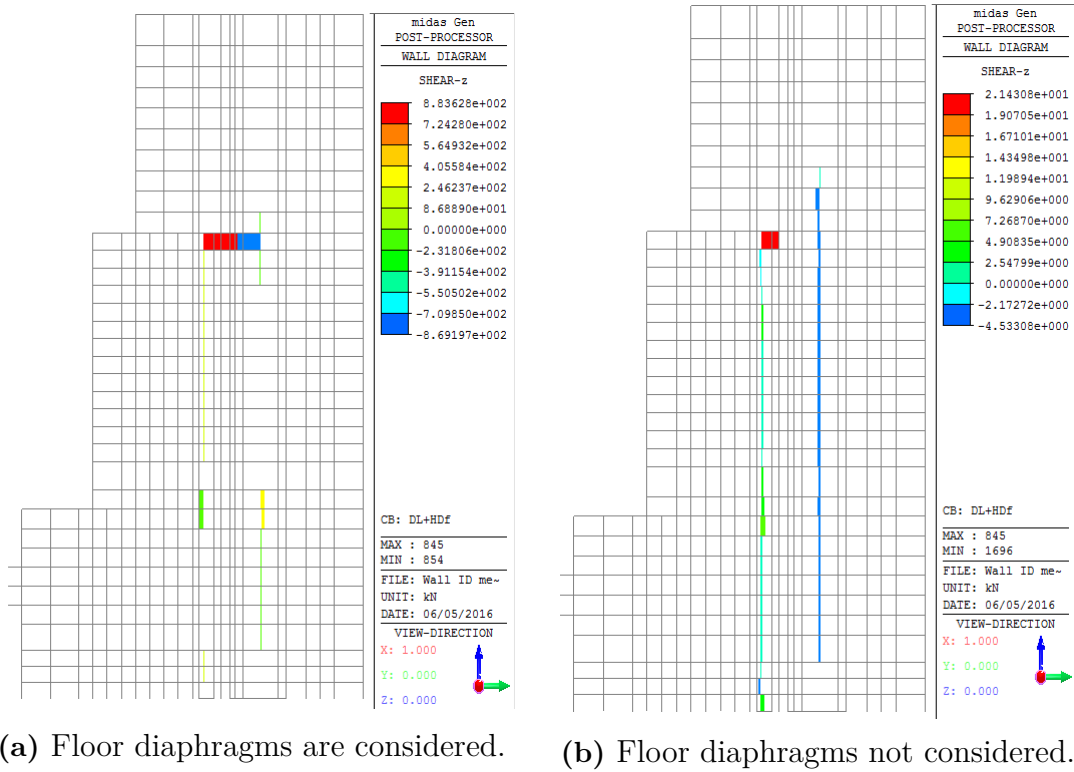


Figure 6.1: Shear force [kN] diagram for vertical load.

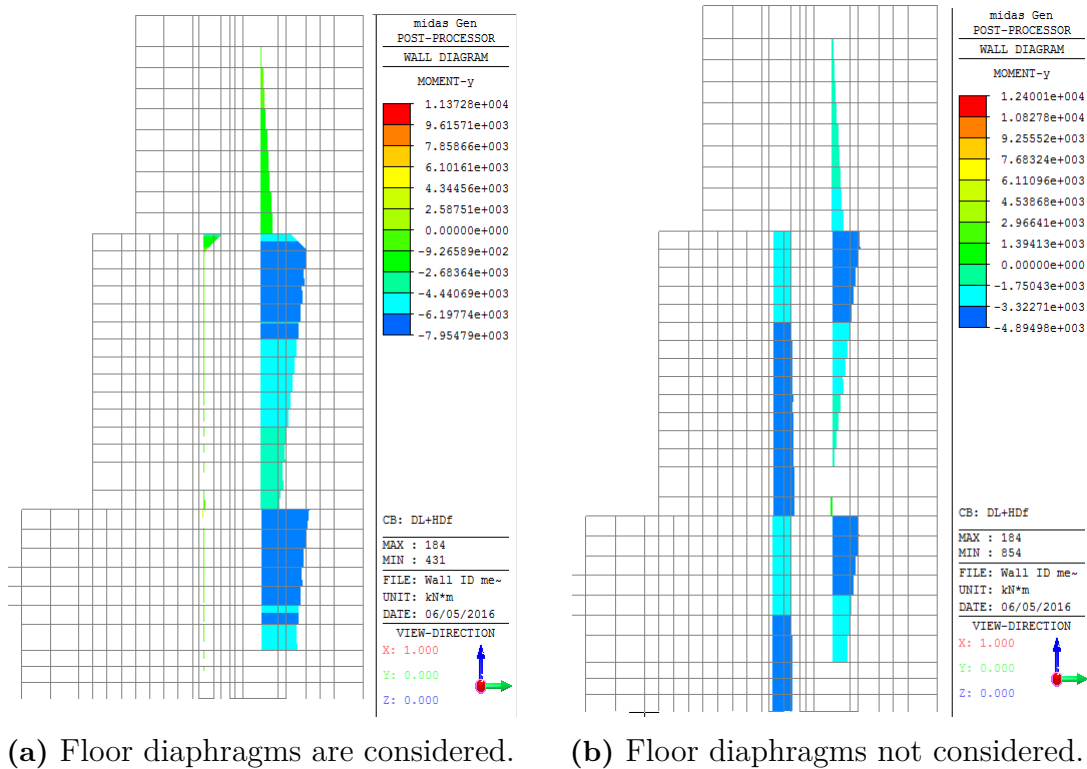
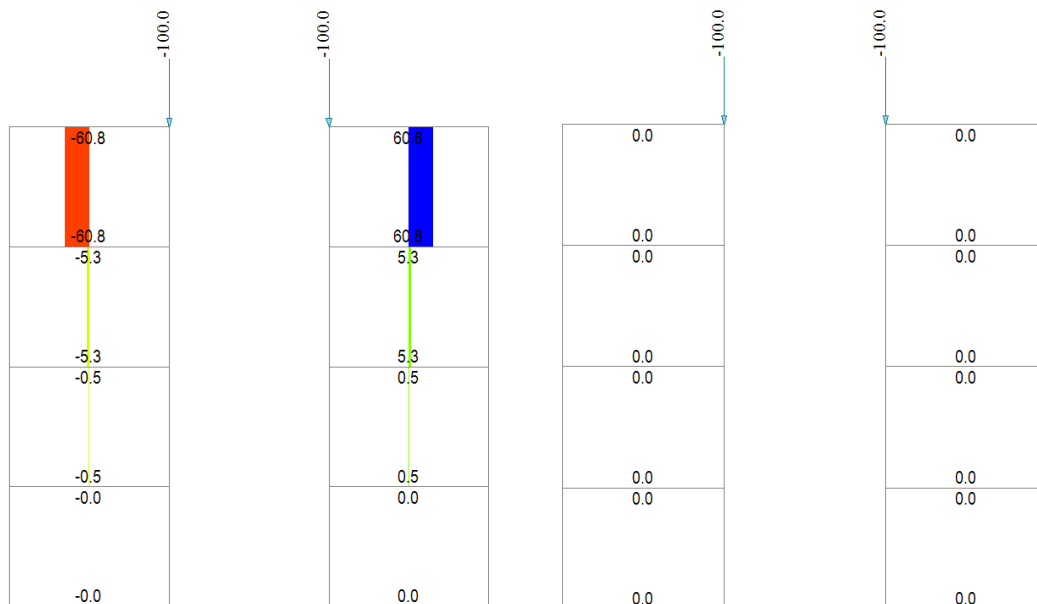


Figure 6.2: Moment diagram [kNm] for vertical load.

Example case

For the sake of clarification and to show how the forces are distributed with and without the consideration of floor diaphragms, an example case as described in Section 5.3 was created. In Figure 6.3, shear force diagrams are shown for a vertical load case. Where the different force distribution is clearly shown between the walls. The corresponding moment diagrams are presented in Figure 6.4 and the moment couple at the top storey, seen in the the model of GCG as well, Figure 6.2, is clearly shown in the figure where the moment is transferred to the more stiff core when floor diaphragms are considered due to the floor diaphragms being very stiff. A case where the walls are loaded unsymmetrical is presented in Figure 6.5. Here, only a point load is applied on the left wall. Due to the walls having the same stiffness and the floor diaphragms are very stiff, the distribution of the moment is equal at the ground for the two walls. This is clearly seen in the shear force diagram where a moment couple occurs in the top wall and then decreases to zero.

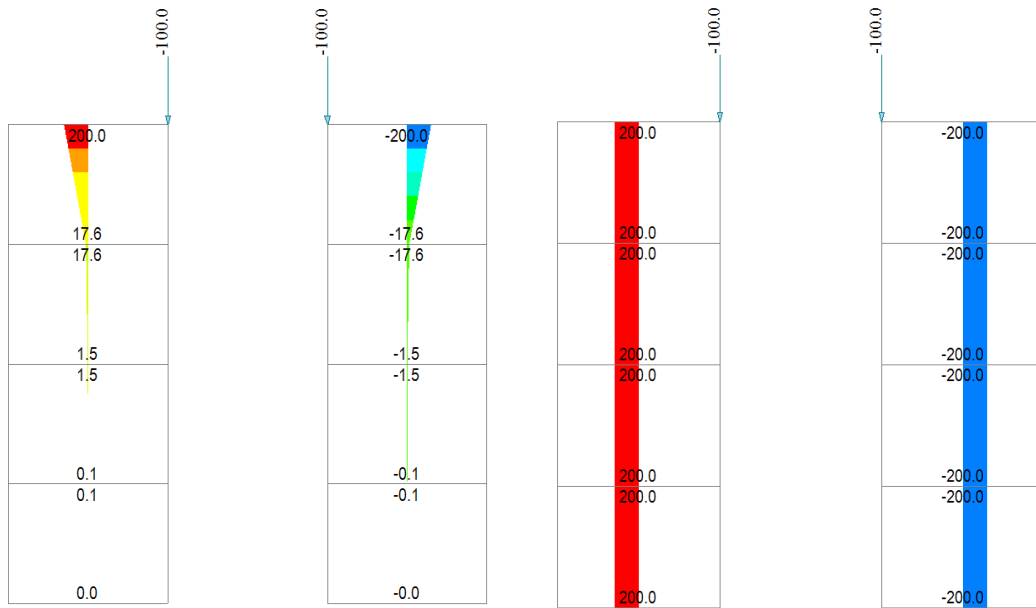


(a) Shear force diagram with floor diaphragms considered for all stories.

(b) Shear force diagram with floor diaphragms not considered.

Figure 6.3: Shear force [kN] diagrams for the example case for a vertical load.

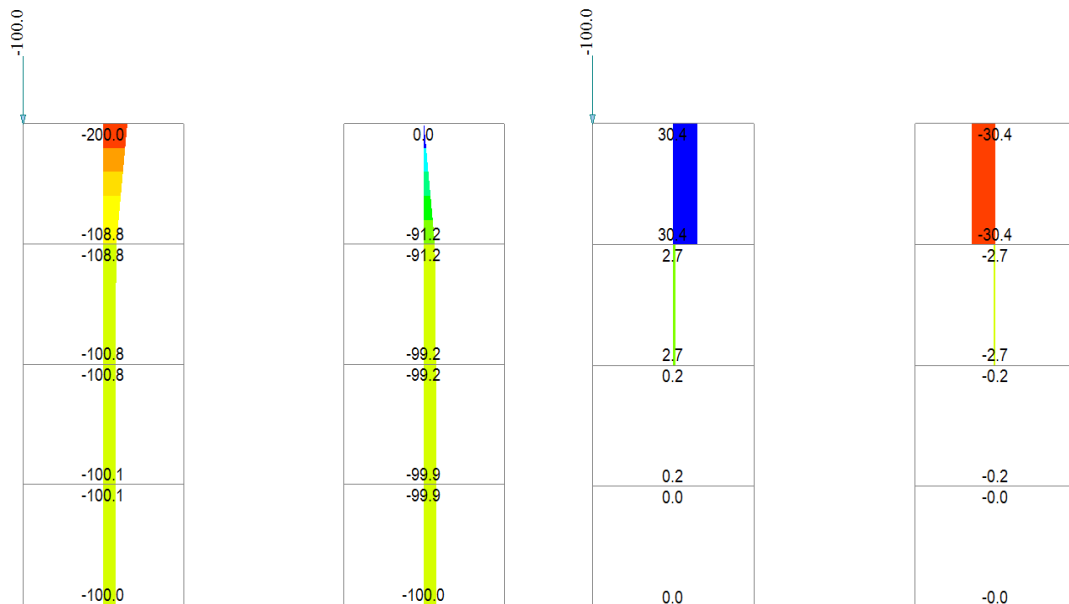
6. Results



(a) Moment diagram with floor diaphragms considered for all stories.

(b) Moment diagram with floor diaphragms not considered.

Figure 6.4: Moment diagrams [kNm] for the example case for a vertical load.



(a) Moment diagram. [kNm]

(b) Shear force diagram. [kN]

Figure 6.5: Moment and shear force diagram when floor diaphragms are considered for all stories and a vertical load is acting on the left wall.

6.1.2 Horizontal load

When horizontal loads are applied to the structure it is shown, for the case when floor diaphragms are considered, that the shear force and moment is distributed to the stiffer core. Studying the shear force diagrams in Figure 6.6, this is very clear. In the model when floor diaphragms are considered there are only shear forces in the right core while in the right figure, where floor diaphragms are not considered, there are no distribution of the shear forces between the cores. In Figure 6.7, the moment diagram for the model is shown and by looking at the values for the moments it is seen that, when floor diaphragms are considered, the moment is distributed to the stiffer, right core. For the case when floor diaphragms are not considered there are no distribution of the moments.

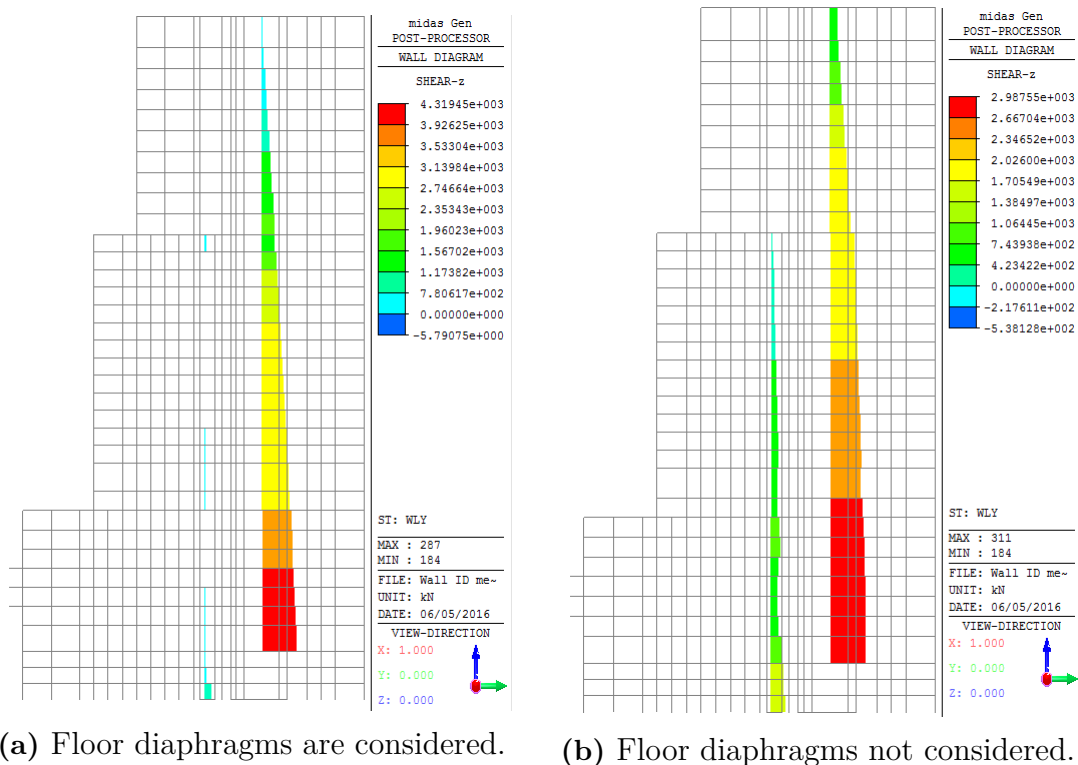


Figure 6.6: Shear force [kN] diagram for horizontal load.

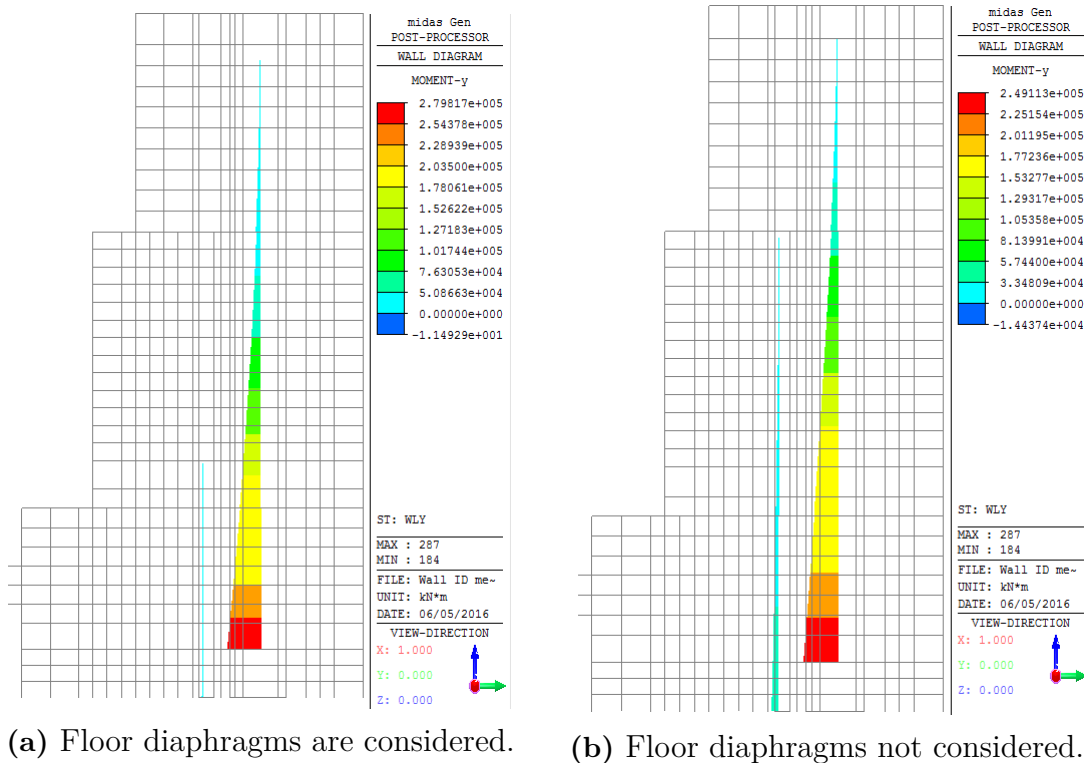


Figure 6.7: Moment diagram [kNm] for horizontal load.

Example case

As for the vertical load case, the shear force and moment distribution is shown with the example case loaded with a horizontal load. A load is applied on the structure as a point load acting in the horizontal direction in the upper left corner with a magnitude of 400 kN. Figure 6.8 presents the shear force diagrams with floor diaphragms considered as well as not considered. It is clearly seen that when floor diaphragms are considered the shear force is equally distributed between the two walls, due to the stiffness of the two walls being the same. For the case without the consideration of floor diaphragms, there are no distribution of the shear force. In Figure 6.9, the moment diagrams are presented with and without the consideration of floor diaphragms. The same principle that occurred for the shear force is shown here, when floor diaphragms are considered, that the moment is equally distributed between the walls. With no floor diaphragms activated, there are no distribution of the moment. In Figure 6.10, where floor diaphragms are considered and the stiffness in the left wall is 50% of the stiffness in the right wall. The stiffer, right wall, will absorb twice the moment and shear force as the left wall.

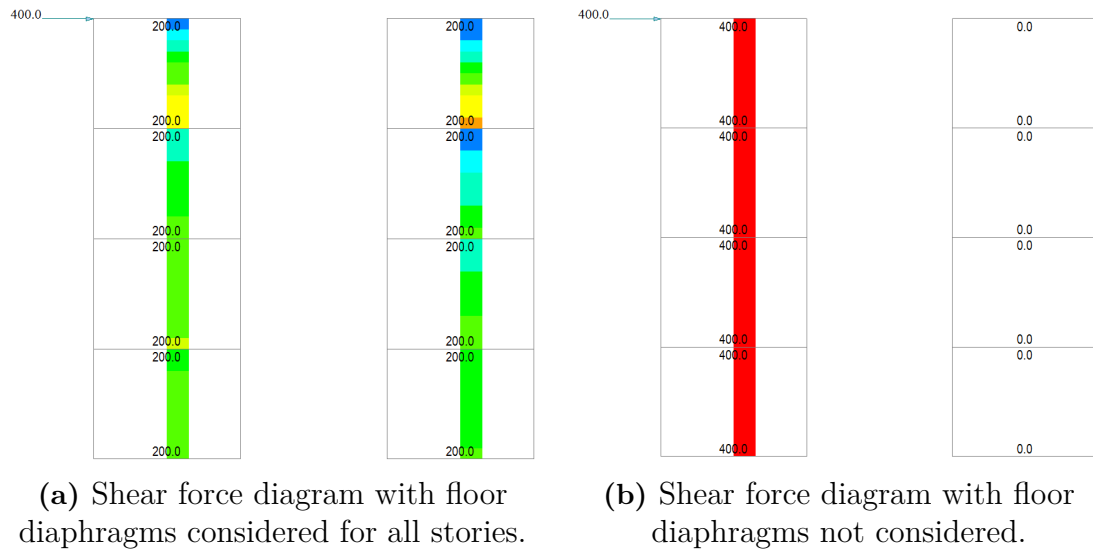


Figure 6.8: Shear force [kN] diagrams for the example case for a horizontal load.

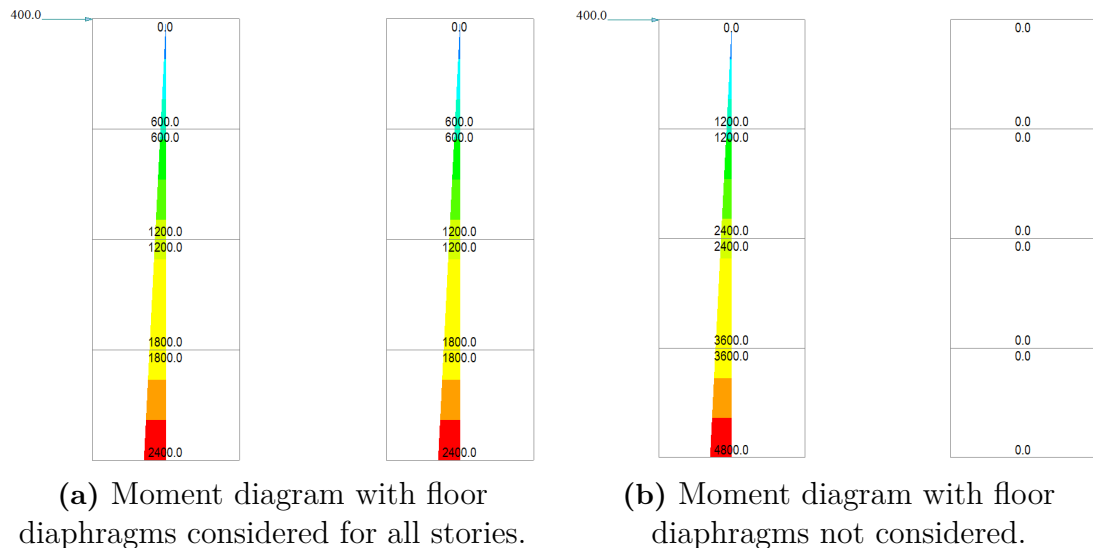


Figure 6.9: Moment diagrams [kNm] for the example case for a horizontal load.

6.1.3 Discussion of results

By looking at the results from the distribution of the shear forces and moments for both the vertical and the horizontal load case, conclusions about the consideration of floor diaphragms can be made.

For the vertical load case, the consideration of floor diaphragms should be used with care as the distributions may be misleading when designing a building. If floor diaphragms are considered, it could lead to an inaccurate distribution of the reaction forces, which in the worst case scenario, could lead to a collapse. This can occur due to the distribution of shear forces and moments which could lead to lower values being designed for in a concrete staircase, elevator shaft or wall, as can be seen in Figure 6.2. The distribution might not occur in reality, since the phenomena where

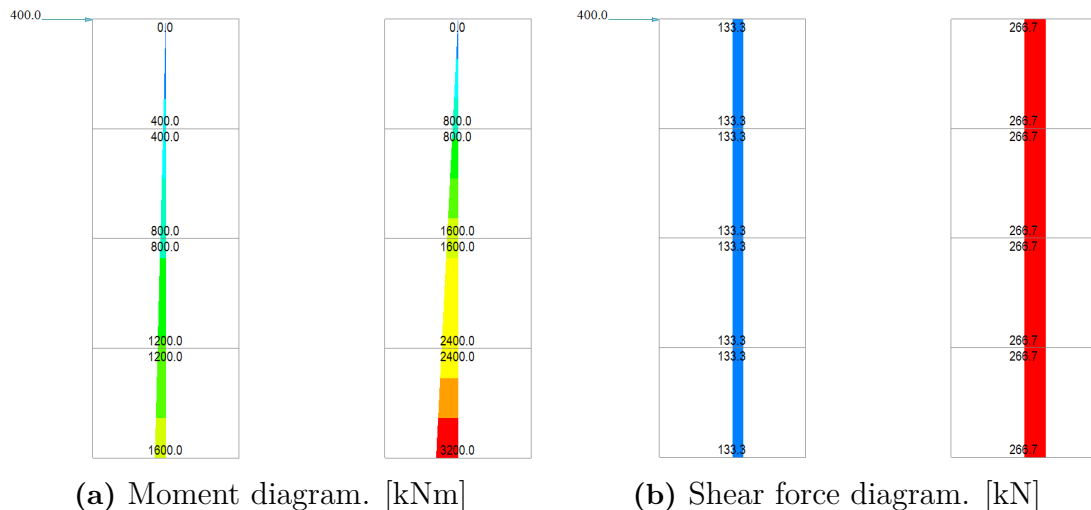


Figure 6.10: Moment and shear force diagram when floor diaphragms are considered for all stories for horizontal load. The stiffness in the left wall is half of the stiffness in the right wall.

the concrete cores are relying on each other is not always wanted.

For the horizontal load case however, the consideration of floor diaphragms are desired if the model is created with wall elements as it is acting as a slab. This provides lateral stiffness of the building and diaphragm action is achieved. When the structure is loaded laterally, the load is transferred in the diaphragms to the vertical elements, which is desired. An important thing to notice is how the wind-load is applied when floor diaphragms are considered. For each storey, the resultant wind-force is placed in the mass centre, or master node, of the diaphragms. If diaphragms are not considered on the other hand, the wind-load is instead placed in each node due to lack of lateral stiffness.

The stiffness of the different load-bearing elements have a huge impact on the distribution of the forces. Stiffer elements absorb more forces which is clear when looking at the force distributions in Göteborg City Gate, where the smaller core has a much lower stiffness than the larger core. This is why it is important, in the vertical load case, to design each core for the forces it is exposed to without floor diaphragms. Otherwise, the forces will get distributed to the most stiff core.

6.2 Analysis of reaction forces

In this section the result of the comparison between the cumulative loads are presented as well as the effect from considering floor diaphragms in the vertical load case. A calculation of the cumulative loads on the building was made by hand. The result was compared to the loads from the FE program. The reaction forces were checked in three different points in the building, in the columns A1, G3 and in the wall between point F2 and F3, see Figure 6.11. The summation of the total reaction force from the building is given from Midas Gen as 225.7 MN, from the meshed

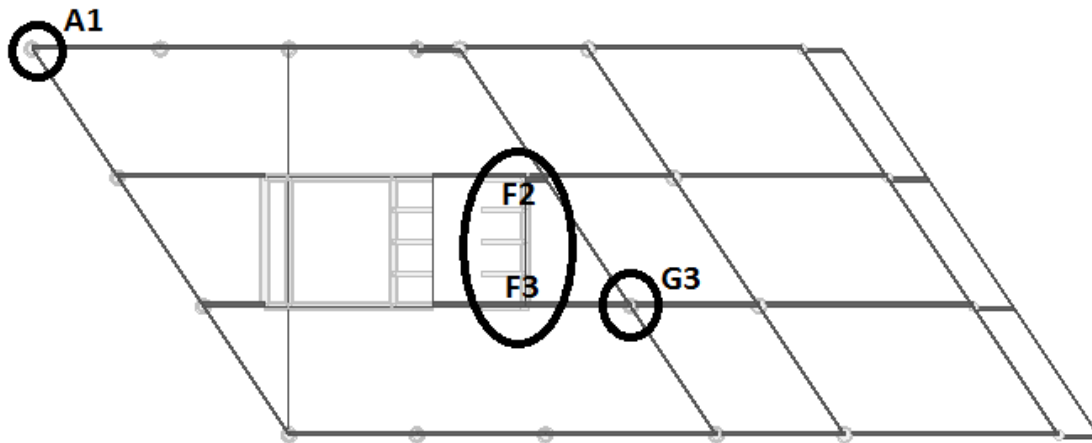


Figure 6.11: Columns and walls checked for cumulative load calculation.

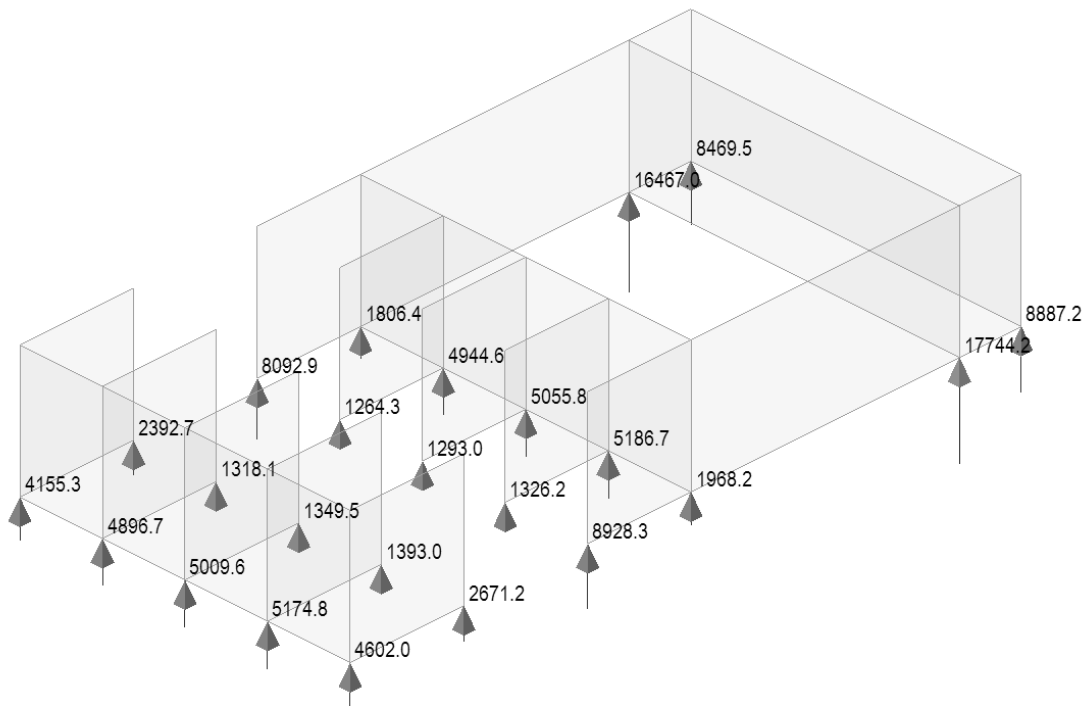
Table 6.1: Comparison between reaction forces from dead load and slab in the model with wall elements and floor load representing the slabs, floor diaphragms are considered.

	Reaction forces from slabs		
	Column A1	Column G3	Wall F2-F3
Calculation by hand [kN]	1456.9	6430.2	12028
Result from model [kN]	1458.1	6345.2	11972
Difference [%]	0.08	1.34	0.47
Reaction forces from dead load in model 1.			
Calculation by hand [kN]	1995.4	2074.6	21022
Result from model [kN]	1995.4	2074.2	21168
Difference [%]	0	0.02	0.69

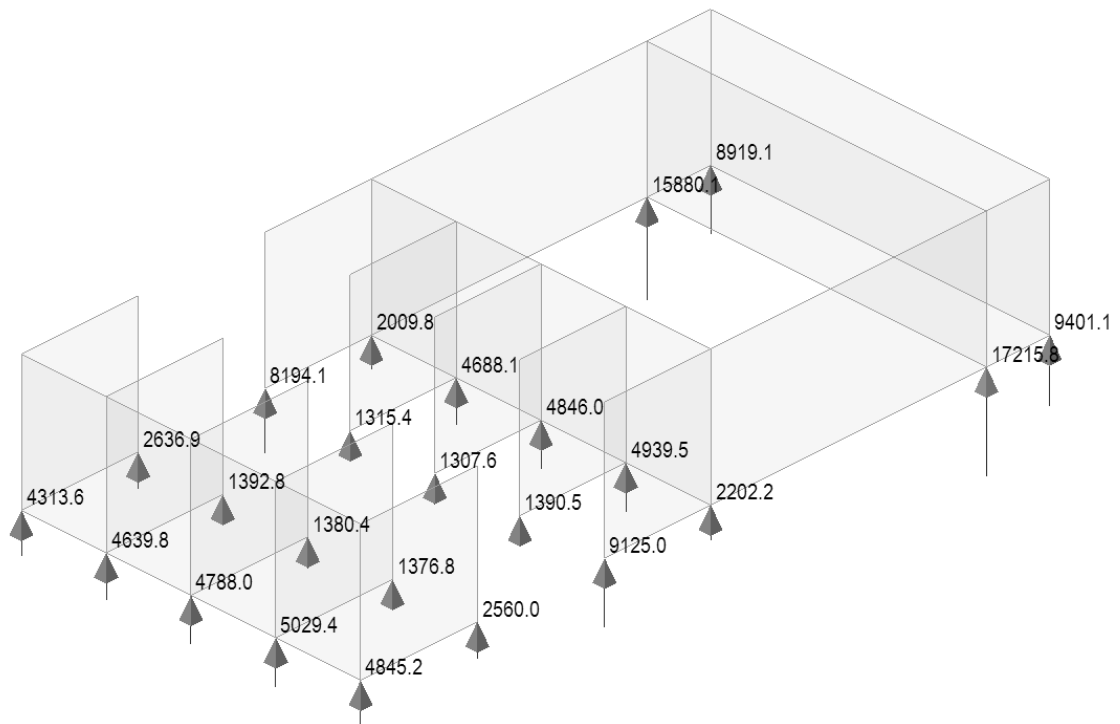
model. For the model with wall elements and floor loads the total reaction force is 224.8 MN. In Table 6.1 there are a comparison between the calculated self-weight in specific elements and the reaction forces from Midas Gen in the same elements in order to validate the numerical FE model. The distribution of forces in the model varies if floor diaphragms are considered or not. This is shown in Figure 6.12 where the reaction forces under each core in the building are shown with and without the consideration of floor diaphragms. A comparison between the total reaction forces under each concrete core is shown in Table 6.2.

Table 6.2: Summation of reaction forces [kN] under each core.

	Floor diaphragm considered	Floor diaphragm not considered
Large core	91434.3	91434.3
Small core	32962.9	32962.9
Summation	124397.2	124397.2



(a) Reaction forces [kN] when floor diaphragms are considered.



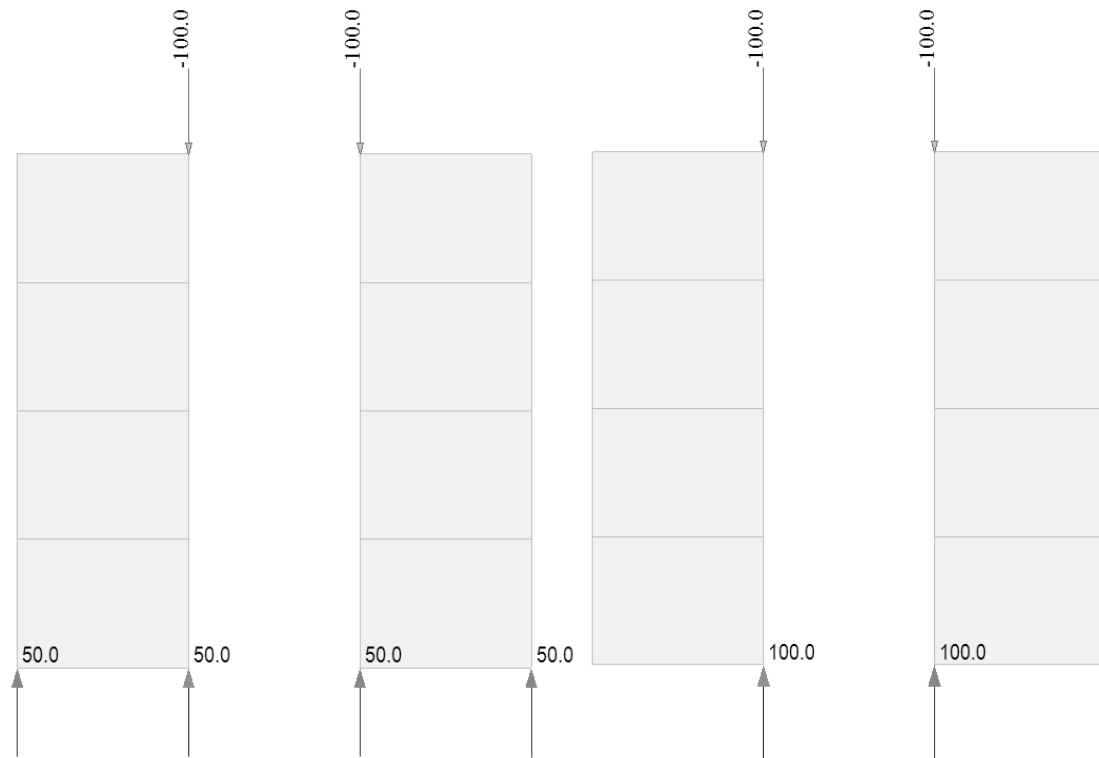
(b) Reaction forces [kN] obtained from model without floor diaphragms.

Figure 6.12: Both models are subjected to self-weight and load from a hollow-core slab and modelled with wall elements, subtype plate, with no beams between the cores.

6.2.1 Discussion of results

When comparing the differences between the two models in Table 6.2, the model with wall elements and the meshed model, the summation of the total reaction force is very similar. The difference is 1 MN or 0.4%.

Table 6.2 shows the effect of floor diaphragms. When considering only vertical loads the floor diaphragms have no impact on the total reaction force. In Figure 6.12 it is shown, however, that the internal distribution of the reaction forces in the cores are different. To illustrate this, an example case is presented in Figure 6.13. Here, the total reaction force for each wall is the same. However, a marked difference in the internal distribution is shown in the comparison between the consideration of floor diaphragms. For the cumulative load calculation of a structure made with precast concrete elements, it is easier to have control of how the loads are distributed with a model created with wall elements and the slab represented by a floor load as it corresponds well with the behaviour of precast concrete slabs. For example, as hollow-core slabs only transfers loads in one direction these are modelled with a one-way floor load. Trying to achieve the same load distribution with a meshed model is a complicated and time consuming task. If the slab is created with a mesh, the stiffness will be the same in all directions and it will not represent a hollow-core slab. To get a proper representation, the engineer has to use either plate-end release, which removes the boundary condition on the edges of the mesh where no load should be transferred, or use fictitious beams, which are placed a small distance from the edge where no support exists, to get the load acting in only one direction. These fictitious beams have with very low stiffness. Both options will, however, generate other problems. For instance, the last option will create major shear forces in the beams and the plate end release will cause abnormal displacements in the slab.



(a) Reaction forces [kN] when floor diaphragms are considered.

(b) Reaction forces [kN] obtained from model without floor diaphragms.

Figure 6.13: Example case where the walls are exposed to a point load of 100 kN applied in the vertical direction. The figure shows the distribution of the reaction forces with and without the consideration of floor diaphragms.

6.3 Analysis of overturning moment

In this section the overturning moment from horizontal load is compared with different standards to FE analyses in Midas Gen. Three different overturning moments can be found in Midas Gen. The first is a summation of all reaction moments from the horizontal wind load, the second is found in the wind load profile and the last is calculated with a reduction factor τ . This reduction factor intends to consider the effect of higher modes and is applied as follows [24]:

- At 10 stories from the top, τ is equal to 1.0.
- At the 20th storey from the top and below, τ is equal to 0.8.
- Between the 10th and the 20th stories from the top, τ is interpolated between 1.0 and 0.8.
- For dynamic analysis, τ can be set to 1.0.

The reduction factor τ is very similar to the size factor c_s which is used in Eurocode [31]. To make a qualified comparison between the overturning moments, four calculations of the static overturning moment are made. One strictly according to Eurocode [31], see Appendix B, one without the size factor c_s , see Appendix C, one

Table 6.3: Summary of overturning moments.

Method	Overturning moment [MNm]
Static: Strictly according to Eurocode	617.0
Static: Without the size factor c_s	736.4
Static: Without the size factor c_s but with τ	680.6
Static: According to EKS10	433.5
Dynamic: According to Eurocode	619.2
Midas Gen: Summation of reaction moments	793.5
Midas Gen: From the wind load profile	701.6
Midas Gen: Overturning moment	634.8

with the reduction factor τ applied as the Midas manual [24] suggests, without the size factor c_s , see Appendix D and one simplified calculation based on tabular values from EKS10 [6], see Appendix E. Finally, a calculation of the dynamic overturning moment according to Eurocode [31] is made, which can be seen in Appendix F. All results of overturning moments are summarised in Table 6.3.

6.3.1 Discussion of results

Looking at the results of the overturning moments a large spread can be noticed depending on the method used for calculation. The largest value is taken from the summation of reaction forces in Midas Gen as 793.5 MNm, while the lowest from calculation according to EKS 10 was 433.5 MNm. This results in a difference of 360 MNm or 45.4%. It is important to make sure the resisting moment is larger than the overturning moment or the structure will overturn. As can be seen in Table 6.3, the choice of overturning moment will have a huge impact when designing the building. Furthermore, it is seen that the overturning moment from Midas Gen of 634.8 MNm corresponds well with the static overturning moment calculated according to Eurocode of 617.0 MNm.

6.4 Analysis of horizontal deflection

In this section the deflection is analysed and compared for the FE model in Midas Gen to calculations made by hand and in the software Frame analysis. The calculations for these are shown in Appendix G and the result is presented in Table 6.4.

6.4.1 Discussion of result

Both the calculation made by hand and in the software Frame analysis are calculated on a cantilever with equivalent stiffness as the concrete core in the building. The deflection is only calculated in the weak direction, x-direction, of the building. Even though, in reality, the building have a influence from torsional deflection as well. This due to the building being unsymmetrical, which Midas Gen is considering but it is neglected in the hand and Frame analysis calculations. This is a reason why

Table 6.4: Comparison of the deflection at the top of the building calculated by hand, in Frame analysis and in Midas Gen. The deflection is caused by wind load in x-direction.

Method	Deflection [m]
By hand	0.253
Frame analysis	0.251
Midas Gen: meshed model with element size 1 meter	0.261
Midas Gen: wall elements with subtype plates	0.283

Table 6.5: Comparison between the methods used to determine the critical buckling load.

Method	Critical load [GN]
Vianello method	6.52
Buckling analysis	7.60
P-delta analysis with wall elements; subtype plate	6.55
P-delta analysis with wall elements; subtype membrane	9.26

the deflections are much greater from the Midas models. The values taken from Midas are the maximum value in the concrete core, the maximum deflection occurs in the edge of the slab, where the influence of torsional deflection is largest. The calculations made by hand are time consuming as the calculation has to be done separately for each storey. Furthermore, only the first order deflection is considered in these calculations.

6.5 Analysis of critical load

In this section the critical buckling load is investigated. To determine the critical buckling load of Göteborg City Gate, four different analyses have been made. One calculation according to the Vianello method described in Section 4.1, one buckling analysis in Midas Gen, described in Section 5.2.2 and two P-delta analyses in Midas Gen, described in Section 5.2.2. The calculations according to Vianello are found in Appendix H and the buckling as well as the P-delta analyses are found in Appendix I. The result from the analyses are presented in Table 6.5.

6.5.1 Discussion of result

Performing a calculation by hand on the structure for the critical buckling load is a good way to get an indication on the range of the result. However, the calculations are made on a cantilever with equivalent stiffness and the structure is simplified in order to complete the calculations. This provides a lower value for the critical buckling load, which is seen in Table 6.5. The value calculated with the Vianello method corresponds well with the P-delta analysis with wall elements with subtype

Table 6.6: Resonance frequencies [Hz] calculated from the models in Midas Gen.

	Mode 1	Mode 2	Mode 3
Membrane walls, fixed beams	0.33	0.41	1.09
Membrane walls, hinged beams	0.33	0.33	1.07
Plate walls, fixed beams	0.33	0.41	1.09
Plate walls, hinged beams	0.33	0.33	1.07
Meshed plate elements size 3 m, fixed	0.34	0.43	0.92
Meshed plate elements size 3 m, hinged	0.34	0.39	0.91
Meshed plate elements size 1 m, fixed	0.33	0.39	0.91
Meshed plate elements size 1 m, hinged	0.33	0.35	0.89

plate.

Between the two critical loads calculated with the P-delta analyses, a difference of 2.71 GN or 29.3% is shown. This is believed to have to do with that membrane elements does not consider out-of-plane bending, while plate elements does. The membrane element represents a shear wall while the plate element represents a more common wall. From the buckling analysis, a value is given between the two P-delta analyses and may be due to the difference in stiffness between the meshed slab and the floor diaphragms.

It should be mentioned that finding the critical buckling load is easier with the buckling analysis than with the P-delta analysis because the later require that the load factor is changed manually until the analysis no longer converges to find the load factor, while the buckling analysis calculates it automatically. On the other hand, the buckling analysis requires a sufficiently fine mesh, which have converged in element size. This can be a very time consuming task, especially for large structures. Furthermore, it is clear that depending on which type of analysis used to find the critical load, major differences in the results will be obtained.

6.6 Analysis of resonance frequencies

In this section an evaluation of the resonance frequencies of the building is carried out. The calculations of the resonance frequencies are described in Section 5.2.2. In Table 6.6 the first three resonance frequencies are presented for the various models investigated. These resonance frequencies are to be compared with the resonance frequencies calculated with Equations 4.43–4.45 for each mode, respectively. This provides the result presented in Table 6.7 together with a comparison to the FE calculations. According to Stafford Smith & Coull [34], a more accurate calculation can be performed in order to predict the fundamental frequency with Equation 4.46. The calculations for these are found in Appendix J with the result of 0.34 Hz. This corresponds very well with the meshed model with element size of 3 meter, from which the values of deflections and storey-weights were taken. Applying Stafford Smith & Coull’s method on deflections calculated by hand the fundamental frequency was 0.30 Hz.

Table 6.7: Calculated resonance frequencies for the three first modes.

	Mode 1	Mode 2	Mode 3
Frequencies calculated by hand. [Hz]	0.38	0.48	0.60
Comparison to frequencies from the FE-models [%]			
Membrane walls, fixed beams	16.6	18.2	-44.8
Membrane walls, hinged beams	16.6	43.7	-44.1
Plate walls, fixed beams	16.6	18.2	-44.8
Plate walls, hinged beams	16.6	43.7	-44.1
Meshed plate elements size 3 m, fixed	11.8	11.6	-34.8
Meshed plate elements size 3 m, hinged	11.8	23.1	-34.1
Meshed plate elements size 1 m, fixed	15.2	23.1	-34.1
Meshed plate elements size 1 m, hinged	15.2	27.1	-32.6

6.6.1 Discussion of result

In Table 6.6 it clearly shows that for all models with wall elements, the subtype of plate or membrane has no impact on the first three resonance frequencies. It also shows that modelling the connection of the beams between the two concrete cores with hinges decreases the second and third resonance frequency while the first is unchanged. This is because the connection of the beams does not influence the stiffness of the structure in the weak direction, where the first resonance frequency occur, but a hinged connection reduces the stiffness in the stiff and rotational direction.

Important to notice is that the models with wall elements does not consider the floor loads as masses when calculating the resonance frequencies. This will provide incorrect results since the mass from the slabs have a major influence on the resonance frequencies. In order to adjust for this, the density of the materials can be modified to get a mass representing the weights from both self-weight and the slab, and thus resonance frequencies that corresponds to the actual mass of the building. However, affecting the mass like this will change the mass distribution which may affect the moment of inertia and thereby also the resonance frequencies.

When performing eigenfrequency analysis on a meshed model, no adjustments for the masses are needed since the slab have a mass. However, the results from the meshed models are not as pure, only working in one direction, as they were for the models with wall elements. The first and second mode, for example, has an influence of rotation as well. This is believed to have to do with the stiffness in the meshed slab against the floor diaphragms. Since the stiffness in the slab is not as stiff as the diaphragms, rotation occurs.

Comparing the simplified calculations by hand with the analyses in Midas Gen, a clear difference is shown. For the first and second mode the differences between the calculations made by hand and the FE models are between 12% up to 44%, and for the third mode the frequency calculated by hand is much lower than all FE models. However, this is not surprising since the equations for predicting the resonance frequencies only includes the buildings height and not geometry nor stiffness.

6.7 Analysis of acceleration

In this section, the accelerations caused by wind-load on the building is analysed, which is a difficult task in Midas Gen, since a time-history function is needed where the wind-load is described with a response spectrum. Generating a time-history function for a building is both difficult and time consuming since it requires the solution of the buildings equation of motion, which is complicated for a large and complex building. It can, however, be created by performing a wind-tunnel experiment on the building [23]. No time-history function was calculated during this Master's thesis due to insufficient time. Furthermore, if a time-history function had been calculated, Midas Gen does not consider the across-wind response. However, the accelerations were still calculated by hand at the top of the building in both the along- and across-wind direction. Only wind-load in the weak direction of the building was considered when calculating the accelerations.

6.7.1 Along-wind acceleration

The calculations of the along-wind response of Göteborg City Gate was made according to the theory in Section 4.2.3. The calculated acceleration was compared with the standard SS-ISO 10137 [33], see Figure 2.11. However, Equation 4.36 that is used to recalculate the mean wind velocity for different return periods does not allow a return period of one year, which is what should be used to be able to compare with the standard SS-ISO 10137. To get around this issue, return periods from 1.0001 years to 5 years was calculated. The result from these are shown in Figure 6.14. Appendix K shows the calculation of the 5 year return period which gave an along-wind acceleration of 0.17 m/s^2 at the top of the building. From the meshed FE model a fundamental frequency of 0.33 Hz was determined. This frequency was used as input to the calculations by hand of the along-wind acceleration. But depending on the model and method used to determine the resonance frequency of a building, different results are found as shown in Section 6.6. To see what effect the different resonance frequencies have on the along-wind acceleration at the top of Göteborg City Gate a graph was plotted, see Figure 6.15.

6.7.2 Across-wind acceleration

The calculation of the across-wind acceleration was performed with the theory presented in Section 4.2.4. A wind-load with a return period of 50 years gave an acceleration of 0.08 m/s^2 at the top of the building, for calculations see Appendix K. In association with the along-wind acceleration, the wind has to be recalculated to a return period of one year to be able to compare the acceleration with the requirements in SS-ISO 10137 [33]. As for the along-wind acceleration, one year is not valid input to Equation 4.36, why Figure 6.16 shows the increase of the across-wind acceleration with regard to different return periods of the wind. The effect on the across-wind acceleration at the top of the building with regards to different frequencies was evaluated as well. This is presented in Figure 6.17.

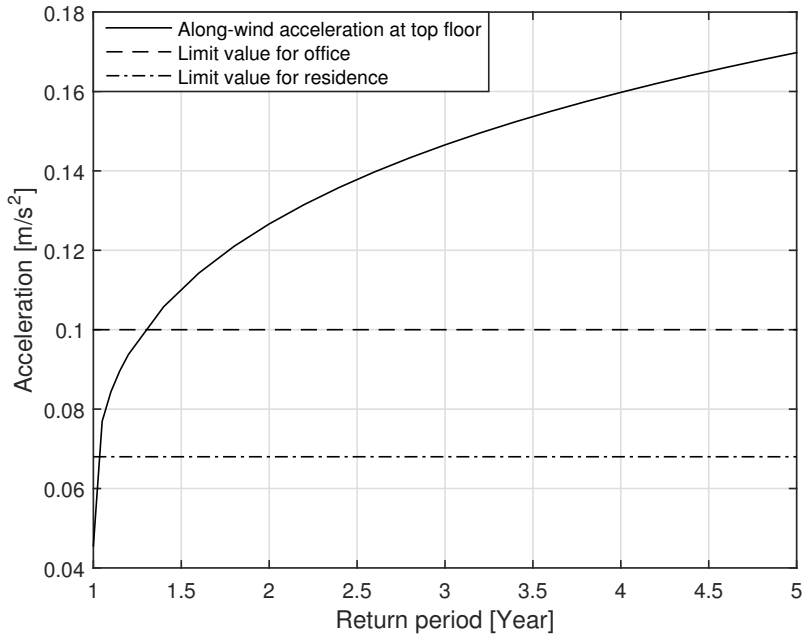


Figure 6.14: Along-wind acceleration at the top of Göteborg City Gate at different return periods for the wind-load. The fundamental frequency of the building is estimated to 0.33 Hz and the limit values come from the SS-ISO standard [33] in Figure 2.11.

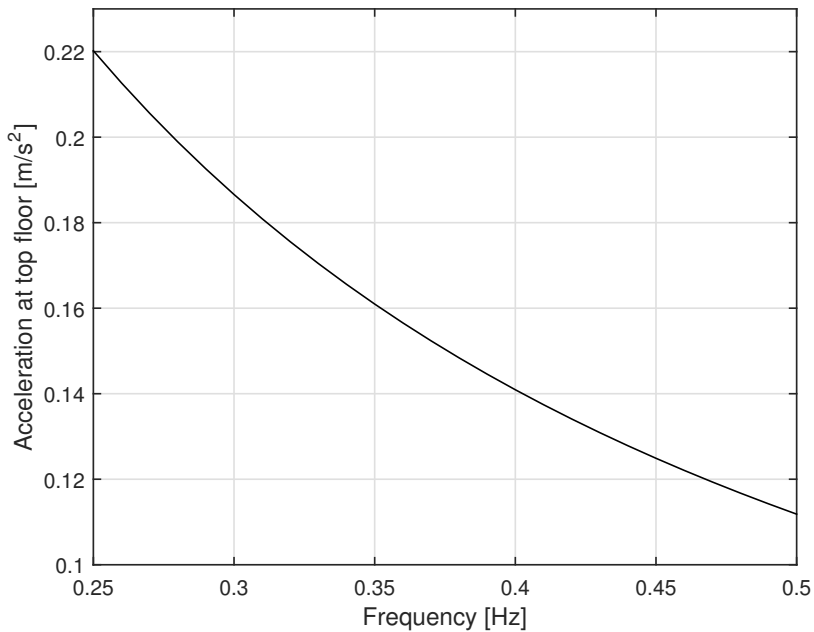


Figure 6.15: Along-wind acceleration at top floor of Göteborg City Gate at different resonance frequencies. Calculated according to the Eurocode standard and with a return period of 5 years.

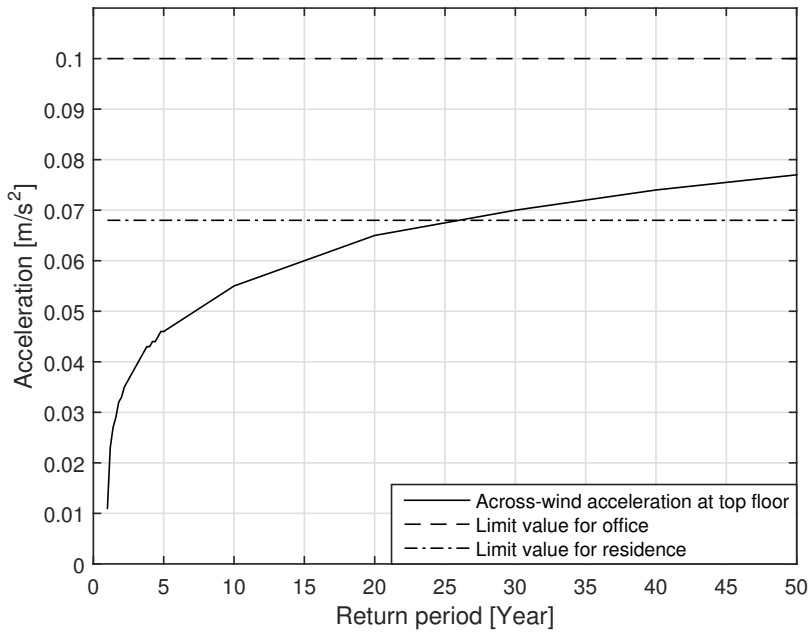


Figure 6.16: Across-wind acceleration at the top floor of Göteborg City Gate at different return periods for the wind-load. The fundamental frequency for the building is 0.33 Hz and the limit values come from the SS-ISO standard [33] in Figure 2.11.

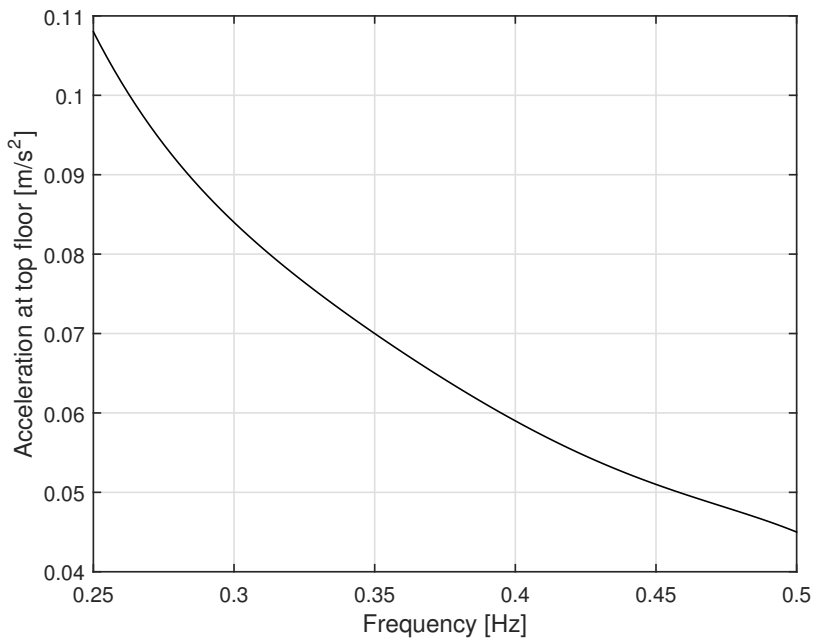


Figure 6.17: Across-wind acceleration at the top storey of Göteborg City Gate for different frequencies calculated for a wind with a return period of 50 years.

6.7.3 Discussion of results

Evaluating the results of the acceleration in both the along- and across-wind directions it gives a clear picture about the relationship between accelerations and resonance frequencies. Figures 6.15 and 6.17 shows that increased fundamental frequency gives decreased acceleration.

Furthermore, comparing the accelerations with the comfort requirements in Figure 2.11 is not as easy as it seems, since a problem occurs with Equation 4.36 when recalculating the wind velocity for different return periods. This because it does not allow one year as input which is the return period that should be used in SS-ISO 10137. However, Figures 6.14 and 6.16 shows how the along- and across-wind acceleration increases with increased return period of the wind. It is seen that the along-wind acceleration increases drastically in the beginning and exceeds the limit value for residents almost immediately. This may indicate that the building has to be redesigned or that it is not suitable to use a return period close to one year as an input to Equation 4.36.

In correlation with what has been discussed, a way to meet the requirements better would be to increase the stiffness of the building, leading to increased resonance frequencies and thus a reduced acceleration.

6.8 Analysis of forces between elements in a pre-fabricated concrete core

In this section the forces between elements are analysed with the theory described in Section 5.2.2. From the model with meshed elements, linear-elastic shear flow was obtained at three cuts, an example of this is shown in Figure 6.19. The model that was created with wall elements gave output in form of moments, shear forces and normal forces in each wall at each cut. The result from these calculations are summarised in Tables 6.8, 6.9 and 6.10. The shear forces were calculated to shear flow in each wall with Equation 5.1 to evaluate the accuracy of the equation presented by Eurocode, Equation 4.47.

6.8.1 Discussion of results

When evaluating the results it is important to keep in mind that the shear flow obtained from the meshed model in Midas Gen are based on linear-elastic theory. What this means is that the FE program is considering the concrete to be uncracked. If a cross-section is in bending or tension the concrete normally cracks, meaning that the linear-elastic shear flow is no longer valid. This may cause a redistribution of the shear flow. Because of this, it is important to investigate whether the cross-section is in compression, tension or bending when calculating the shear flow in a building.

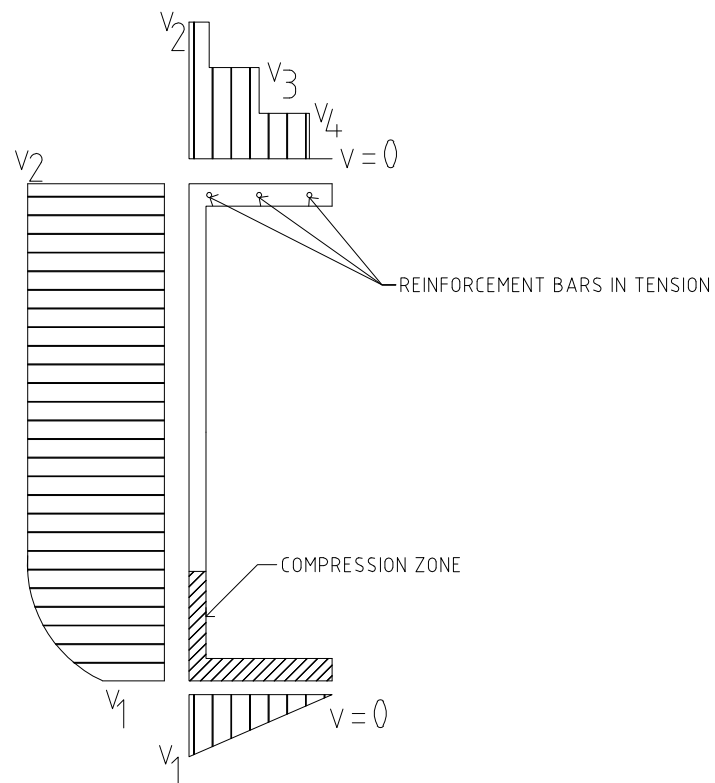


Figure 6.18: Shear flow example of a cracked C-beam in bending.

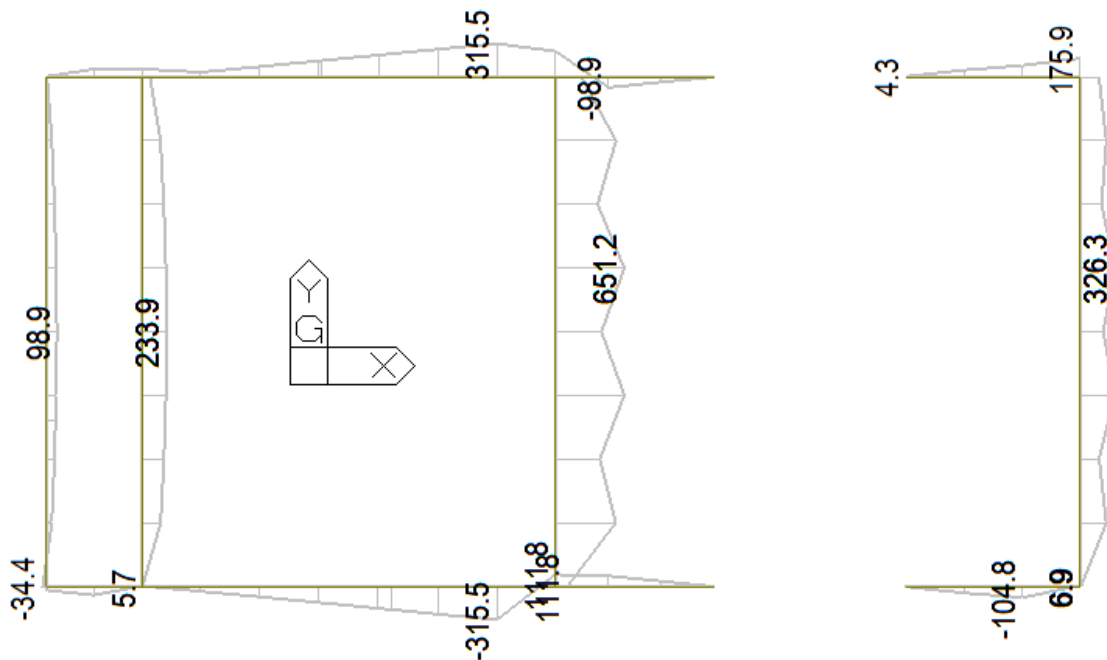


Figure 6.19: Linear-elastic shear flow [kN/m] in the cut at 21.3 meters generated from wind in the x-direction, average nodal.

11	12	3	7
1	2	4	8
13	14	5	9
		6	10

Figure 6.20: Description of the wall numbering used in Tables 6.8, 6.9 and 6.10.

In Table 6.10, which presents the results from the cut at 90 meters it can be observed that all the walls are in compression by looking at the normal forces. This would imply that linear-elastic theory is applicable. By looking at the shear force on wall 1 and 2 loaded in the y -direction it can be noted that the value is zero. This is because Midas Gen calculates the summation of the shear forces in the element and symmetry of the positive and negative shear force leads to the total adding up to zero. Since in the meshed model the elements are smaller, shear flow in this direction will still be calculated. Furthermore, it should be noted that the cut at 90 meters are in level with a slab. This will give local effects caused by the force from the slab which may be difficult to interpret.

From the cuts at 21.3 and 60 meters it can be observed that all the wall elements no longer are in pure compression. This means that the linear-elastic theory may not be applicable on these walls.

Assuming the concrete is fully cracked when in tension means that theoretically no shear flow will be consumed by the concrete. This means that the reinforcement will have to absorb all the shear flow. From the compression zone the shear flow will then be kept constant until it reaches the reinforcement and a decrease of the shear flow will occur and then kept constant until the next bar. This means that the placement of the reinforcement will have a large impact on the shear stress as a larger distance between the bars will increase the shear stress in the reinforcement, see Figure 6.18. Since the compression zone is independent of the horizontal placement of the reinforcement in the top flange, the value of the shear flow v_2 will be unchanged. However, a nonlinear analysis should be performed in order to see how the actual shear flow is distributed when a concrete element no longer can be considered as uncracked.

Table 6.8: Cut at 21.3 meters where WLX and WLY are wind in the x-direction and y-direction respectively, N is the normal force from wind and self-weight, M is the moment from wind, V is the shear force from wind, $v(z)$ is the shear flow calculated with Equation 5.1, v_{Elastic} is the linear-elastic shear flow and the wall numbers refer to Figure 6.20. Underlined values denotes if the linear-elastic shear flow is greater than the shear flow calculated from the shear force.

WLX						
Wall	N [kN]	M [kNm]	V [kN]	$v(z=0.67L)$ [kN/m]	$v(z=L)$ [kN/m]	v_{Elastic} [kN/m]
1	-10475	30456	416	78	52	<u>99</u>
2	-10604	30498	1490	279	186	<u>234</u>
3	-7390	475	1296	972	648	572
4	-4358	478	1382	1036	691	651
5	-1298	478	1382	1036	691	651
6	1767	475	1296	972	648	572
7	50	458	519	389	259	246
8	-4029	464	611	459	306	326
9	-1062	464	611	459	306	326
10	-1898	458	519	389	259	246
11	-6544	-1	170	170	114	74
12	-28670	-4	1131	261	174	<u>316</u>
13	2592	1	-170	-170	-114	-83
14	10956	4	-1131	-261	-174	<u>-316</u>
WLY						
Wall	N [kN]	M [kNm]	V [kN]	$v(z=0.67L)$ [kN/m]	$v(z=L)$ [kN/m]	v_{Elastic} [kN/m]
1	-21711	0	0	0	0	<u>-117</u>
2	-18161	0	0	0	0	<u>-74</u>
3	-798	4	162	122	81	100
4	-729	1	61	46	31	34
5	-660	-1	-61	-46	-31	-33
6	-590	-4	-162	-122	-81	-100
7	-2169	0	10	7	5	4
8	-2112	0	4	3	2	2
9	-2043	0	-4	-3	-2	-2
10	-1962	0	-10	-7	-5	-4
11	-3842	83	241	241	161	123
12	-8957	6751	1354	313	208	222
13	-3634	83	241	241	161	230
14	-8056	6751	1355	313	208	224

Table 6.9: Cut at 60 meters where WLX and WLY are wind in the x-direction and y-direction respectively, N is the normal force from wind and self-weight, M is the moment from wind, V is the shear force from wind, $v(z)$ is the shear flow calculated with Equation 5.1, v_{Elastic} is the linear-elastic shear flow and the wall numbers refer to Figure 6.20. Underlined values denotes if the linear-elastic shear flow is greater than the shear flow calculated from the shear force.

WLX						
Wall	N [kN]	M [kNm]	V [kN]	$v(z=0.67L)$ [kN/m]	$v(z=L)$ [kN/m]	v_{Elastic} [kN/m]
1	-5785	11054	738	138	92	105
2	-5903	11126	1072	201	134	145
3	-3305	175	526	394	263	223
4	-2172	176	584	438	292	264
5	-1036	176	584	438	292	264
6	97	175	526	394	263	222
7	-2424	140	357	267	178	171
8	-1522	140	436	327	218	212
9	-622	140	436	327	218	212
10	276	140	356	267	178	171
11	-2772	-1	-13	-13	-9	<u>-48</u>
12	-12329	39	90	21	14	<u>83</u>
13	581	1	13	13	9	<u>39</u>
14	2321	39	-90	-21	-14	<u>-84</u>
WLY						
Wall	N [kN]	M [kNm]	V [kN]	$v(z=0.67L)$ [kN/m]	$v(z=L)$ [kN/m]	v_{Elastic} [kN/m]
1	-9954	0	0	0	0	<u>-58</u>
2	-8739	0	0	0	0	<u>-33</u>
3	-900	2	118	89	59	<u>55</u>
4	-859	1	44	33	22	19
5	-824	-1	-45	-33	-22	-18
6	-795	-2	-118	-89	-59	-55
7	-938	0	4	3	2	<u>17</u>
8	-913	0	2	1	1	<u>8</u>
9	-889	0	-2	-1	-1	<u>-7</u>
10	-868	0	-4	-3	-2	<u>-18</u>
11	-1804	30	150	150	100	<u>73</u>
12	-5161	2468	857	198	132	116
13	-1701	30	150	150	100	81
14	-4709	2468	857	198	132	118

Table 6.10: Cut at 90 meters where WLX and WLY are wind in the x-direction and y-direction respectively, N is the normal force from wind and self-weight, M is the moment from wind, V is the shear force from wind, $v(z)$ is the shear flow calculated with Equation 5.1, v_{Elastic} is the linear-elastic shear flow and the wall numbers refer to Figure 6.20. Underlined values denotes if the linear-elastic shear flow is greater than the shear flow calculated from the shear force.

WLX						
Wall	N [kN]	M [kNm]	V [kN]	$v(z=0.67L)$ [kN/m]	$v(z=L)$ [kN/m]	v_{Elastic} [kN/m]
1	-2732	3264	251	47	31	<u>-83</u>
2	-2760	-3312	-590	-111	-74	<u>-90</u>
3	-1244	-53	-433	-325	-216	-160
4	-893	-53	-472	-354	-236	-207
5	-541	-53	-472	-354	-236	-207
6	-193	-53	-433	-325	-216	-160
11	-1025	1	-44	-44	-29	<u>48</u>
12	-4540	24	-316	-73	-49	<u>-64</u>
13	-4	1	-44	-44	-29	<u>67</u>
14	-41	24	-316	-73	-49	<u>-64</u>
WLY						
Wall	N [kN]	M [kNm]	V [kN]	$v(z=0.67L)$ [kN/m]	$v(z=L)$ [kN/m]	v_{Elastic} [kN/m]
1	-3784	0	0	0	0	<u>74</u>
2	-3493	0	0	0	0	<u>24</u>
3	-564	-1	-64	-48	-32	-38
4	-537	-1	-24	-18	-12	-12
5	-518	1	24	18	12	11
6	-507	1	64	48	32	36
11	-711	-7	-79	-79	-53	-41
12	-2423	611	-442	-102	-68	-47
13	-653	7	79	79	53	38
14	-2175	611	442	102	68	47

If the shear flow calculated with Eurocode is greater than the elastic in both directions the equation can be considered to give a conservative value. This is not always the case, as the linear-elastic shear flow might consist of a peak that can be spread to a larger area. Since the shear flow is spread in the cross-section, the total elastic shear flow in a wall may still be smaller than the shear flow calculated according to Eurocode, which is constant. The Eurocode equation should therefore still be safe to use.

It is difficult to claim that the equation presented by Eurocode always gives a conservative value of the shear flow. However, it seems to be safe to use in most cases. Especially if combining the results from wind in both x- and y-direction. Then only 3% of the linear elastic shear flow exceeds the shear flow calculated with Equation 5.1. What should be kept in mind is that the equation contains an internal lever

arm, z , which does not exist when a section is completely in compression or tension. However, using $z = 0.67h$ should give a conservative shear flow. The fact that it is not conservative in some cases can depend on the mesh size and local effects from slabs. If the model would have a smaller mesh and floor diaphragms, that has no bending stiffness, instead of meshed slabs the results could have been better.

6.9 Vertical displacement

In this section the displacement is analysed and as mentioned in Section 3.5, a construction stage analysis should be performed when designing a high-rise building. The differences between an analysis with and without construction stage regarding deflection are shown in Figures 6.21 and 6.22. The results from the displacement between the two models shows that the deflections at the top storey are smaller with a construction stage analysis. To notice is that the deflections in the columns with construction stage analysis, the maximum deflection occurs in the middle.

6.9.1 Vertical displacement in column

To present the displacement in each step for the construction stage analysis a model of a concrete column with five stories was created, with only self-weight to cause deformations, see Figure 6.23. The elastic strain is calculated with Hooke's law as

$$\epsilon = \frac{\sigma}{E}$$

where:

σ is the stress calculated as: $\sigma = \frac{F}{A}$
 E is the Young's modulus

The force in each element was calculated from the self-weight and acts in the centre of each element due to symmetry. The area of the column is 1 m^2 and the length of each segment is $L=5$ meters. The deformation for the first construction step is presented in Figure 6.24. For the second construction step there are two options available to show, the current step deformation and the summation of the deformations at each node from earlier steps, shown in Figure 6.25. Figure 6.26a shows the step deformation for the last construction step. In Figure 6.26b the summation of the deformations in all earlier construction steps are presented and the deformation at the top of the column is 0.08 millimetres since it only deforms in the last step. In addition, the deformation is greater at the mid-level of the column since the deformations are added from the earlier construction steps. In Figure 6.27, the column with the deformations are shown without a construction stage analysis.

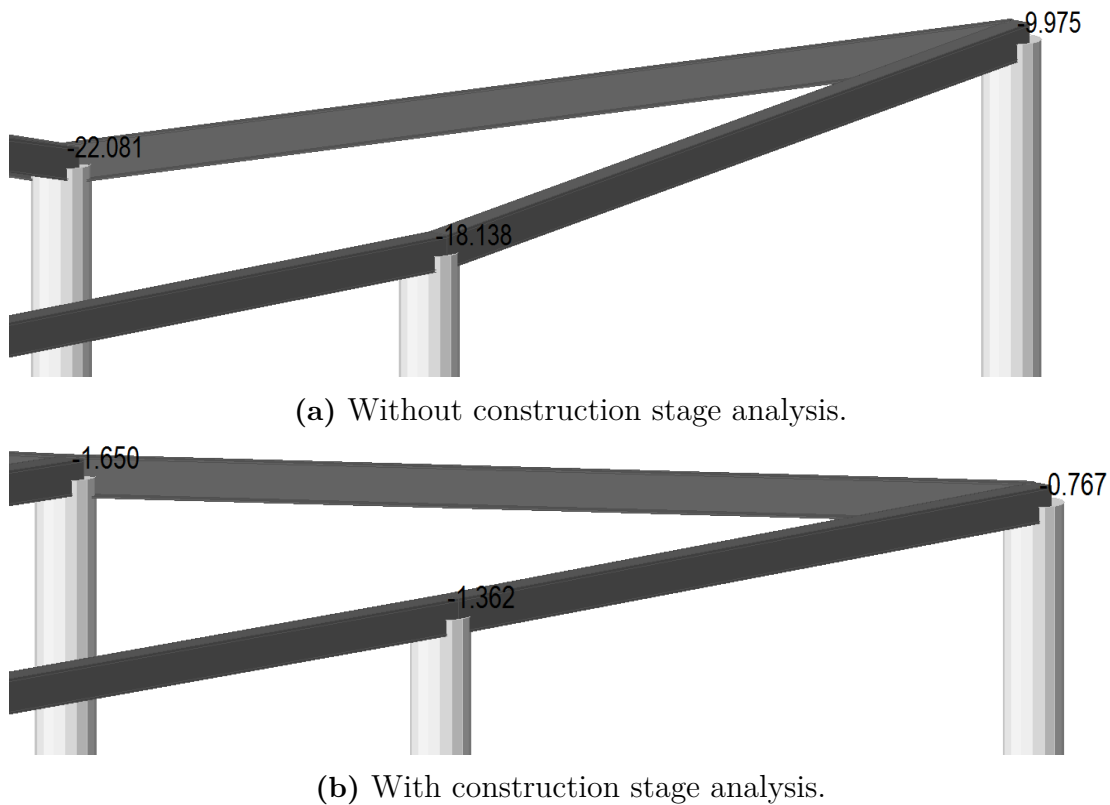
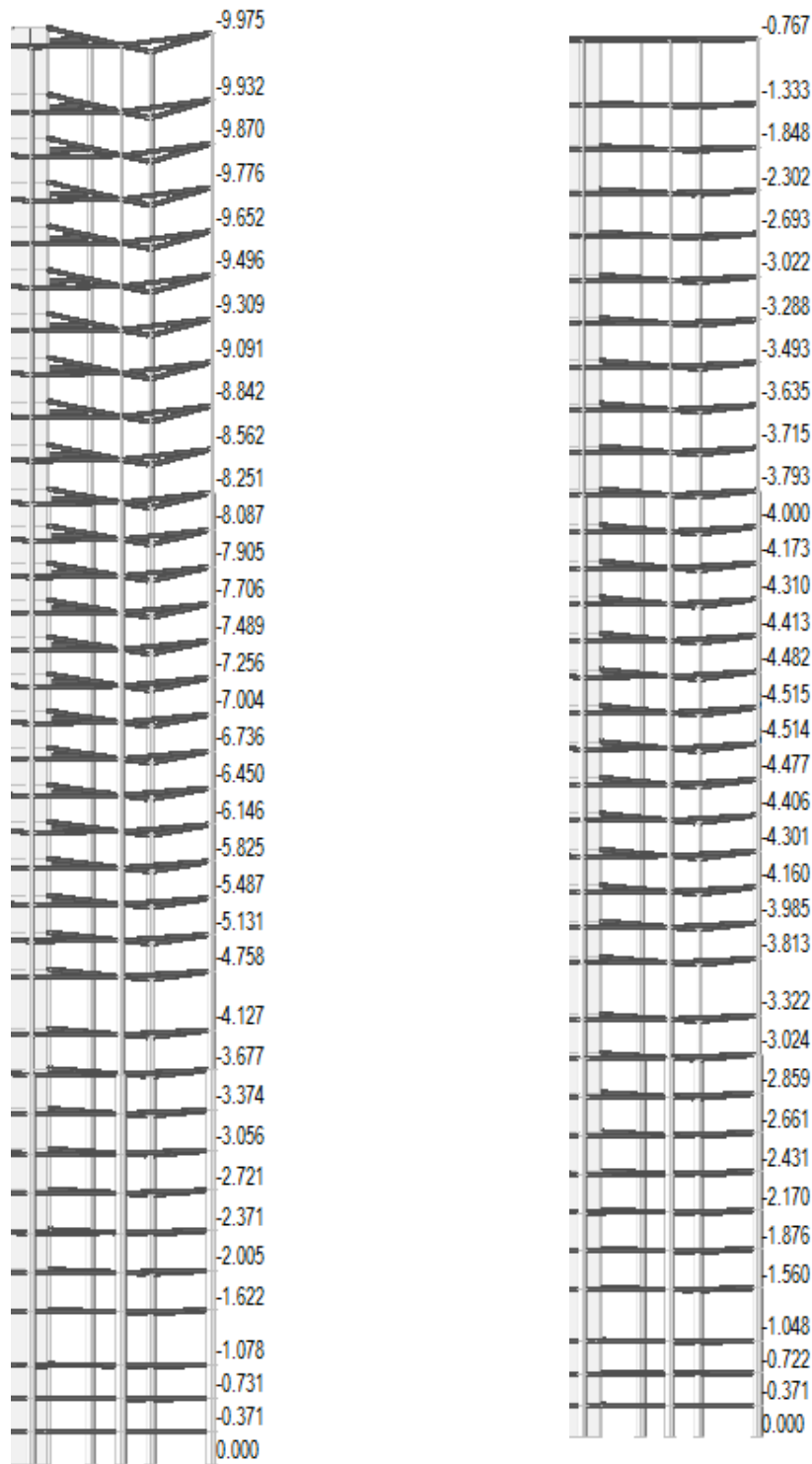


Figure 6.21: Deformation [mm] from self-weight and floor loads. The column is located in position A1, which can be seen in Appendix A.

6.9.2 Discussion of results

The deformations in the column in the example case and the deformations in Göteborg City Gate follows the same trend. By comparing the deformations with and without construction stage analysis it is obvious that the deformation at the top becomes smaller and that the largest deformation occurs in the middle when performing a construction stage analysis. The reason that the deformations are largest at the middle of a structure is that the construction stage adds the deformations from earlier steps in each position and every storey is built at its original level. This means that in the construction stage analysis the deformations that occurred in earlier steps does not affect the new segment. In addition, all segments gets a deformation in each step from the new segment. All nodal deformations for every step is then added together. From this it is possible to find out how much each storey will need to be compensated for on site.



(a) Without construction stage analysis. Maximum deflection at the top storey. (b) With construction stage analysis. Maximum deflection in the middle.

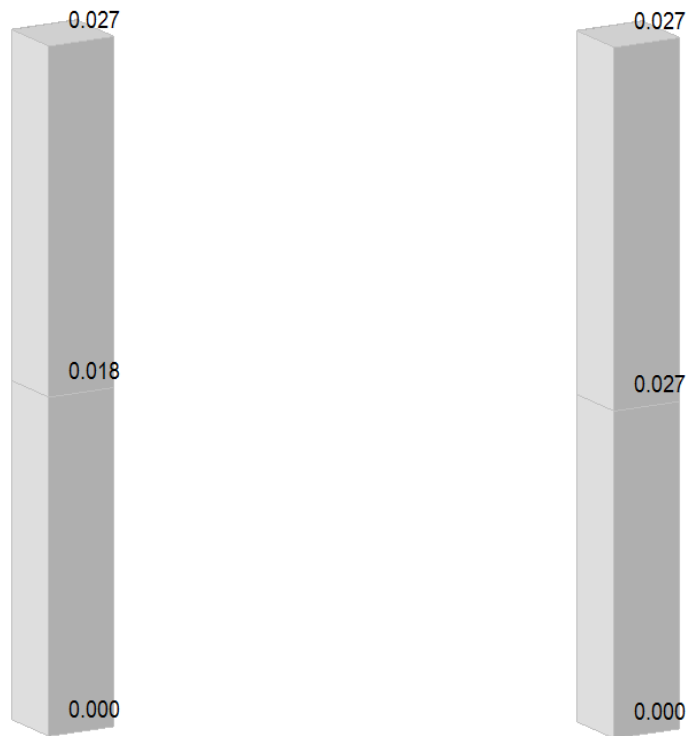
Figure 6.22: Deformed shape from self-weight and floor loads. Deflections [mm] are from column located in position A1, which can be seen in Appendix A.



Figure 6.23: Model of concrete column to demonstrate deformations with construction stage analysis. Each section of the column has a width and depth of 1 meter and a height of 5 meters, giving a total height of 25 meters.

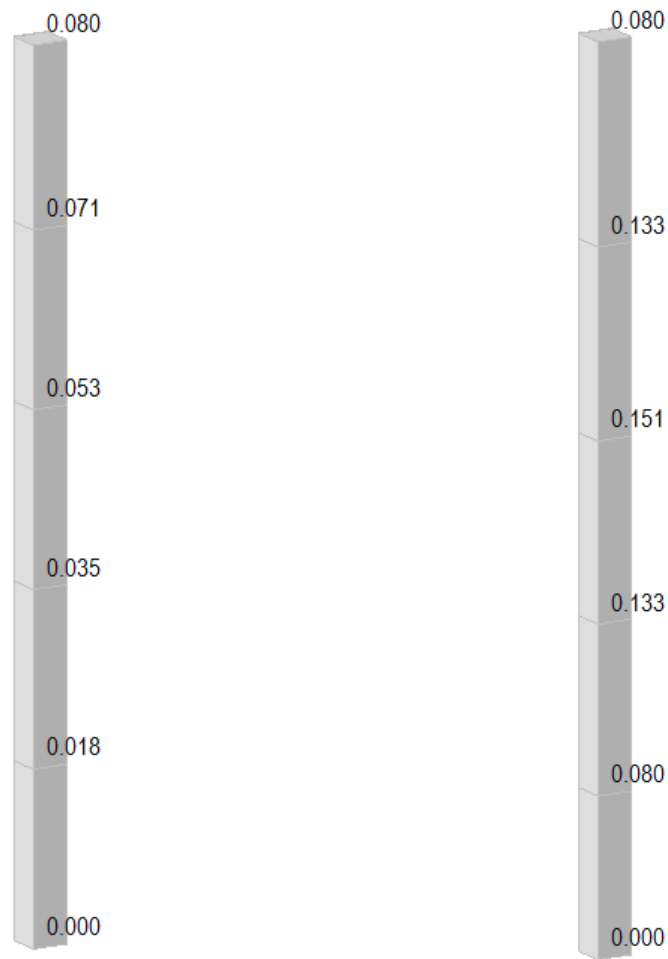


Figure 6.24: Deformation [mm] of column at first construction step. Dimensions are 1x1x5 meters.



(a) Current step deformation for second construction step. **(b)** Summation of deformations at second construction step.

Figure 6.25: Deformation [mm] of column at second construction step. Dimensions are 1x1x10 meters.



(a) Current step deformation for last construction step.

(b) Summation of deformations at last construction step.

Figure 6.26: Deformation [mm] of column at last construction step. Dimensions are 1x1x25 meters.



Figure 6.27: Deformation [mm] of column without construction stage analysis. Dimensions are 1x1x25 meters.

7 Conclusions and further studies

Modelling high-rise buildings in finite element software means dealing with many different problems and difficulties, some of which are evaluated and discussed in this Master's thesis.

Through investigations it is found that when modelling a building, that are to be constructed with prefabricated concrete elements, the use of wall elements is a good way to create a model that represents the buildings global behaviour. This because they are time efficient, both in modelling and analyses, as well as providing reliable results. Hollow-core slabs are commonly used prefabricated slabs and span in one direction. In order to represent the load from these in a finite element model they can be modelled as a one-way floor load. This will provide a proper cumulative load calculation in order to design the foundation. For vertical and horizontal loads on a building, advantage can be taken to study each load-case separately. The force distributions and reaction forces due to vertical loading should be analysed without the consideration of floor diaphragms. This because the floor diaphragms are very stiff and can thereby redistribute forces latterly between elements in a building, resulting in unwanted shear forces and misleading results. When analysing horizontal load, however, the consideration of floor diaphragms are very useful. This because they have diaphragm action, transferring the horizontal forces to the stabilising units.

Studying a building more in detail, such as the forces between prefabricated elements, which requires calculations of the shear flow to design the connections, a meshed model of the building is recommended. Advantage with a meshed model is that the shear flow is provided directly, which is efficient when a building is geometrically complex and the force distribution is difficult to interpret. However, it is difficult and time consuming to model a building with a sufficiently dense mesh. If the mesh has not converged, i.e. not providing the same result as a courser mesh, influence from slabs and point loads will result in local effects. These effects are difficult to interpret and can give unreliable results. On the other hand, for simpler structures where the force distribution is easy to calculate, the shear flow can be calculated directly from the shear forces in a model with wall elements.

Dynamic response to wind-loads and resonance frequencies should be evaluated when designing high-rise buildings. However, when calculating the resonance frequencies, issues may occur when defining the mass and stiffness of the buildings. This, especially when modelling with floor-load, since they are loads and therefore not considered in an eigenfrequency analysis. Regarding the accelerations of a building

in a finite element software, issues occur when describing the wind-load as a time-history function. This, because the time-history function is obtained by solving the buildings equation of motion, which for complex and large structure are difficult, or by performing a wind-tunnel experiment. However, Eurocode [31] provides an alternative method to estimate the along-wind acceleration and Stafford Smith & Coull [34] presents a method to estimate the across-wind acceleration.

Due to the limited time of the Master's thesis and the complexity of both global and material behaviour, more investigations are needed regarding structural design of high-rise buildings. Especially when analysing the shear flow in complex geometric structures, where the force distribution is difficult to establish. This, in addition with the non-linear behaviour of cracked concrete and possible redistribution of forces caused by changes in stiffness. Regarding dynamic analyses, such as the accelerations of a building, further investigations can be made to describe wind-loads as time-history functions, for use in finite element software.

Bibliography

- [1] Peter Adler. *Bygga industrialiserat*. Lund: AB Svensk Byggtjänst, 2005.
- [2] *Advanced structural forms*. URL: <http://pentscivil.blogspot.se/2011/07/advanced-structural-forms.html> (visited on 05/25/2016).
- [3] R. B. Agarwal. *CHAPTER 4 1-BEAM ELEMENT, ME 273 Lecture Notes*. URL: <http://www.engr.sjsu.edu/ragarwal/ME273/pdf/Chapter%204%20-%20Beam%20Element.pdf> (visited on 04/13/2016).
- [4] K-J. Bathe. *Finite element procedures*. New York: Prentice Hall, 2006.
- [5] Biography.com. *Alexander Graham Bell Biography*. URL: <http://www.biography.com/people/alexander-graham-bell-9205497> (visited on 02/22/2016).
- [6] Boverket. *Boverkets föreskrifter och allmänna råd om tillämpning av europeiska konstruktionsstandarder*. Tech. rep. BFS 2015:6 EKS 10. Boverket, 2015.
- [7] A.S.G Bruggeling and G.F Huyghe. *Prefabrication with concrete*. Rotterdam: A.A. Balkema, 1991.
- [8] Byggnyheter.se. *Henning Larsen Architects*. 2015. URL: <http://www.byggnyheter.se/2015/05/henning-larsen-architects-ritar-nytt-h-ghus-i-g-teborg> (visited on 03/11/2016).
- [9] Andrew Charleson. *Seismic Design for Architects*. 2008. URL: <http://www.nexus.globalquakemodel.org/gem-building-taxonomy/overview/glossary/braced-frame--lfbr> (visited on 03/25/2016).
- [10] Anil.K Chopra. *Dynamics of Structures, Theory and Applications to Earthquake Engineering*. Englewood Cliffs, New Jersey: Prentice Hall, 1995.
- [11] Gulf Construction. *Precast concrete*. 2014. URL: http://www.gulfconstructiononline.com/news/160379_BPC-claims-record-with-tallest-precast-building.html (visited on 02/23/2016).
- [12] Roy R. Craig and Andrew J. Kurdila. *Fundamentals of Structural Dynamics*. Second edition. New Jersey: John Wiley & Sons, 2006.
- [13] CTBUH. *Burj Khalifa*. URL: <http://skyscrapercenter.com/building/burj-khalifa/3> (visited on 02/23/2016).
- [14] CTBUH. *Council of Tall Buildings and Urban Habitat: Height Criteria*. URL: <http://www.ctbuh.org/TallBuildings/HeightStatistics/Criteria/tabid/446/language/en-US/Default.aspx> (visited on 02/22/2016).
- [15] CTBUH. *Council of Tall Buildings and Urban Habitat: Tall Buildings in Numbers*. 2010. URL: www.ctbuh.org/LinkClick.aspx?fileticket=rlKQFdZyhwg%3D (visited on 02/23/2016).
- [16] Johann Eisele and Ellen Kloft. *High-Rise Manual*. Birkhäuser Verlag AG, 2003.
- [17] Rafik R. Gerges and Kal Benuska. "Across-Wind Response of High-Rise Buildings". In: *STRUCTURE magazine* (2013), pp. 8–10.

- [18] Marshall Gerometta. *Council of Tall Buildings and Urban Habitat, Height: The History of Measuring Tall Buildings*. Dec. 2009. URL: <http://www.ctbuh.org/AboutCTBUH/History/MeasuringTall/tabid/1320/language/en-US/Default.aspx> (visited on 02/23/2016).
- [19] History.com. *Home Insurance Building*. 2010. URL: <http://www.history.com/topics/home-insurance-building> (visited on 02/22/2016).
- [20] HSB. *Några fakta om Turning Torso*. 2015. URL: <https://www.hsb.se/malmo/om-boende/vara-hyresratter/malmo-landmarke-turning-torso/nagra-fakta-om-turning-torso/> (visited on 02/22/2016).
- [21] Tord Isaksson and Annika Mårtensson. *Byggkonstruktion, Regel- och formelsamling*. Second edition. Lund: Studentlitteratur AB, 2010.
- [22] Mogens Lorentsen, Tage Petersson, and Håkan Sundquist. *Stabilisering av byggnader*. Stockholm, Sweden, 1995.
- [23] Gui-Niu Mao, Xiao-Lei Han, and Xue-Wei Chen. *WIND LOAD SIMULATION AND WIND-INDUCED VIBRATION TIME-HISTORY ANALYSIS OF TALL BUILDING STRUCTURES*. Tech. rep. China: International Symposium on Innovation & Sustainability of Structures in Civil Engineering, 2009.
- [24] Ltd Midas Information Technology Co. *Midas Gen On-line manual*. 2015. URL: manual.midasuser.com/EN_Common/Gen/845/index.htm (visited on 05/05/2016).
- [25] *Most Efficient Structural System Against Wind Loads*. URL: <http://www.whatsonthere.com/2012/02/23/most-efficient-structural-system-against-wind-loads/> (visited on 05/25/2016).
- [26] Ola Nylander. *Svensk Bostad 1850-2000*. Lund: Studentlitteratur AB, 2013.
- [27] Otis. *Otis historia*. URL: <http://www.otis.com/site/se/Pages/OtisHistory.aspx?menuID=6> (visited on 02/22/2016).
- [28] Ove Pettersson. *Knäckning*. Tech. rep. Bulletin 24. Lund, Sweden: Division of Structural Mechanics, Lund Institute of Technology, 1971.
- [29] Guenter Axel Rombach. *Finite-element design of concrete structures, Practical problems and their solutions*. Second edition. 40 Marsh Wall, London E14 9TP: Institution of Civil Engineers (ICE) Publishing, 2011.
- [30] SIS. *Eurocode 1: Actions on structures - Part 1-1: General actions - Densities, self-weight, imposed loads for buildings*. Tech. rep. SS-EN 1991-1-1. Swedish Standards Institute, 2002.
- [31] SIS. *Eurocode 1: Actions on structures 1-Part 1-4: General actions 1-Wind actions*. Tech. rep. SS-EN 1991-1-4:2005. Swedish Standards Institute, 2005.
- [32] SIS. *Eurocode 2: Design of concrete structures 1-Part 1-1: General rules and rules for buildings*. Tech. rep. SS-EN 1992-1-1:2005. Swedish Standards Institute, 2005.
- [33] SIS. *Bases for design of structures 1-Serviceability of buildings and walkways against vibration*. Tech. rep. SS-ISO 10137:2008. Swedish Standards Institute, 2008.
- [34] Bryan Stafford Smith and Alex Coull. *Tall Building Structures: Analysis and Design*. USA: Wiley-Interscience publication, 1991.

- [35] *Structural Forms Systems for Tall Building Structures*. URL: <http://www.internationaljournalssrg.org/IJCE/2014/Volume1-Issue4/IJCE-V1I4P106.pdf> (visited on 03/27/2016).
- [36] Bungale S. Taranath. *Structural Analysis and Design of Tall Buildings, Steel and Composite Construction*. 6000 Broken Sound Parkway NW, Suite 300 Boca Raton, FL 33487-2742: CRC Press, 2011.
- [37] OC. Zienkiewicz and RL. Taylor. *The finite element method*. Volume 1 and 2. London: MacGraw Hill, 1994.

A Drawings of Göteborg City Gate

Table A.1: Explanations to drawings.

V1	Wall, concrete, thickness 550 mm
V2	Wall, concrete, thickness 450 mm
V3	Wall, concrete, thickness 350 mm
V4	Wall, concrete, thickness 300 mm
P1	Column, concrete, diameter 1000 mm
P2	Column, concrete, diameter 800 mm
P3	Column, concrete, diameter 600 mm
B1	Beam, Steel, HSQ, see Figure A.1
B2	Beam Steel, UPE, see Figure A.2

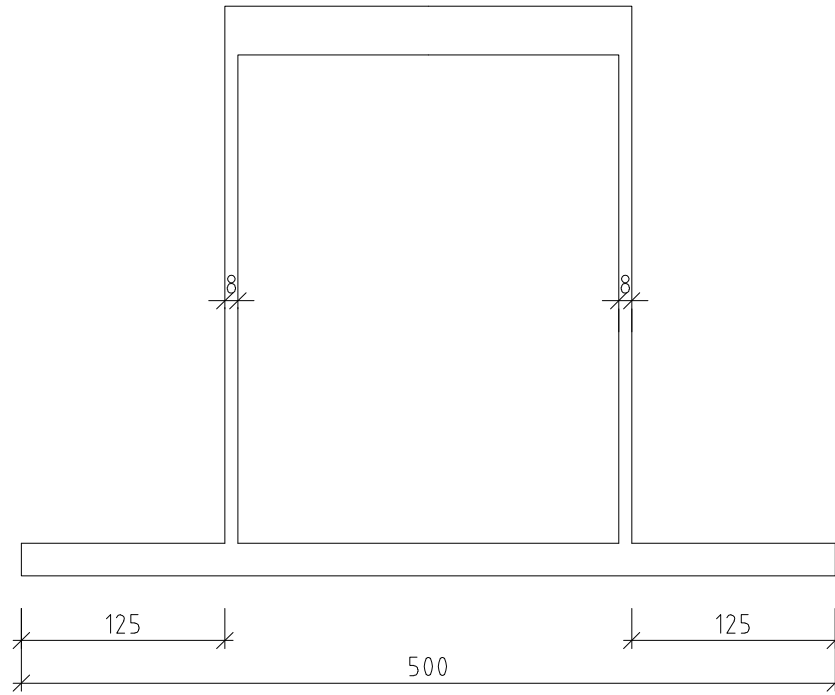


Figure A.1: HSQ-beam.

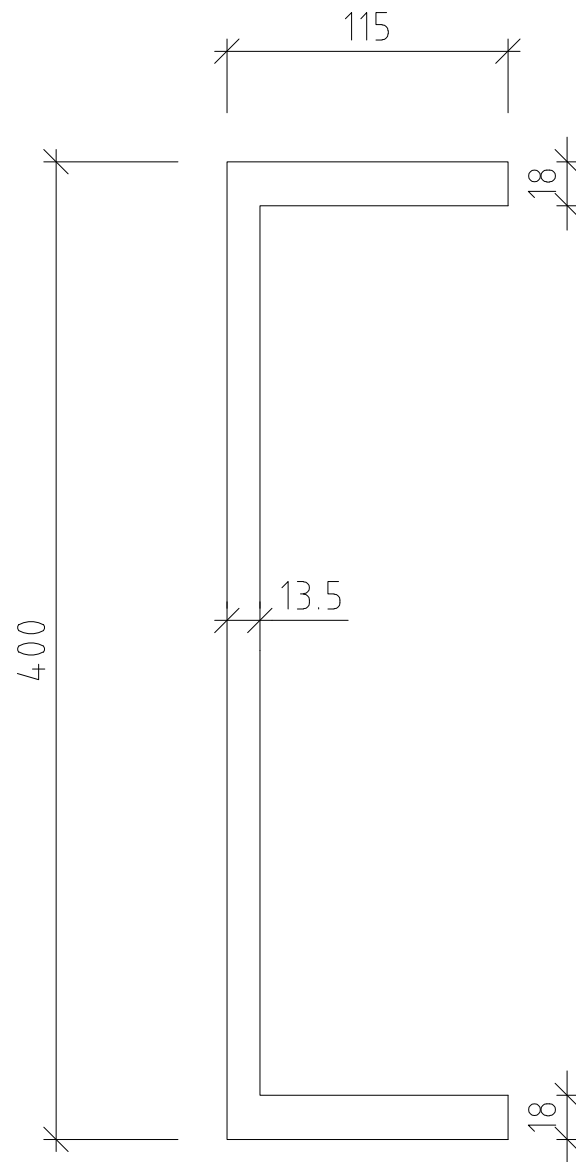


Figure A.2: UPE-beam.

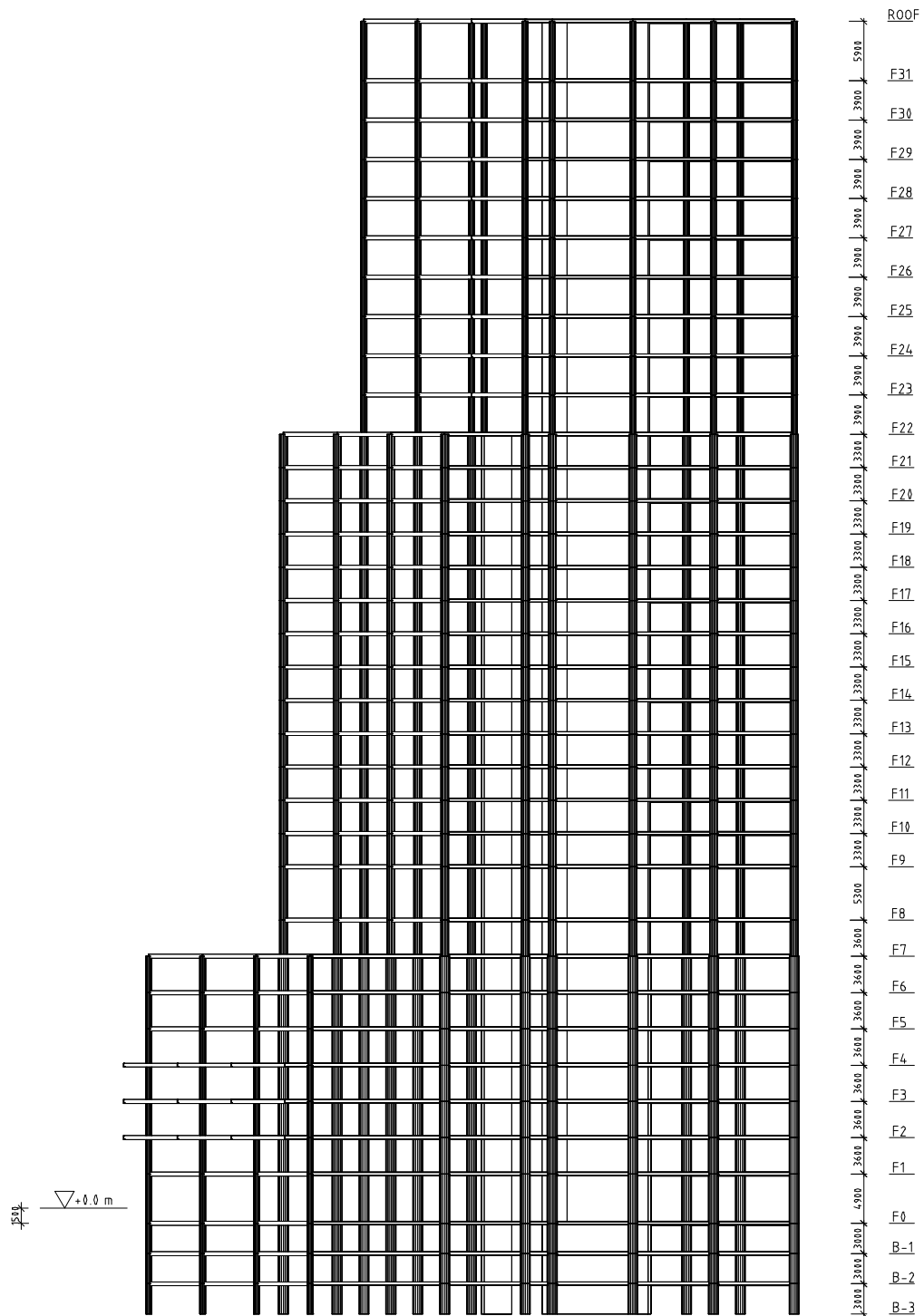


Figure A.3: View in x-direction.

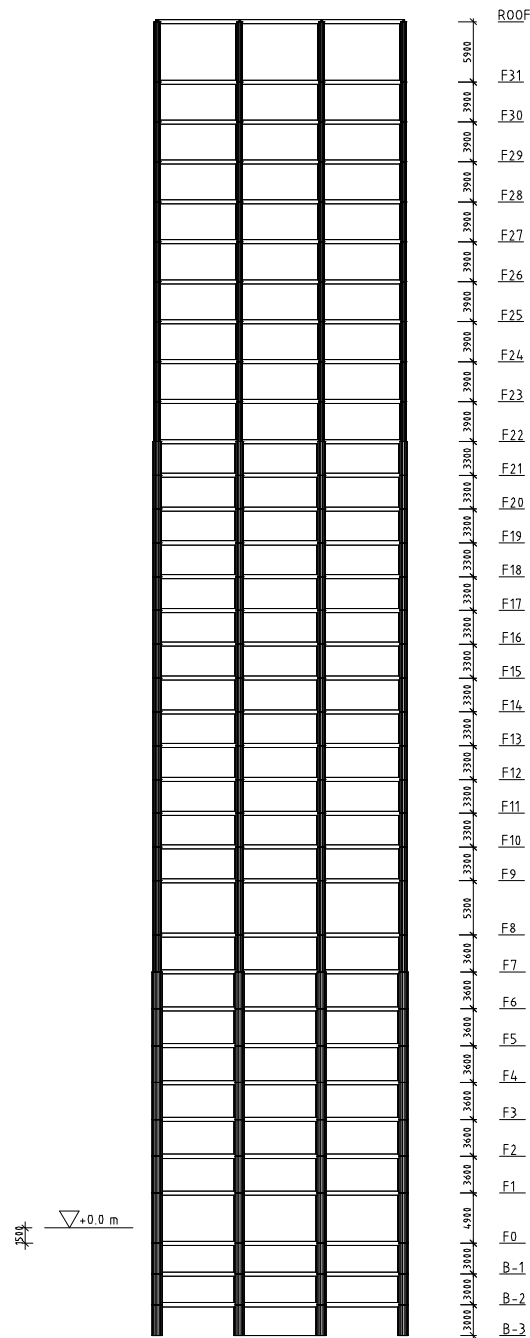


Figure A.4: View in y-direction.

A. Drawings of Göteborg City Gate

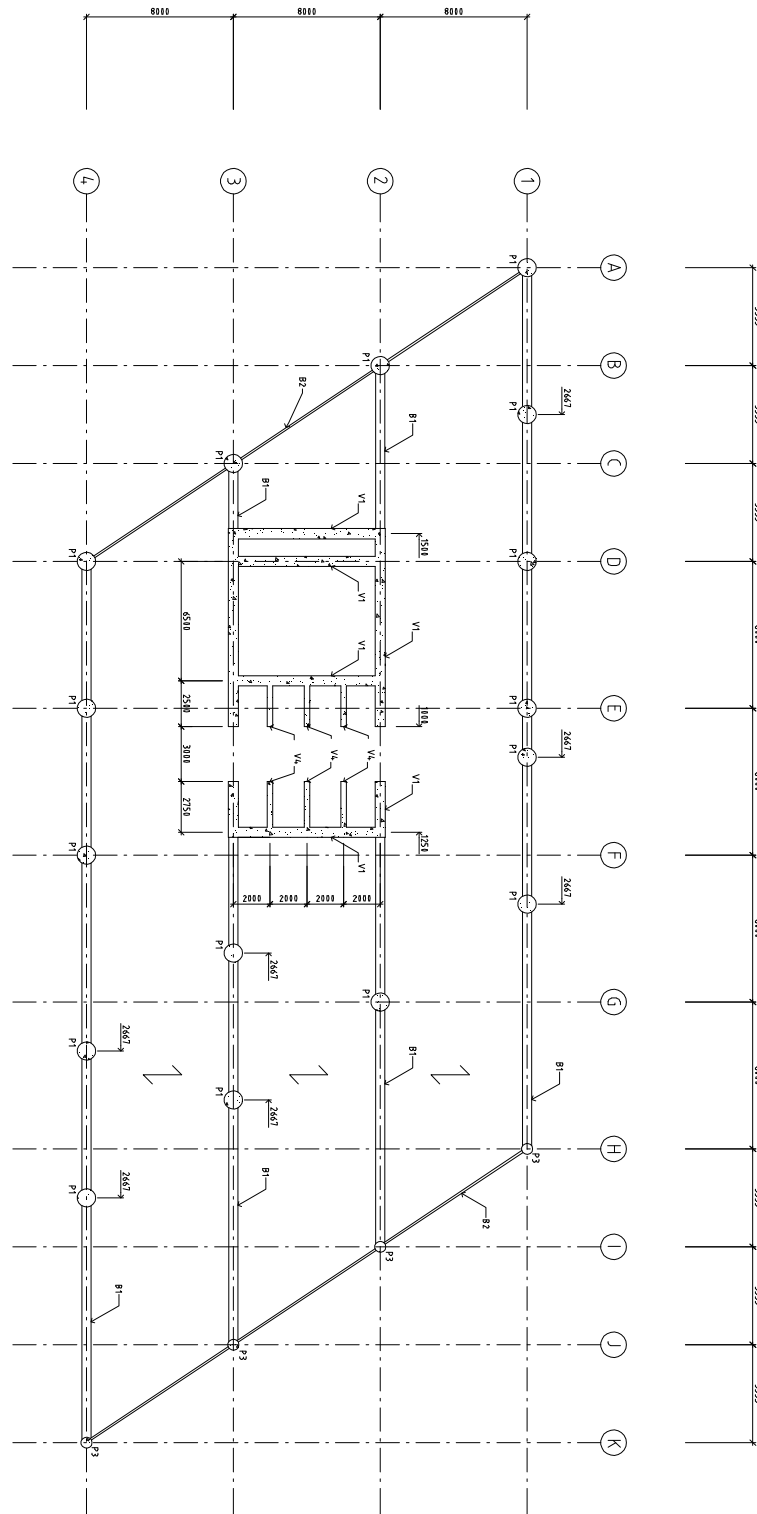


Figure A.5: Floor plan of storey B-3 to F1 and F5 to F7 in Figure A.3 and A.4, see Table A.1 for explanations.

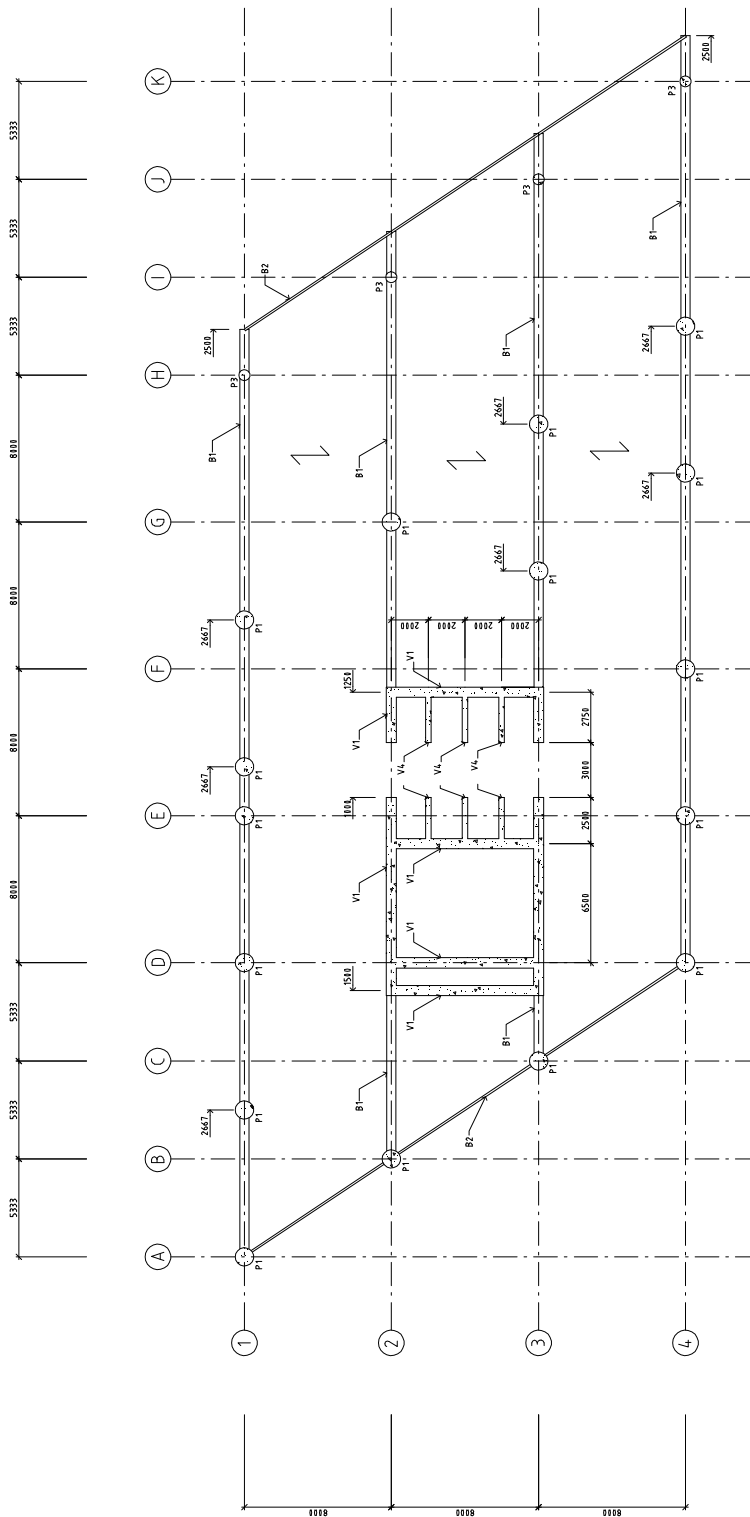


Figure A.6: Floor plan of storey F2 to F4 in Figure A.3 and A.4, see Table A.1 for explanations.

A. Drawings of Göteborg City Gate

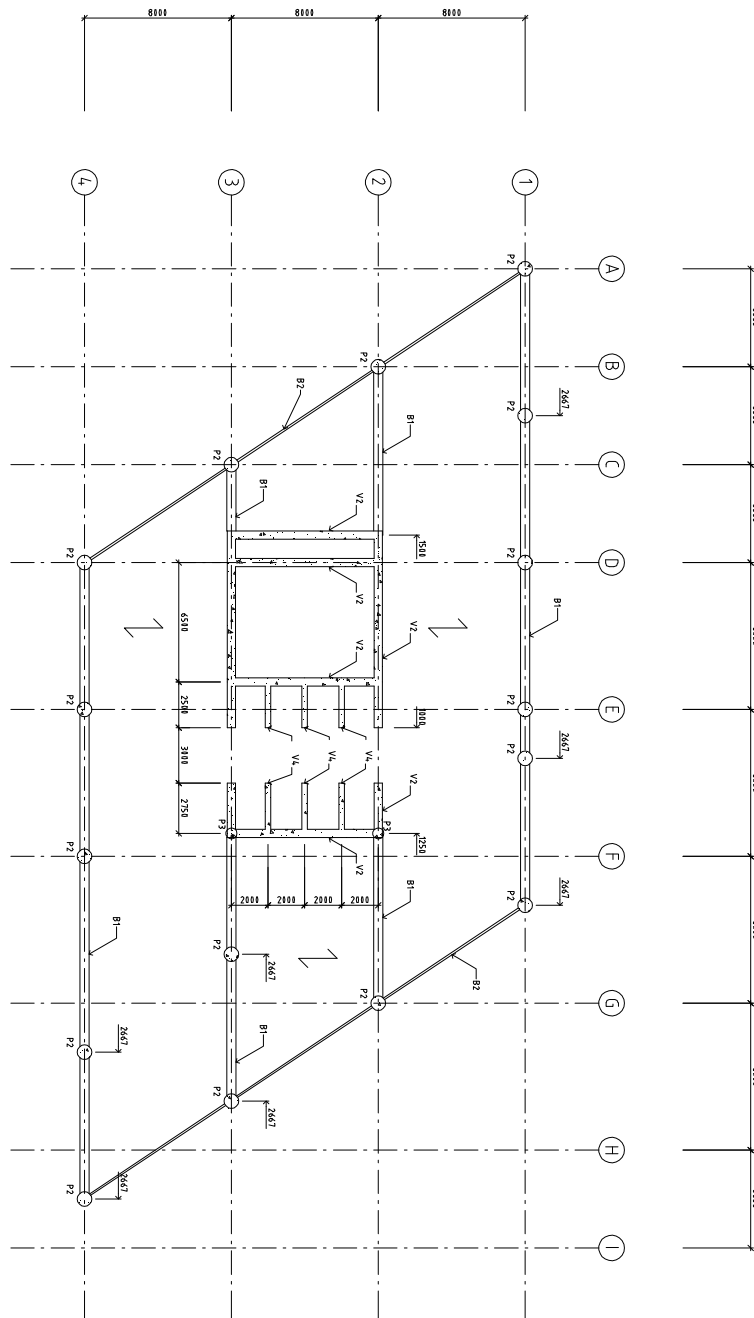


Figure A.7: Floor plan of storey F8 to F22 in Figure A.3 and A.4, see Table A.1 for explanations.

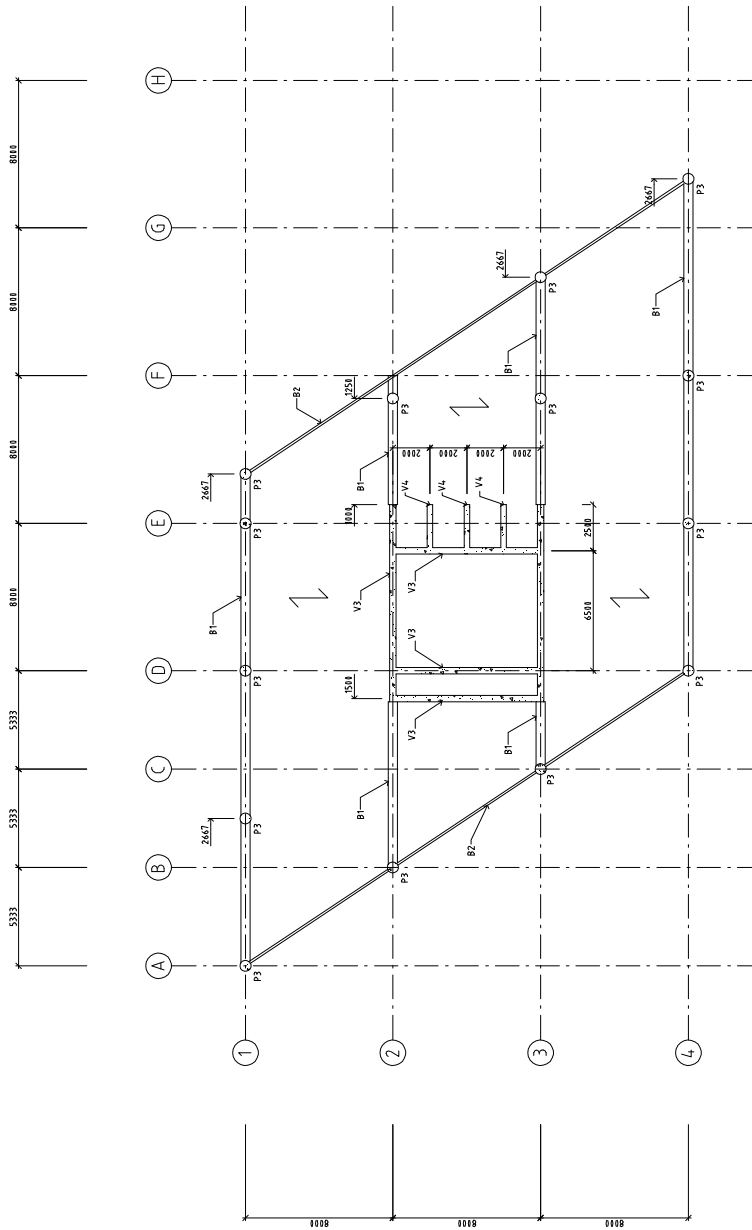


Figure A.8: Floor plan of storey F23 to ROOF in Figure A.3 and A.4, see Table A.1 for explanations.

B Static wind-load - Strictly according to EC

Table B.1: Input for calculations of static wind-load strictly according to EC.

C_{dir}	1	z_0 [m]	0.3
C_{season}	1	z_{min} [m]	5
$v_{b,0}$ [m/s]	25	z_{max} [m]	200
v_b [m/s]	25	z_s [m]	72.48
Terrain category	3	$c_0(z_s)$	1
k_r	0.22	$c_r(z_s)$	1.18
k_l	1	$V_m(z_s)$ [m/s]	29.5
σ_v	5.38	$I_v(z_s)$	0.18
Height [m]	120.8	$L(z_s)$ [m]	161.6
Depth [m]	24	B^2	0.51
Width [m]	64	c_s	0.84
λ	2.64		
Ψ_λ	1		
ρ [kg/m ³]	1.25		
d/b	0.375		

C Static wind-load with no c_s factor

Table C.1: Input for calculations of static wind-load strictly according to EC.

C_{dir}	1	z_0 [m]	0.3
C_{season}	1	z_{min} [m]	5
$v_{b,0}$ [m/s]	25	z_{max} [m]	200
v_b [m/s]	25	z_s [m]	72.48
Terrain category	3	$c_0(z_s)$	1
k_r	0.22	$c_r(z_s)$	1.18
k_l	1	$V_m(z_s)$ [m/s]	29.5
σ_v	5.38	$I_v(z_s)$	0.18
Height [m]	120.8	$L(z_s)$ [m]	161.6
Depth [m]	24	B^2	0.51
Width [m]	64	c_s	1.0
λ	2.64		
Ψ_λ	1		
ρ [kg/m ³]	1.25		
d/b	0.375		

D Static wind-load with τ factor

Table D.1: Input for calculations of static wind-load strictly according to EC.

C_{dir}	1	z_0 [m]	0.3
C_{season}	1	z_{min} [m]	5
$v_{\text{b},0}$ [m/s]	25	z_{max} [m]	200
v_{b} [m/s]	25	z_{s} [m]	72.48
Terrain category	3	$c_0(z_{\text{s}})$	1
k_{r}	0.22	$c_{\text{r}}(z_{\text{s}})$	1.18
k_{l}	1	$V_{\text{m}}(z_{\text{s}})$ [m/s]	29.5
σ_{v}	5.38	$I_{\text{v}}(z_{\text{s}})$	0.18
Height [m]	120.8	$L(z_{\text{s}})$ [m]	161.6
Depth [m]	24	B^2	0.51
Width [m]	64	c_{s}	1.0
λ	2.64		
Ψ_{λ}	1		
ρ [kg/m ³]	1.25		
d/b	0.375		

E Wind-load according to EKS10

Table E.1: Input for calculations of static wind-load according to EKS10.

v_b [m/s]	25
Terrain category	3
Height [m]	120.8
Depth [m]	24
Width [m]	64

F Dynamic wind-load

Table F.1: Input values for calculations of dynamic wind-load.

δ_s	0.10	$V_m(z_s)$ [m]	29.55
δ_d	0	$L(z_s)$ [m]	161.55
ρ [kg/m ³]	1.25	$f_L(z_s, n)$	1.80
$E_{concrete}$ [GPa]	35.22	$S_L(z_s)$	0.09
$n_{1,x}$ [Hz]	0.33	$I_v(z_s)$	0.18
m_e [kg/m]	179359	B^2	0.51
Height [m]	120.8	η_h	6.21
Width [m]	64	η_b	3.29
z_0 [m]	0.3	R_h	0.15
z_{min} [m]	5	R_b	0.26
z_s [m]	72.48	c_s	0.84

Table F.2: Base shear and overturning moment for dynamic wind-load calculations.

Storey	F_w [kN]	Moment [kNm]
Foundation	44.4	0.0
0	189.6	284.4
1	286.4	1832.8
2	298.0	2979.7
3	326.1	4435.2
4	345.6	5944.6
5	368.1	7655.7
6	348.0	8491.3
7	322.2	9020.7
8	413.1	13055.2
9	418.0	15423.9
10	328.9	13220.2
11	336.4	14632.3
12	343.4	16071.1
13	350.0	17535.1
14	356.2	19022.7
15	362.1	20532.5
16	367.7	22063.5
17	373.1	23614.6
18	378.2	25184.8
19	383.0	26773.3
20	387.7	28379.3
21	392.2	30002.1
22	395.8	31584.6
23	400.0	33478.2
24	404.7	35448.8
25	204.6	18719.6
26	206.8	19724.5
27	208.8	20738.5
28	210.9	21761.4
29	212.8	22792.8
30	214.7	23832.6
31	216.5	24880.4
Roof	331.6	40059.7
Base shear:	10725	
Overturning moment:		619176

G Deflection

The deflection at the top of the building is calculated in order to compare with the deflection given from the model in Midas. The deflection is calculated with load-cases from Isaksson [21] where each storey represents a cantilever beam fixed in one end and free in the other. The free-end is exposed for a point-load from the wind acting on the facade of the building. For calculation model see Figure G.1.

The deflection v_b for each storey is calculated as

$$v_B = \frac{PL^3}{3EI}$$

The buildings top deflection is then super positioned for each storey to get the total deflection. In addition, the contribution from the angle is also considered when calculating the deflection. The angle is calculated for each storey and then multiplied with the length from that storey to the top of the building, see Figure G.2.

The angle at the top of each storey is calculated as

$$\theta_B = \frac{PL_e^2}{2EI}$$

Since the angle, θ_B , is small the deflection at the top, v_{top} , can be calculated as

$$v_{top} = \theta_B * L$$

Both the contribution from deflection as well as the deflection from the angle is calculated for each storey in Table G.1 and then summarised to get the total deflection at the top of the building to: $v_{top} = 0.2533$ m. A verification of this was also made in the software Frame Analysis with a model as similar as possible to the Midas Gen model. The result from this is shown in Figure G.3.

The deflection was calculated in Midas Gen as well. For this a meshed plate model was used with fixed beams between the cores. The Result from this is shown in Table G.2

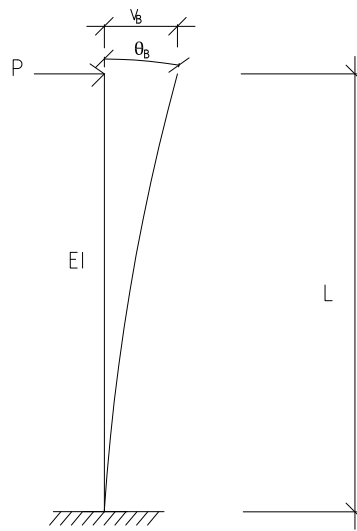


Figure G.1: Calculation model for deflection of a fixed cantilever beam exposed to point-load at free end.

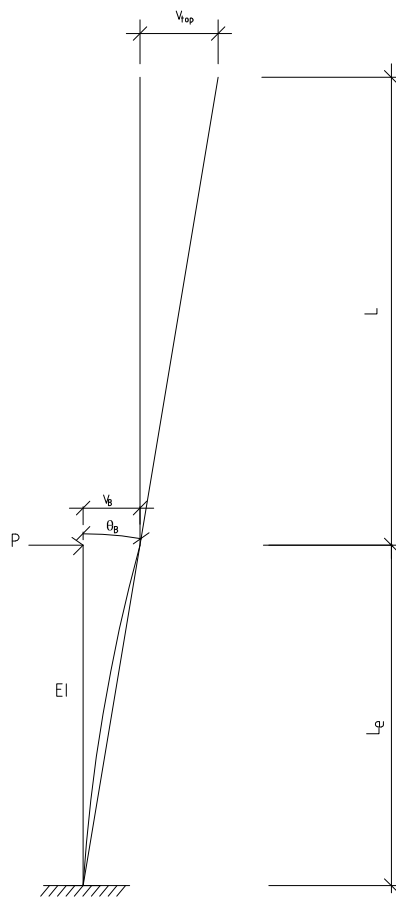


Figure G.2: Calculation model for deflection at top from contribution of the angle on each storey.

Table G.1: Deflection calculated for top of the building. Contribution from deflection and angle for each storey.

Height [m]	Force [kN]	EI [kNm ²]	Deflection [m]	Deflection θ [m]
0	0.0	11976913200	0	0
1.5	433.7	11976913200	0.0000	4.8600E-06
6.4	515.6	11976913200	0.0000	1.0086E-04
10	445.3	11976913200	0.0000	2.0598E-04
13.6	453.8	11976913200	0.0000	3.7563E-04
17.2	445.3	11976913200	0.0001	5.6976E-04
20.8	436.8	11976913200	0.0001	7.8892E-04
24.4	436.8	11976913200	0.0002	1.0466E-03
28	391.3	11976913200	0.0002	1.1883E-03
31.6	427.4	9876392400	0.0004	1.6217E-03
36.9	413.0	9876392400	0.0006	2.0567E-03
40.2	316.9	9876392400	0.0006	1.8201E-03
43.5	316.9	9876392400	0.0008	2.0641E-03
46.8	316.9	9876392400	0.0010	2.3067E-03
50.1	317.8	9876392400	0.0012	2.5518E-03
53.4	320.0	9876392400	0.0015	2.8012E-03
56.7	322.5	9876392400	0.0018	3.0448E-03
60	324.8	9876392400	0.0022	3.2741E-03
63.3	327.0	9876392400	0.0026	3.4862E-03
66.6	341.4	9876392400	0.0031	3.8141E-03
69.9	354.7	9876392400	0.0038	4.1153E-03
73.2	354.7	9876392400	0.0043	4.2354E-03
76.5	354.7	9876392400	0.0050	4.3192E-03
79.8	353.9	9876392400	0.0056	4.3530E-03
83.7	353.0	5229817800	0.0067	4.4269E-03
87.6	353.0	5229817800	0.0078	4.4372E-03
91.5	353.0	5229817800	0.0091	4.3624E-03
95.4	353.0	5229817800	0.0105	4.1920E-03
99.3	353.0	5229817800	0.0121	3.9156E-03
103.2	353.0	5229817800	0.0138	3.5223E-03
107.1	353.0	5229817800	0.0156	3.0014E-03
111	353.0	5229817800	0.0177	2.3419E-03
114.9	443.0	5229817800	0.0250	1.9237E-03
120.8	267.0	5229817800	0.0179	0

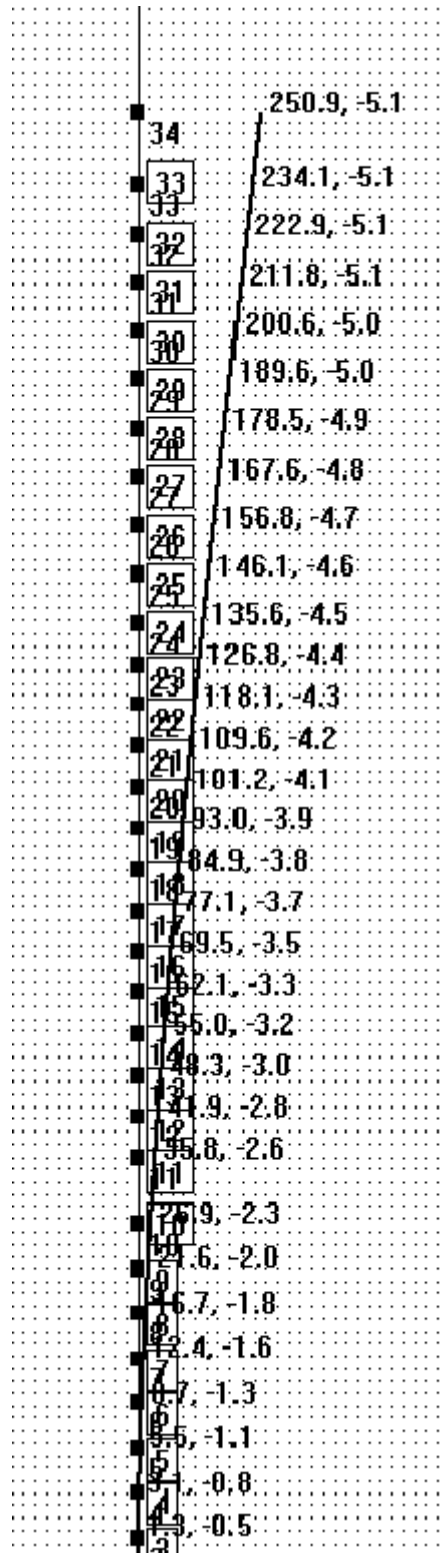


Figure G.3: Deflection calculated in Frame analysis. [mm]

Table G.2: Deflection calculated in Midas Gen with a model with plate elements with a mesh of 1 m.

Load Case	Story	Level [m]	Height [m]	Maximum Displacement [m]	Average Displacement [m]
WLX	Roof	119.3	120.8	0.271	0.261
WLX	33F	113.4	114.9	0.256	0.246
WLX	32F	109.5	111	0.246	0.235
WLX	31F	105.6	107.1	0.235	0.225
WLX	30F	101.7	103.2	0.225	0.215
WLX	29F	97.8	99.3	0.214	0.204
WLX	28F	93.9	95.4	0.204	0.194
WLX	27F	90	91.5	0.193	0.184
WLX	26F	86.1	87.6	0.183	0.174
WLX	25F	82.2	83.7	0.172	0.163
WLX	24F	78.3	79.8	0.165	0.155
WLX	23F	75	76.5	0.157	0.147
WLX	22F	71.7	73.2	0.149	0.138
WLX	21F	68.4	69.9	0.141	0.130
WLX	20F	65.1	66.6	0.133	0.122
WLX	19F	61.8	63.3	0.124	0.114
WLX	18F	58.5	60	0.116	0.106
WLX	17F	55.2	56.7	0.108	0.098
WLX	16F	51.9	53.4	0.100	0.091
WLX	15F	48.6	50.1	0.093	0.083
WLX	14F	45.3	46.8	0.085	0.076
WLX	13F	42	43.5	0.078	0.069
WLX	12F	38.7	40.2	0.070	0.062
WLX	11F	35.4	36.9	0.063	0.055
WLX	10F	30.1	31.6	0.052	0.045
WLX	9F	26.5	28	0.049	0.040
WLX	8F	22.9	24.4	0.042	0.034
WLX	7F	19.3	20.8	0.036	0.028
WLX	6F	15.7	17.2	0.030	0.023
WLX	5F	12.1	13.6	0.024	0.018
WLX	4F	8.5	10	0.018	0.014
WLX	3F	6.7	8.2	0.013	0.010
WLX	2F	4.9	6.4	0.013	0.009
WLX	1F	0	1.5	0.007	0.005
WLX	B1	-3	-1.5	0.005	0.003
WLX	B2	-6	-4.5	0.002	0.001
WLX	B3	-9	-7.5	-0.001	0.000

H Vianello method

The calculations for the Vianello method are presented in this Appendix. In Table H.1 are the input used in the calculations followed by the iterations used to calculate the critical load.

Table H.1: Input for calculations of critical load according to Vianello.

Height bottom part [m]	27.3
Height middle part [m]	77.9
Height top part [m]	27.3
Total height [m]	120.8
Moment of inertia bottom part, weak direction [m ⁴]	340.1
Moment of inertia middle part, weak direction [m ⁴]	280.4
Moment of inertia top part, weak direction [m ⁴]	168.5
Young's modulus, concrete [GPa]	35.22

Table H.2: Final Vianello iteration

Storey	Height [m]	v'	v _{calc}	v _a /v _{calc}
0	0	0.00	0.00	
1	3.9	7.41	7.41	0.256
2	7.8	21.24	28.65	0.256
3	11.7	34.11	62.76	0.256
4	15.6	46.07	108.83	0.256
5	19.5	57.15	165.98	0.256
6	23.4	67.41	233.39	0.256
7	27.3	76.89	310.29	0.256
8	31.2	86.47	396.76	0.256
9	35.1	96.23	492.98	0.256
10	39.0	105.19	598.17	0.256
11	42.9	113.41	711.58	0.256
12	46.8	120.94	832.51	0.256
13	50.7	127.67	960.18	0.256
14	54.6	133.52	1093.70	0.256
15	58.5	138.56	1232.26	0.256
16	62.3	142.86	1375.12	0.256
17	66.2	146.49	1521.61	0.256
18	70.1	149.52	1671.13	0.256
19	74.0	152.03	1823.16	0.256
20	77.9	154.07	1977.23	0.256
21	81.8	155.87	2133.10	0.256
22	85.7	158.02	2291.12	0.256
23	89.6	159.68	2450.80	0.256
24	93.5	160.95	2611.76	0.256
25	97.4	161.90	2773.65	0.256
26	101.3	162.55	2936.20	0.256
27	105.2	162.95	3099.15	0.256
28	109.1	163.18	3262.33	0.256
29	113.0	163.28	3425.61	0.256
30	116.9	163.32	3588.94	0.256
31	120.8	163.33	3752.26	0.256
Multiplicator:		$\frac{Pv_0L}{EI_3}$	$\frac{Pv_0L^2}{EI_3}$	
Sum:				7.94

From the final iteration in table ?? the value of the factor, k_v , can be taken as 7.94. The critical load is then calculated to:

$$N_{cr} = k_v \frac{EI_3}{L_h^2} = 7.94 \frac{35.22 \cdot 340.1}{120.8^2} = 6.52 \text{ GN} \quad (\text{H.1})$$

I Buckling and P-delta analyses in Midas

The buckling shape for the building calculated with Midas can be seen in Figure I.1. The corresponding critical load factor for the buckling analysis is 33.79. From this the critical load can be calculated by multiplying the critical load factor with the applied load, which in this case was the self-weight of the building of 225.745 MN, from Section 6.2. The critical load is then calculated to

$$P_{cr} = 225.745 \cdot 33.79 = 7628 \text{ MN} = 7.6 \text{ GN}$$

In order to see what the result would yield with larger elements a similar model with quadratic and triangular model with a size of 3 meter was analysed. The critical load factor was given to 34.51. The corresponding critical load for the second model was then calculated to

$$P_{cr} = 225.745 \cdot 34.51 = 7.79 \text{ GN}$$

The difference between the two models is small whereas the size of the mesh can be seen as converged. Furthermore applying wind load to the buckling analyses did not give a different result.

In the P-delta analyses the critical load factor was manually interpolated to 29 for the model with wall elements, subtype plate, and 41 for the model with wall elements, subtype membrane. This correspond to critical loads of:

$$P_{cr} = 225.745 \cdot 29 = 6.55 \text{ GN}$$

$$P_{cr} = 225.745 \cdot 41 = 9.26 \text{ GN}$$

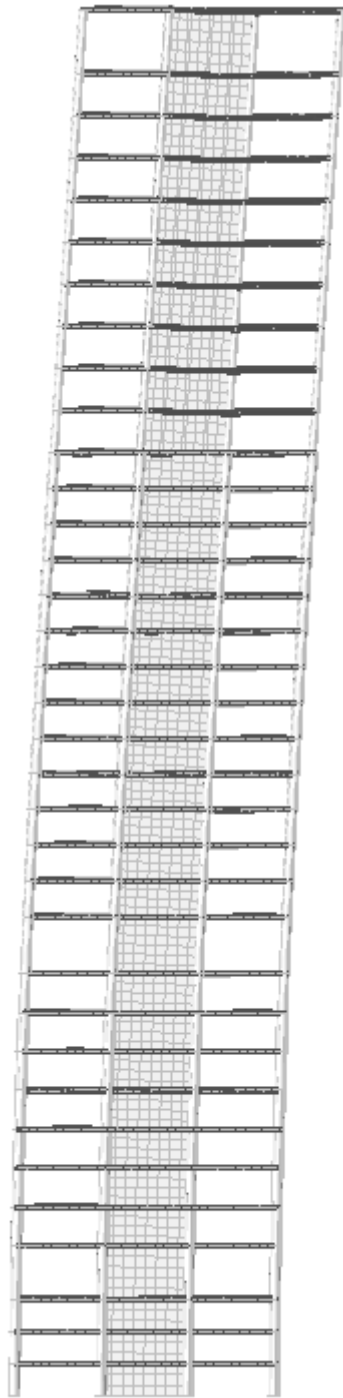


Figure I.1: Buckling shape calculated in Midas. The model is meshed with quadratic and triangular elements with a size of 1 m.

J Fundamental frequency according to Stafford Smith & Coull

In order to calculate the fundamental frequency according to Stafford Smith & Coull as

$$n_0 = \frac{1}{2\pi} \left(\frac{g \sum F_i u_i}{\sum W_i u_i^2} \right)^{1/2} \quad (\text{J.1})$$

where:

- g is the acceleration due to gravity
- F_i is the equivalent lateral load at the floor levels
- u_i is the calculated static horizontal deflection at i th level
- W_i is the weight of the i th floor

the output from Midas Gen in Table J.1 is used for input in the equation.

Table J.1: Output from Midas in order to calculate the fundamental frequency.
The data is taken from a meshed model with element size of 3 meter.

Storey	Wind x-direction [kN]	Displacement [m]	Weight [kN]
Roof	267.0	0.2537	3745.5
32	443.6	0.2386	4816.0
31	353.0	0.2284	4267.0
30	353.0	0.2183	4267.0
29	353.0	0.2082	4267.0
28	353.0	0.198	4267.0
27	353.0	0.1879	4267.0
26	353.0	0.1778	4267.0
25	353.0	0.1677	4267.0
24	353.0	0.1576	4267.0
23	353.0	0.1488	5602.0
22	354.7	0.1407	6144.1
21	354.7	0.1327	6144.1
20	354.7	0.1247	6144.1
19	341.4	0.1167	6144.1
18	327.1	0.1089	6144.1
17	324.8	0.1011	6144.1
16	322.5	0.0935	6144.1
15	320.0	0.086	6144.1
14	317.8	0.0787	6144.1
13	316.9	0.0716	6144.1
12	316.9	0.0646	6144.1
11	316.9	0.0579	6144.1
10	413.0	0.0515	7121.4
9	427.4	0.0417	7268.0
8	391.3	0.0371	8230.6
7	436.8	0.0313	8748.3
6	436.8	0.0258	8748.3
5	445.3	0.0209	8987.4
4	453.8	0.0162	8987.4
3	445.3	0.0119	8987.4
2	515.6	0.008	9570.5
1	433.7	0.0039	9191.0
0	0	0	-

K Calculations of acceleration

Along-wind acceleration

Calculations of the along-wind acceleration for a wind with a return period of 5 years.

Table K.1: Input for acceleration calculation.

Height [m]	120.8	$L(z_s)$ [m]	161.55
Width [m]	64	$V_m(z_s)$ [m/s]	29.55
ρ [kg/m ³]	1.25	Return period [years]	5
ζ	1	$V_{m,s}(z_s)$ [m/s]	25.27
K_x	1.50	$I_v(z_s)$	0.18
$m_{1,x}$ [kg/m]	179359	$f_L(z_s, n)$	2.11
$n_{1,x}$ [Hz]	0.33	$S_L(z_s)$	0.08
$k_{p,nat}$	3.44	η_h	7.26
δ_s	0.10	η_b	3.85
δ_d	0	R_h	0.13
z_0 [m]	0.3	R_b	0.23
z_s [m]	72.48		

Table K.2: Calculations for along-wind acceleration.

Storey	Height [m]	c_f	δ_a	δ	R^2	R
Foundation	0	2.2	0.038	0.138	0.083	0.288
0	1.5	2.2	0.038	0.138	0.083	0.288
1	6.4	2.2	0.038	0.138	0.083	0.288
2	10	2.2	0.038	0.138	0.083	0.288
3	13.6	2.2	0.038	0.138	0.083	0.288
4	17.2	2.2	0.038	0.138	0.083	0.288
5	20.8	2.2	0.038	0.138	0.083	0.288
6	24.4	2.2	0.038	0.138	0.083	0.288
7	28	2.2	0.038	0.138	0.083	0.288
8	31.6	2.2	0.038	0.138	0.083	0.288
9	36.9	2.2	0.038	0.138	0.083	0.288
10	40.2	2.2	0.038	0.138	0.083	0.288
11	43.5	2.2	0.038	0.138	0.083	0.288
12	46.8	2.2	0.038	0.138	0.083	0.288
13	50.1	2.2	0.038	0.138	0.083	0.288
14	53.4	2.2	0.038	0.138	0.083	0.288
15	56.7	2.2	0.038	0.138	0.083	0.288
16	60	2.2	0.038	0.138	0.083	0.288
17	63.3	2.2	0.038	0.138	0.083	0.288
18	66.6	2.2	0.038	0.138	0.083	0.288
19	69.9	2.2	0.038	0.138	0.083	0.288
20	73.2	2.2	0.038	0.138	0.083	0.288
21	76.5	2.2	0.038	0.138	0.083	0.288
22	79.8	2.2	0.038	0.138	0.083	0.288
23	83.7	2.2	0.038	0.138	0.083	0.288
24	87.6	2.2	0.038	0.138	0.083	0.288
25	91.5	2.2	0.038	0.138	0.083	0.288
26	95.4	2.2	0.038	0.138	0.083	0.288
27	99.3	2.2	0.038	0.138	0.083	0.288
28	103.2	2.2	0.038	0.138	0.083	0.288
29	107.1	2.2	0.038	0.138	0.083	0.288
30	111	2.2	0.038	0.138	0.083	0.288
31	114.9	2.2	0.038	0.138	0.083	0.288
Roof	120.8	2.2	0.038	0.138	0.083	0.288

Table K.3: Along-wind acceleration.

Storey	$\Phi_1(z)$	$c_0(z)$	$\sigma_{a,x}$	x_a [m/s ²]
Foundation	0	1	0	0
0	0.012	1	0.001	0.002
1	0.053	1	0.003	0.009
2	0.083	1	0.000	0.000
3	0.113	1	0.006	0.019
4	0.142	1	0.007	0.024
5	0.172	1	0.009	0.029
6	0.202	1	0.010	0.034
7	0.232	1	0.011	0.039
8	0.262	1	0.013	0.044
9	0.305	1	0.015	0.052
10	0.333	1	0.016	0.057
11	0.360	1	0.018	0.061
12	0.387	1	0.019	0.066
13	0.415	1	0.020	0.070
14	0.442	1	0.022	0.075
15	0.469	1	0.023	0.080
16	0.497	1	0.025	0.084
17	0.524	1	0.026	0.089
18	0.551	1	0.027	0.094
19	0.579	1	0.029	0.098
20	0.606	1	0.030	0.103
21	0.633	1	0.031	0.108
22	0.661	1	0.033	0.112
23	0.693	1	0.034	0.118
24	0.725	1	0.036	0.123
25	0.757	1	0.037	0.129
26	0.790	1	0.039	0.134
27	0.822	1	0.041	0.140
28	0.854	1	0.042	0.145
29	0.887	1	0.044	0.151
30	0.919	1	0.045	0.156
31	0.951	1	0.047	0.161
Roof	1.000	1	0.049	0.170

Across-wind acceleration

Calculations of the across-wind acceleration for a wind with a return period of 50 years.

Table K.4: Input for calculation of across-wind response.

H [m]	120.8
D [m]	64
W [m]	24
n_0 [Hz]	0.33
β	0.04
V_H [m/s]	32.3
ρ [kg/m ³]	169.8

Table K.5: Calculations of across-wind response.

a_r	1.609
v	0.162
B	0.600
R	0.190
S	0.040
F	0.190
g_p	3.720
a_w [m/s ²]	0.077

L Calculation of shear-flow in a C-beam

To be able to validate the shear forces in the building a simple test where made regarding a C-beam in steel with a point-load in mid-span. Input data and assumptions for the C-beam where:

- Self-weight is negligible.
- Web stiffeners are placed at the supports and under the point-load, which result in the assumption that the torsion angle at the supports are negligible.
- Free warping occurs at the supports.
- The material of the beam is steel and it is assumed to be linear-elastic and isotropic.
- Young's modulus is 210 GPa.
- Poisson's ratio is 0.3.

Information regarding dimensions and load-case can be seen in Figure L.1.

With a combination of Bernoulli-Euler beam theory about straight bars in bending without torsion and both St Venantsk and Vlasovsk beam theory about torsion, the shear stresses can be calculated for the C-beam in a section in the middle between the point-load and support, a quarter of the length in from support. The result from this is shown in Figure L.2.

With the same input the result from the hand calculations are reproduced with the finite element program Midas Gen. This result is shown in Figure L.3.

From this it can be concluded that linear-elastic shear-flow can be calculated accurately with programs like Midas Gen.

L. Calculation of shear-flow in a C-beam

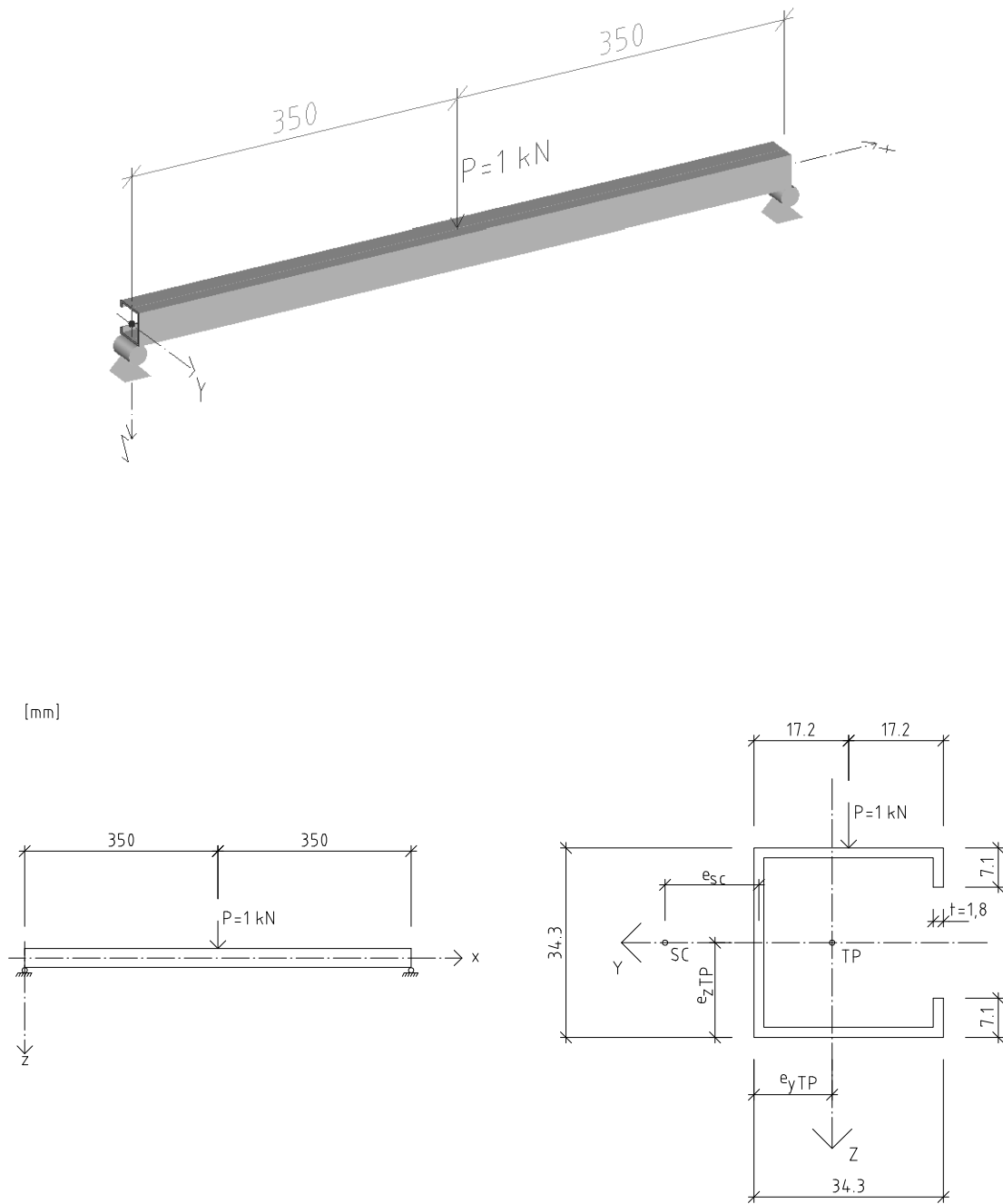


Figure L.1: Input for the C-beam.

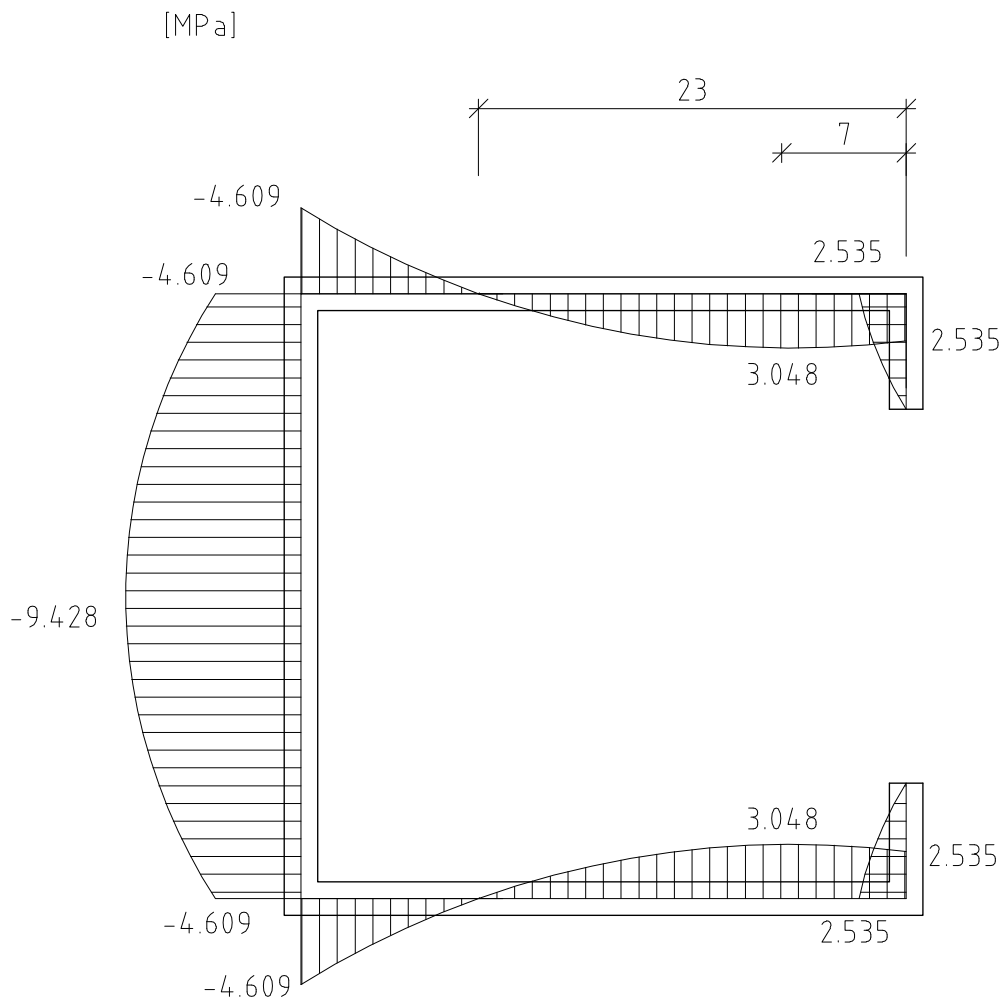


Figure L.2: Shear stresses in C-Beam a quarter of the length in from the support according to hand calculation.

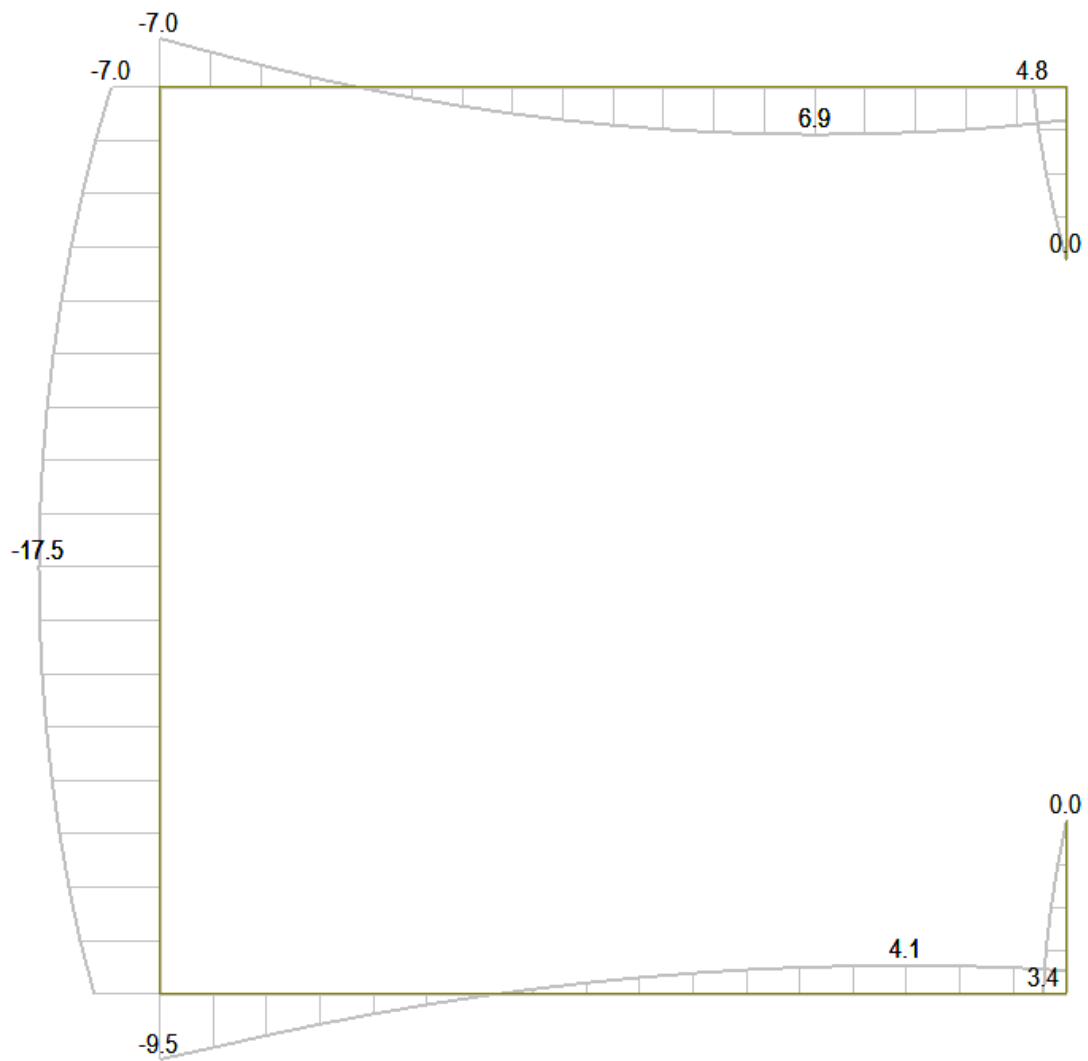


Figure L.3: Shear-flow in C-Beam a quarter of the length in from the support according to Midas Gen. Divide values with the thickness of 0.0018 m to get shear stress. [kN/m]